Enzyme Immobilization on to Magnetic Microparticles Functionalized with Polydopamine

Xinyue Wang

Thesis submitted to the University of Ottawa

in partial Fulfillment of the requirements for the

Doctorate in Philosophy degree in Chemical Engineering

Department of Chemical and Biological Engineering

Faculty of Engineering

University of Ottawa

Résumé

Les enzymes sont des biocatalyseurs extrêmement efficaces. Cependant, leurs applications industrielles ont souvent été limitées en raison de leur plage étroite de pH et de température optimaux, ainsi que de leur faible récupérabilité, réutilisabilité et stabilité. L'immobilisation des enzymes sur des supports appropriés s'est avérée être une approche efficace pour résoudre ces problèmes. Cette thèse présente une approche innovante utilisant des microparticules modifiées par de la polydopamine comme supports pour l'immobilisation des enzymes. L'immobilisation de trois enzymes de poids moléculaires et de structures très différents, dont l'alcalase et deux lipases, a été étudiée par des investigations expérimentales et une analyse bioinformatique. Les microparticules ont été fonctionnalisées par un revêtement de polydopamine (PDA), puis greffées soit avec du glutaraldéhyde (GA), soit avec du polyéthylènimine (PEI) comme espaceur pour l'immobilisation des enzymes. Divers paramètres, y compris les conditions de fonctionnalisation, les concentrations de GA, les propriétés et la concentration des enzymes, la structure et la concentration de l'espaceur, ainsi que les conditions d'immobilisation, ont été systématiquement étudiés pour évaluer leurs effets sur la densité de charge, l'activité enzymatique et l'activité enzymatique spécifique. Les résultats ont révélé des améliorations significatives de la stabilité en température et en pH, un élargissement des plages de pH et de température optimaux, ainsi qu'une meilleure récupérabilité et réutilisabilité, l'alcalase immobilisée maintenant 72,3 % de son activité relative après 10 utilisations consécutives. L'immobilisation des deux lipases a été étudiée en utilisant soit GA, soit PEI comme espaceur. Parmi les divers poids moléculaires de PEI testés (600 Da, 1800 Da et 10000 Da), le PEI avec un poids moléculaire de 600 Da a fourni l'immobilisation des protéines enzymatiques la plus efficace, tandis que le PEI avec 1800 Da a maintenu les activités enzymatiques spécifiques les plus élevées et a donné l'activité enzymatique la plus élevée par unité de masse des enzymes immobilisées. Les conditions d'immobilisation optimales ont été identifiées comme une concentration de lipase de 4,25 mg/ml, un pH de 6, un temps d'immobilisation de 5 heures et une température de 10°C. La lipase immobilisée a démontré une plage de pH optimale plus large

et une meilleure stabilité thermique, conservant 50 % de son activité après 10 cycles de réactions enzymatiques, indiquant une excellente réutilisabilité et stabilité.

Abstract

Enzymes are highly efficient biocatalysts. However, their industrial applications have been in many scenarios limited due to their narrow pH and temperature optima, poor recoverability, reusability, and stability. Immobilizing enzymes on appropriate carriers has been proven to be an effective approach addressing these issues. This thesis introduces an innovative approach utilizing polydopamine-functionalized microparticles as carriers for enzyme immobilization. The immobilization of three enzymes of vastly different molecular weights and structures, including alcalase and two lipases, was studied by experimental investigations and bioinformatic analysis. The microparticles were functionalized by coating with polydopamine (PDA), which were then grafted with either glutaraldehyde (GA) or polyethyleneimine (PEI) as the spacer for immobilization of enzymes. Various parameters, including functionalization conditions GA concentrations, enzyme properties and concentration, spacer structure and concentration, as well as immobilization conditions, were systematically investigated to assess their effects on the loading density, enzymatic activity, and specific enzymatic activity. The results revealed significant improvements in temperature and pH stability, broadening of pH and temperature optima, and improved recoverability and reusability with the immobilized alcalase maintaining 72.3% of its relative activity after 10 consecutive uses. The immobilization of the two lipases were studied using either GA or PEI as the spacer. Among various PEI molecular weights tested (600 Da, 1800 Da, and 10000 Da), PEI with a molecular weight of 600 Da provided the most effective immobilization of enzymatic proteins, while PEI with 1800 Da maintained the highest specific enzyme activities and resulted in the highest enzymatic activity per unit mass of immobilized enzymes. Optimal immobilization conditions were identified as a lipase concentration of 4.25 mg/ml, pH 6, immobilization time of 5 hours, and temperature of 10°C. The immobilized lipase demonstrated a broader optimal pH range and improved thermal stability, retaining 50% of its activity after 10 cycles of enzymatic reactions, indicating excellent reusability and stability.

Collaborator's Contributions

Chapter 3

Christopher Q. Lan provided experimental guidance, discussion of the results, correction of the manuscript and corresponding author.

Jason Zhang provided the lab and lab equipment.

Hongying Zhou, Zitong Xu and Huan Wu performed some of the experiments, such as sample collection and absorbance measurements.

Chapter 4

Christopher Q. Lan provided experimental guidance, discussion of the results, correction of the manuscript corresponding author.

Jason Zhang provided the lab and lab equipment.

Xiao Hong helped to correct the bioinformatics related figures.

Freeman Lan helped to revise the manuscript

Chapter 5

Christopher Q. Lan provided experimental guidance, discussion of the results, correction of the manuscript and corresponding author.

Jason Zhang provided the lab and lab equipment.

Xiao Hong helped to correct the bioinformatics related figures.

List of current and anticipated publications

Peer-reviewed articles:

1. Wang X., Zhou H., Xu Z., Wu H., Lan C., Zhang J. Immobilization of alcalase on polydopamine functionalized magnetic particles. (2024) Biochemical Engineering Journal
2. Li A., Wang, X., Dafoe J., Yang T., Lan C. Development of alcalase-polyacrylonitrile nanofibrous biocatalytic membranes for protein hydrolysis. (2024) Industrial& Engineering Chemistry Research
3. Wang X., Hong, X., Lan, C., Zhang J. Immobilization of lipase on polydopamine (PDA) functionalized magnetic microparticles with spacers. (Submitted to Bioresource Technology)
4. Wang X., Lan, C., Zhang J. Immobilization of two lipase using PEI and investigation of their immobilization behaviors. (In preparation)
5. Wang X., Hong, X, Lan, C., Zhang J. The frontier of enzyme technology: novel conjugation approaches in immobilization and modification (2024) Biotechnology Advances (Under review)
6. Zhou H., Wang J., Xu Z., Wang X, Lan, C., Zhang J. Two-step cultivation of Neochloris oleoabundans in a novel horizontal thin-layer algal reactor: Interplay of pH and dissolved inorganic carbon (2024) Biochemical Engineering Journal
7. Xu Z., Ma G., Zhou H., Wang X., Rana D., Matsuura T., Lan C., Ployamidoaminer dendrimer-modified polyvinylidene fluoride microporous membranes for protein separation (2024) Reactive and Functional Polymers

Conference presentation:

1. Biochemical and Biological Engineering & Synthetic Biology 2023
2. Canadian Chemical Engineering Conference (CSChE 2023)

Acknowledgements

As I conclude my thesis, I reflect on the past few years of my Ph.D. program, a journey marked by challenges, opportunities, confusion, and hope. I began my Ph.D. in the winter of 2020, only to face the outbreak of the pandemic, which brought my laboratory research to a standstill. There were moments when I considered giving up, but with my own perseverance and the encouragement of family and friends, I pressed on and gradually completed this work.

First and foremost, I want to extend my most heartfelt thanks to Professor Christopher Q. Lan. I am deeply grateful to Professor Lan for giving me the opportunity to pursue a Ph.D. in the first place. This was the beginning of all the opportunities that followed. I appreciate Professor Lan's support and guidance whenever I encountered difficulties in proposing topics, conducting experiments, or writing papers.

Next, I want to thank Professor Jason Zhang. Although Professor Zhang only became my co-supervisor in 2021, his assistance has been indispensable throughout my Ph.D. journey. I am grateful to Professor Zhang for providing labs and experimental equipment, as well as for his concern and support.

I would also like to thank my lab colleagues: Dr. Hooman Chamani, for his help in initiating my project; Dr. Hongying Zhou, Dr. Zitong Xu, and Huan Wu, for their companionship over the years; Mr. Franco Ziroldo, for his assistance in repairing centrifuges and vacuum furnaces; and Mr. Gérard Nina, for programming, software maintenance, and the instruments I used in my experiments. My sincere thanks also go to my high school classmate, Dr. Hong, for his help with bioinformatics research.

I am deeply thankful to my most important friend and partner, Mr. Zhang, for your unwavering care and companionship.

Lastly, I wish to express my gratitude to my parents. Without your unconditional support, I would not have been able to focus on my studies with such peace of mind.

Finally, I want to thank myself. Thank you for your perseverance and hard work, for never giving up, which has made this life experience so memorable and irreplaceable. This experience has not only earned me a Ph.D. degree but also given me the courage and confidence to face all difficulties and challenges in future.

Table of Contents

List of Figures

List of Tables

List of Abbreviation

AAR	Amino Acid Residues
APTES	3-Aminopropyl Triethoxysilane
Asp	Aspartic Acid
BSA	Bovine Serum Albumin
DA	Dopamine
DSC	Differential Scanning Calorimetry
EDC	1-Ethyl-3-(3-dimethylaminopropyl) carbodiimide
ELISA	Enzyme-Linked Immunosorbent Assay
FE	Free Enzyme
FT-IR	Fourier Transform Infra-Red spectroscopy
GA	Glutaraldehyde
Glu	Glutamic Acid
IE	Immobilized Enzyme
IMER	Immobilized Enzyme Microreactor
ITC	Isothermal Titration Calorimetry
LCR	Lipase sourced from *Candida rugosa*
LCS	Lipase sourced from *Candida sp.*
LD	Loading Density
Lys	Lysine
MOF	Metal-Organic Framework
MPP	Magnetic Polydopamine-modified Particles

MPPG Magnetic Polydopamine-modified particles grafted with Glutaraldehyde

MPPP Magnetic Polydopamine-modified particles grafted with Polyethyleneimine

MPs Magnetic Particles

Mw Molecular Weight

NHS N-hydroxysuccinimide

OD Optical Density

PBS Phosphate Buffered Saline solution

PDA Polydopamine

PDB Protein Database Bank

PEI Polyethyleneimine

PEI-10000 Polyethyleneimine with a molecular weight of 10000 Da

PEI-1800 Polyethyleneimine with a molecular weight of 1800 Da

PEI-600 Polyethyleneimine with a molecular weight of 600 Da

p-NP p-Nitrophenol

p-NPP p-Nitrophenol Palmitate

RSM Response Surface Methodology

SA Specific Activity

SA_{IE} Specific Activity of Immobilized Enzyme

SASA Solvent Accessible Surface Area Method

SEM Scanning Electron Microscopy

Ser Serine

Thr Threonine

Tyr Tyrosine

VSM Vibrating Sample Magnetometer

XPS X-ray Photoelectron Spectroscopy

XRD X-ray Diffraction

Chapter 1 Introduction

Enzymatic reactions are distinguished by their mild operating conditions, high efficiency, and remarkable selectivity, making enzymes the preferred catalysts across a wide range of applications, including food production, pharmaceuticals, detergents, chemicals, agriculture, and environmental industries[1]. However, in certain applications such as enzyme-based biosensors, as well as industrial and environmental processes involving costly enzymes, the limitations of free enzymes become apparent[2]. Challenges such as limited reusability and the inability to support continuous operation can hinder their effectiveness. In these contexts, enzyme immobilization emerges as a critical strategy, providing enhanced stability, reusability, and enabling continuous processes. Immobilized enzymes are not just a viable alternative but often the most practical solution for optimizing enzyme performance in such applications, thereby broadening their industrial relevance and cost-effectiveness[3,4].

1.1 Problem statement

Enzyme immobilization can be defined as restriction of enzyme mobility in a fixed space, which can provide advantages such as easy enzyme recovery, reutilization of enzyme, continuous enzymatic reaction, improved microenvironment to enhance enzymatic performance and stability, and better control of product quality[1], making it highly applicable in diverse fields such as enzymatic conversional processes[5], biosensors[6], immunomagnetic separation[7], magnetophoretic [8], drug delivery[9], etc.

The rational selection of immobilization methods and accurate evaluation of the immobilization effectiveness are critical to successful applications. Commonly used parameters for assessing immobilization effectiveness include loading density, activity, and specific activity. The loading

density refers to the amount of enzymes immobilized per unit mass or volume of carriers. It is affected by parameters such as surface/volume ratio of carriers, density of functional groups on modified carrier surfaces, the effectiveness of crosslinking agents, the concentration of enzyme concentration and the properties of bioactive molecules (e.g., molecular size, configuration, number and availability/location of functional groups on molecular surface). The measurement of enzyme activity is crucial for determining the retention rate of activity following immobilization. The activity of immobilized enzymes is influenced by two key factors: (1) the preservation of the native conformation of the immobilized molecules and (2) the accessibility of these molecules on the carrier surfaces. These factors are determined by (1) the location and strength of the bonds formed between functional groups of the bioactive molecules and the carrier surface, which can impact the configuration and orientation of the molecules; and (2) the length and flexibility of the spacer linking the enzyme to the carrier surface, which may influence steric hindrance during substrate and product mass transfer, thereby affecting the accessibility of active sites. Therefore, systematic studies on the interactions between the enzymatic proteins and carriers in immobilization using different spacers would provide not only valuable information on development of highly efficient immobilized enzymes but also knowledge that could have more general impacts on the immobilization of bioactive molecules. This approach is plausible because in comparison to other bioactive molecules, the functionality of enzymes is in general easier to quantify as enzymatic activity.

There are many enzyme immobilization technologies that have been developed up to this point. Proper immobilization methods can retain or even enhance enzymatic performance. However, there are also challenges in enzyme immobilization technology, such as identifying proper carriers for good dispersity and reusability, spacers to help immobilized enzymes retain relatively high activity

and the right bonding reactions (physical or chemical) to high loading density and stability of immobilized enzymes.

Magnetic Fe_3O_4 particles (MPs), which have been widely studied as carriers for enzyme immobilization, offer excellent dispersibility in suspensions, enabling rapid reaction kinetics, easy separation and identification, and efficient targeted delivery[10]. The immobilization of enzymes on MPs has garnered significant attention due to their strong magnetic responsiveness, which facilitates efficient mixing and convenient recovery of immobilized enzymes in reactors using an external magnetic field[11,12]. This study investigates the immobilization of alcalase on polydopamine (PDA)-modified magnetic particles (MPP) using two different spacers: glutaraldehyde (GA) and polyethyleneimine (PEI). The effects of spacer type (GA or PEI), spacer length, spacer concentration, and immobilization method on key parameters—such as loading density, activity, specific activity, and overall enzymatic performance—will be systematically evaluated.

The enzymes selected for immobilization in this thesis are alcalase (EC 3.4.21.62) and two lipases (EC 3.1.1.3). Alcalase 2.4 L, derived from *Bacillus licheniformis*, is a protease with a molecular weight of 27.41 kDa. The two lipases are sourced from *Candida sp.* and *Candida rugosa*, with molecular weights of approximately 270 kDa and 57 kDa, respectively. The purpose of choosing the two enzymes is threefold. Firstly, the two enzymes are of practical significance. Alaclase is a proteinase that has been widely used to produce peptides from hydrolysing proteins for reduced allergenicity and improved solubility and stability[13]. Lipases are important biocatalysts in production of biodiesel and numerous other applications[14]. Secondly, the same lipase will be immobilized using both GA and PEI as spacers to investigate the impact of different spacers on immobilization outcomes. Lastly, bioinformatics analysis will be employed to compare the number and distribution of potential reactive residues on the surfaces of the two different lipases, allowing for an examination of the differences between theoretical predictions and experimental results.

As abovementioned, the results of the proposed studies would have implications far beyond the immobilized enzymes and could be extended to immobilization of other bioactive proteins in applications such as magnetic separation[15] and detection[16] and drug delivery.

1.2 Research Objectives

The goal of this thesis is twofold, 1) to elucidate the effects of important parameters on the immobilization efficiency of proteins on magnetic nanoparticles, which include the properties of proteins, the properties of carriers (i.e., magnetic nanoparticles), and the properties and concentration of spacers and coating reagents; and 2) to develop immobilized enzymes that are stable, highly efficient, and easy to recycle. More specifically, the following objectives are to be pursued:

(1) Compare different methods for the synthesis of MPs and determine the method to be used in this study.

(2) Investigate the feasibility of using GA to immobilize alcalase and evaluate the effects of different immobilization conditions on the results, the enzymatic performance of the immobilized alcalase has be assessed.

(3) Investigate the effects of using GA and PEI of varying lengths to immobilize lipase, with a focus on optimizing immobilization conditions. The performance of the immobilized enzymes was then evaluated under different conditions.

(4) From a bioinformatics perspective, comparing different spacers for the same lipase examines how spacer properties, such as length and flexibility, affect enzyme immobilization and active site accessibility. Similarly, for two different lipases with the

same spacer, bioinformatics analysis reveals how structural differences, such as surface charge and hydrophobicity, influence immobilization efficiency and enzyme activity.

(5) Investigate the impact of varying lengths of polyethyleneimine (PEI) on the immobilization results of two lipases with different molecular weights. Response surface methodology (RSM) was employed to optimize the immobilization conditions. The performance of the immobilized enzymes was then evaluated.

1.3 Thesis Structure

This thesis is organized into six chapters. The second chapter provides a comprehensive review of current knowledge on enzyme immobilization methods, focusing on both alcalase and lipase. It begins with an introduction to these enzymes, highlighting their properties and applications. The chapter then discusses the various immobilization techniques, specifically the use of glutaraldehyde (GA) and polyethyleneimine (PEI) as spacers. It examines the potential of these methods for enzyme immobilization, including their advantages and challenges. The chapter aims to summarize the advancements in immobilization research, offering insights into the benefits and limitations of each approach. The third chapter explores the feasibility of using glutaraldehyde (GA) for the immobilization of alcalase on polydopamine (PDA)-modified magnetic microparticles (MPs). This chapter focuses on optimizing the immobilization conditions and evaluating the enzymatic performance of the immobilized alcalase. Chapter 4 investigates the feasibility of using both glutaraldehyde (GA) and polyethyleneimine (PEI) for the immobilization of lipase. The study reveals that PEI is more suitable than GA for lipase immobilization. This chapter also focuses on optimizing the immobilization conditions for lipase and evaluating the enzymatic performance of the immobilized enzyme. The next chapter explores the immobilization of two different lipases using polyethyleneimine (PEI). Bioinformatics methods

were employed to predict the immobilization outcomes, which were then compared with experimental results. Response surface methodology (RSM) was used to optimize the immobilization conditions, followed by testing the performance of the immobilized enzymes. Finally, Chapter 6 provides a comprehensive conclusion.

1.4 Reference

1. Dwevedi, A. Enzyme immobilization: Advances in industry, agriculture, medicine, and the environment. *Enzyme Immobilization: Advances in Industry, Agriculture, Medicine, and the Environment* 1–132 (2016) doi:10.1007/978-3-319-41418-8.

2. Ansari, S. A. & Husain, Q. Potential applications of enzymes immobilized on/in nano materials: A review. *Biotechnol Adv* 30, 512–523 (2012).

3. Maghraby, Y. R., El-Shabasy, R. M., Ibrahim, A. H. & Azzazy, H. M. E. S. Enzyme Immobilization Technologies and Industrial Applications. *ACS Omega* 8, 5184–5196 (2023).

4. Liu, S. *et al.* Smart chemistry of enzyme immobilization using various support matrices – A review. *Int J Biol Macromol* 190, 396–408 (2021).

5. Di Cosimo, R., Mc Auliffe, J., Poulose, A. J. & Bohlmann, G. Industrial use of immobilized enzymes. *Chem Soc Rev* 42, 6437–6474 (2013).

6. Asal, M., Özen, Ö., Şahinler, M., Baysal, H. T. & Polatoğlu, İ. An overview of biomolecules, immobilization methods and support materials of biosensors. *Sensor Review* 39, 377–386 (2019).

7. Chung, T. H., Chang, J. Y. & Lee, W. C. Application of magnetic poly(styrene-glycidyl methacrylate) microspheres for immunomagnetic separation of bone marrow cells. *J Magn Magn Mater* 321, 1635–1638 (2009).

8. Forbes, T. P. & Forry, S. P. Microfluidic magnetophoretic separations of immunomagnetically labeled rare mammalian cells. *Lab Chip* 12, 1471–1479 (2012).

9. Thanh, B. T. *et al.* Immobilization of Protein A on Monodisperse Magnetic Nanoparticles for Biomedical Applications. *J Nanomater* 2019, (2019).

10. Bilal, M., Zhao, Y., Rasheed, T. & Iqbal, H. M. N. Magnetic nanoparticles as versatile carriers for enzymes immobilization: A review. *Int J Biol Macromol* 120, 2530–2544 (2018).

11. Vaghari, H. *et al.* Application of magnetic nanoparticles in smart enzyme immobilization. *Biotechnol Lett* 38, 223–233 (2016).

12. Díaz-Hernández, A. *et al.* Characterization of Magnetic Nanoparticles Coated with Chitosan: A Potential Approach for Enzyme Immobilization. *J Nanomater* 2018, (2018).

13. Margelefsky, E. L., Zeidan, R. K. & Davis, M. E. Cooperative catalysis by silica-supported organic functional groups. *Chem Soc Rev* 37, 1118–1126 (2008).

14. Giardina, P. *et al.* Laccases: A never-ending story. *Cellular and Molecular Life Sciences* 67, 369–385 (2010).

15. Al-Qodah, Z., Al-Shannag, M., Al-Busoul, M., Penchev, I. & Orfali, W. Immobilized enzymes bioreactors utilizing a magnetic field: A review. *Biochem Eng J* 121, 94–106 (2017).

16. Nazari, M., Kashanian, S. & Rafipour, R. Laccase immobilization on the electrode surface to design a biosensor for the detection of phenolic compound such as catechol. *Spectrochim Acta A Mol Biomol Spectrosc* 145, 130–138 (2015).

Chapter 2 Literature Review

2.1 Immobilization methods

The primary methodologies for enzyme immobilization can be categorized into four principal groups: physical adsorption, covalent bonding, self-crosslinking and entrapment. In real-world applications, it is commonplace for researchers to integrate two or more of these strategies to enhance the efficacy and stability of the immobilized enzymes[1]. Figure 2-1 shows the schematics of the four immobilization methods.

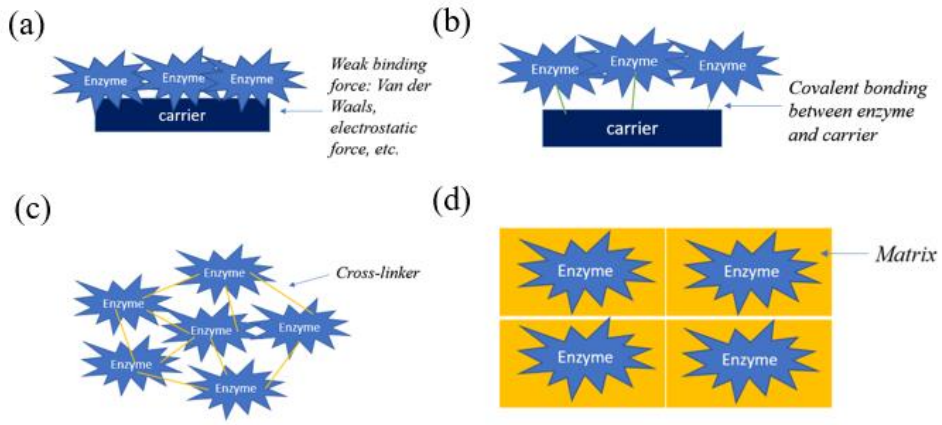

Figure 2-1 Schematic of four immobilization methods: a) Adsorption, b) Covalent bonding, c) Self-crosslinking and d) Entrapment.

2.1.1 Adsorption

The adsorption technique predominantly secures enzymes onto carriers through weak binding forces, including Van der Waals forces, electrostatic interactions, and other non-covalent bonds. This approach is recognized for its simplicity and cost-effectiveness[2]. Given the gentle nature of the binding, the adsorption method minimally impacts the enzyme's structure, thereby largely preserving its activity.

Several methods for immobilizing enzymes using physical adsorption exist. Enzymes can be immobilized onto carriers through surface features such as hydrogen bonding or hydrophobic interactions. Common carriers for this purpose include activated carbon, porous ceramics, and silica gel[3–5]. In physical adsorption for enzyme immobilization, ion exchange adsorption and hydrophobic interactions are also involved. Ion exchange adsorption refers to the immobilization of enzymes onto carriers with ion exchange functionalities, where enzymes are adsorbed and fixed by interacting with ions on the carrier. Such carriers typically include anion exchange resins and cation exchange resins[6,7]. Conversely, hydrophobic interactions involve the binding of enzyme molecules, which usually possess hydrophilic or hydrophobic regions on their surfaces, to the corresponding hydrophobic or hydrophilic regions on the carrier surface. This method is commonly employed with hydrophobic carriers, such as hydrophobic resin[8].

In comparison to the covalent bonding approach, as evidenced by the data presented in Table 1, employing physical adsorption for enzyme immobilization yields a higher retention of activity. Nonetheless, this method is vulnerable to enzyme leakage attributed to desorption, thus constituting a notable limitation, particularly within rigorous industrial settings. The stability of immobilized enzymes may be compromised by variations in factors such as pH, temperature, and ionic strength. Furthermore, the potential leaching of enzymes presents a risk of contaminating the ultimate product, thereby introducing complexities in ensuring product purity[9].

2.1.2 Covalent bonding

Covalent bonding refers to immobilizing enzymes on carriers by covalent bonds. The functional groups on the carrier react with the amino acid residues from enzyme (such as amino groups, carboxyl groups, cysteine sulfhydryl groups, histidine imidazole groups, serine and threonine hydroxyl groups, and tyrosine phenol groups) to form covalent bonds[8]. The table below enumerates several commonly employed methods for enzyme immobilization through covalent bonding,

juxtaposing their respective characteristics. Table 2-1 further delineates recent investigations leveraging covalent bonding for enzyme immobilization. It is discernible from the table that the advantage of utilizing covalent bonding lies in its superior reusability compared to physical adsorption.

Using covalent bonding to immobilize enzymes has several significant advantages and disadvantages. Its advantages include high stability and durability, as covalent bonds are stronger than physical adsorption or other non-covalent bonds, which makes the immobilized enzymes less likely to leach. This property makes them suitable for long-term use and industrial applications[10]. Meanwhile, the disadvantages of covalent bonding include the cumbersome procedural steps, potential loss of enzymatic activity due to conformational changes upon immobilization, and the irreversibility of the reaction[11].

Table 2-1 Comparison of immobilization enzymes using adsorption and covalent bonding

Immobilization Method	Carrier	Type of Enzyme	Activity	Retention of Activity	Activity	Application	Refs
Adsorption	Cloisite 30B	α-amylase	2.39 ± 0.03		35.9%		[12]
	Glyoxyl-based	levansucrase		98%		Synthesis of lactosucrose	[13]
	Na-sepiolite	Lipase		56.7%	54%/1		[14]
	ZIF-8	Lipase		3.8-fold	68%/5	Produce biodiesel	[15]
Covalent Bonding	Cloisite 30B	α-amylase	2.17 ± 0.05 U/mg		79.7%		[12]
	MOF	Catalase			62%/4		[16]
	MOF	glucose oxidase				tumor vasculature targeted catalytic therapy	[17]
	Zinc sulfide-chitosan hybrid nanoparticles	α-amylase	K_m increased			food industry	[18]

2.1.3 Crosslinking and self-cross-linking

Crosslinking is a chemical process that joins two or more molecules via covalent bonds. This technique, which similarly employs covalent bonds, involves chemically immobilizing enzymes onto carrier materials using cross-linking agents. Unlike the straightforward covalent bonding method, crosslinking utilizes agents that link enzyme molecules together while simultaneously anchoring them to the carrier. These agents often feature multiple reactive functional groups, enabling the formation of covalent bonds both among enzyme molecules and between the enzymes and the carrier. Common cross-linking agents include glutaraldehyde, N-hydroxysuccinimide (NHS), carbodiimides (e.g., EDC), disulfide cross-linkers, and isocyanates[19,20].

The use of cross-linking agents results in a robust attachment between the enzyme and the carrier, typically stronger than that achieved by simple covalent bonding. Moreover, by tweaking the cross-linking conditions, the activity of the enzyme can be modulated to better suit specific reaction environments. However, there are notable drawbacks to the cross-linking method for enzyme immobilization. Multipoint cross-linking might obscure active sites or alter the enzyme's conformation and configuration, thus diminishing its activity. Excessive cross-linking can overly restrict the enzyme, limiting its mobility and thereby reducing its catalytic efficiency[21].

The self-crosslinking approach bears similarities to traditional crosslinking but differs significantly in its initial phase. In self-crosslinking, the crosslinking reaction first occurs within the enzyme molecules themselves. Only after this internal crosslinking are the enzyme molecules immobilized onto a carrier. Like other methods, self-crosslinking creates crosslinked structures between enzyme molecules, which can lead to the masking of active sites if the crosslinking is excessive[21] .

2.1.4 Entrapments

Entrapment involves immobilizing enzymes by physically or chemically fixing them within carriers that possess a specialized network structure, such as polyacrylamide, collagen, or gelatin[22–24].

This method includes various techniques such as entrapment gel, microencapsulation, and fiber encapsulation. Entrapment gel utilizes natural or synthetic polymers like sodium alginate and polyacrylamide. Here, the enzyme solution is mixed with monomers or pre-polymers and then polymerized to form a gel matrix that entraps the enzyme molecules within[25]. Microencapsulation involves creating small capsules that contain enzymes, with these microcapsules typically made from polymer materials to ensure the enzyme is securely encapsulated[26]. Fiber encapsulation, on the other hand, involves embedding enzymes within fiber materials, prepared using techniques such as wet spinning, dry spinning, or other fiber formation methods[27].

The entrapment method provides significant protection to enzymes from mechanical shear forces and direct exposure to external conditions, thereby enhancing enzyme stability[28]. It also facilitates the concurrent entrapment of multiple enzymes, which is particularly beneficial for applications requiring multi-enzyme systems. However, this method is generally more suited to enzymes that catalyze reactions involving small molecule substrates and products. This is due to the significant diffusion resistance experienced by enzymes immobilized via entrapment, which can impact enzyme kinetics[4]. Additionally, the materials used for entrapment may undergo aging and degradation over time, potentially compromising the stability and activity of the immobilized enzymes[25].

2.2 Carriers for enzyme immobilization

The carriers employed for enzyme immobilization serve as support materials for the fixation of enzyme molecules. Various carriers are selected based on distinct performance criteria in practical

applications. Generally, carriers utilized for enzyme immobilization must adhere to the following requirements[29,30].

Primarily, the material chosen as a carrier must demonstrate both physical and chemical stability within the context of its intended application. It is essential that the carrier exhibits sufficient mechanical strength to endure stresses from agitation and flow during practical operations. Furthermore, it is critical for the carrier to maintain chemical stability within the pH and temperature ranges pertinent to enzyme immobilization applications. The carrier should not react with substrates or products, nor should it degrade or decompose under operational conditions[31].

Another important consideration is the structure of the carrier. A porous structure or a large specific surface area is advantageous as it allows for a higher density of enzyme loading[32]. The presence of functional groups on the carrier's surface is paramount. Ideally, the surface should have various functional groups, such as hydroxyl, carboxyl, or aldehyde groups, which can react with residues on the enzyme molecule to form covalent bonds, thereby enhancing the binding of the enzyme to the carrier[33].

Carriers are generally categorized into three types based on their chemical composition: inorganic carriers, organic carriers, and composite carriers. Each type offers unique advantages and is suitable for specific applications. The selection of an appropriate carrier material is a critical aspect of the enzyme immobilization process design, influenced by anticipated applications, desired enzyme activity retention, and cost-effectiveness considerations. In practical scenarios, choosing carriers often requires balancing its physicochemical properties with production costs[9].

2.2.1 Inorganic carriers

Inorganic carriers are fundamental to the field of enzyme immobilization, enhancing enzyme stability, reusability, as well as heat and chemical tolerance. These benefits make enzyme immobilization systems more reliable and cost-effective for industrial production. Typically,

inorganic carriers exhibit robust physical and chemical stability, allowing them to maintain their structural integrity under a variety of environmental conditions. This stability prolongs the lifespan of enzymes, increases their efficiency, and enhances loading density, making inorganic carriers critical in applications such as bioprocessing and biomedicine[34].

Unmodified inorganic carriers typically employ physical adsorption or other non-covalent methods for enzyme immobilization. Recently, popular materials in this domain include ceramics, zeolites, and graphene[35].

2.2.1.1 Ceramics

Ceramics, as a category of inorganic support materials, offer distinct advantages due to their versatility in synthesizing desired morphologies and geometries. Silica (SiO2)[36] is notably the most prevalent among ceramics for enzyme immobilization, with other materials like alumina (Al2O3)[37], titanium dioxide (TiO2)[38], and zirconia (ZrO2) [50] also being effectively utilized.

2.2.1.2 Zeolites

Zeolites typically immobilize enzymes through physical adsorption and deposition. The adsorption strength is influenced by the affinity between enzyme molecules and the zeolite surface, which can be adjusted by modifying the Si/Al or SiO_2/Al_2O_3 ratio. Increasing the loading density is possible by enhancing the specific surface area of the zeolite. However, due to the relatively small pore size of zeolites, they are not always suitable for immobilizing larger enzymes, which typically range from 3-30 nm in molecular size[35,39]. Conversely, overly large pore sizes can reduce the specific surface area and thus decrease enzyme loading density[40].

2.2.1.3 Graphene

Graphene, known for its extensive specific surface area and functional groups such as carboxyl, hydroxyl, and epoxy groups, readily bonds with enzymes[41]. Both graphene and its derivative,

graphene oxide, possess exceptional physicochemical properties, including electrical, optical, thermal, and mechanical strengths, making them highly advantageous for enzyme immobilization. Graphene oxide, in particular, is notable for its abundance of oxygen-containing functional groups on its single-layer two-dimensional sheets, such as hydroxyl, carboxyl, epoxy, carbonyl, phenolic, lactone, and quinone groups. These properties make graphene-based materials excellent candidates for enzyme immobilization carriers. The use of graphene-based biocatalytic systems spans various biotechnological applications, including biocatalytic conversions, pollutant degradation, biosensors, biofuel cells, and microchip bioreactors[42].

2.2.2 Organic carriers

Organic carriers utilized in enzyme immobilization are predominantly classified into two categories: natural polymer carriers and synthetic polymer carriers. Each type has distinct properties that suit specific requirements for enzyme immobilization, impacting enzyme functionality and operational stability.

2.2.2.1 Natural Polymer Carriers

Natural polymers, such as polysaccharides and proteins, are extensively utilized in enzyme immobilization due to their ability to enhance the stability of immobilized enzymes (IE) and their bioactivity, which are essential for maintaining enzyme functionality and stability. Alginate, particularly barium alginate, is widely recognized for its gelation properties that provide a mild environment conducive to enzyme activity, as evidenced in studies by[43,44]. Chitosan, another versatile natural polymer known for its ability to enhance the stability of IE and its biodegradability,

is frequently used in forms such as gels, microspheres, or films. Its tunable surface properties facilitate a variety of binding mechanisms, making it a preferred choice for enzyme immobilization[45]. Cellulose is favored for its abundant functional groups and its ability to enhance the stability of IE, typically employed through simple mixing or coprecipitation methods to achieve effective and economical immobilization[46]. Additionally, collagen, as a proteinaceous substrate, provides a natural environment that supports the preservation of enzyme activity. Enzymes are generally attached to collagen surfaces via chemical bonds or non-covalent interactions with amino acid residues, thus maintaining their native conformation and activity[47]. Collectively, these natural polymers play a pivotal role in enhancing the efficiency and effectiveness of enzyme immobilization processes.

2.2.2.2 Synthetic Polymer Carriers

Synthetic polymers are highly valued in enzyme immobilization for their robust mechanical strength and their ability to be customized to resist microbial degradation and meet specific physicochemical requirements. Among the commonly used synthetic carriers, ethylene polymers stand out due to their durability and versatility in various applications, as demonstrated in studies focusing on the impact of macroporous polystyrene microspheres on lipase immobilization[48]. Polyacrylates are noted for their flexibility and are particularly used in immobilizing enzymes like glucoamylase, taking advantage of their functional groups to facilitate enzyme binding[34]. Polyvinyl Alcohol (PVA) is another favored material, chosen for its chemical stability and mechanical robustness, which are crucial for prolonged enzyme activity[49]. Polyacrylamide (PAM) is frequently selected for gel formation due to its ease of processing and effective encapsulation properties, which are essential for maintaining enzyme integrity[50]. Additionally, biodegradable polymers such as Polylactic Acid (PLA) and Polylactic-co-glycolic Acid (PLGA) are extensively utilized not only in the medical and bioengineering fields but also as enzyme carriers, appreciated for their ability to

enhance the stability of IE and favorable degradation profiles[51]. These synthetic polymers collectively enhance the operational stability and efficiency of immobilized enzymes, making them indispensable in advanced biotechnological applications.

2.2.3 Composite carrier

In the realm of enzyme immobilization, the development of composite carriers has become a focal point, merging the beneficial properties of inorganic materials, natural polymers, and synthetic polymers. These composites aim to enhance and optimize carrier properties to improve enzyme performance.

2.2.3.1 Inorganic-organic Composite Carriers

Inorganic-organic composite carriers are increasingly utilized in enzyme immobilization, leveraging their robust properties to enhance enzyme functionality and operational stability.

Metal-Organic Frameworks (MOFs), known for their tunable pore structures and surface functionalization, provide a highly organized framework that not only maintains enzymatic activity but also facilitates easier recovery and reuse. The specific design of MOFs contributes to excellent stability and reactivity, making them ideal for enzyme immobilization[52,53]. Similarly, silicon-based materials, including silica gel, silica nanoparticles, and silicates, are selected for their large surface areas and porous structures. These characteristics are conducive to maintaining the structural integrity and functionality of enzymes, thus supporting their use in sensitive biochemical processes[54–56]. Additionally, nanocomposites, which often consist of metal nanoparticles or magnetic nanoparticles combined with organic molecules or polymers, offer versatile platforms for enzyme immobilization. Their inherent magnetic properties simplify the separation and purification processes, thereby enhancing the practicality and efficiency of industrial applications[57–59]. Porous ceramics such as alumina and zirconia are also employed, prized for their high stability and

mechanical strength. These materials are especially valuable in applications requiring high durability and resistance to harsh conditions, such as continuous flow reactions or high-temperature processes[60,61].

Together, these inorganic-organic composite carriers play a pivotal role in advancing enzyme immobilization technologies, offering tailored environments that enhance enzyme stability, functionality, and industrial applicability.

2.2.3.2 Natural Polymer-Synthetic Polymer Composite Carriers

Blending natural and synthetic polymers to create composite carriers capitalizes on the ability of natural materials to enhance the stability of IE alongside the mechanical strength and chemical stability of synthetic counterparts. These hybrid materials are versatile and highly effective in various applications, from industrial biocatalysis to medical diagnostics.

For example, blends of gelatin and chitosan with synthetic polymers like polyacrylic acid or polyethyleneimine form supportive matrices that are widely employed in enzyme immobilization, as detailed by Khan et al. and J. Wang et al.[62,63]. Furthermore, carriers based on biodegradable polymers such as polylactic acid or polycaprolactone, when combined with natural polymers, not only enhance environmental sustainability but also provide robust platforms for enzyme immobilization. This approach has been explored in works by Samadian et al. and Weng et al.[64,65]., highlighting their efficacy and environmental benefits. Hydrogel composite carriers, which include base materials like sodium polyacrylate, or gelatin hydrogels mixed with synthetic polymers or nanomaterials, offer unique hydration properties and a soft gel-like consistency. These characteristics are beneficial for preserving enzyme activity and stability under physiological conditions, as evidenced by research from Hata et al. and Maroufi et al.[66,67]. Lastly, nanofiber composite carriers, fabricated using technologies such as electrospinning, incorporate a blend of natural polymers, synthetic polymers, and nanomaterials to create ultrafine fibers. These fibers

provide high surface area-to-volume ratios, which are critical for enhancing enzyme loading and activity, a technique effectively demonstrated by Erdal & Güngör and Rather et al.[68,69].

2.3 Immobilized enzyme property

Enzyme immobilization is undoubtedly a critical technology for advancing biocatalysis into the realm of flow chemistry. The primary objective is to maximize the catalytic activity and operational stability of the immobilized enzymes[70]. In order to assess the impact of immobilization on flow biocatalysis, it is imperative to quantify the following parameters using standard quantitative metrics:

2.3.1 Enzyme Loading

The amount of enzyme loaded onto the phase must be measured to determine the efficiency of the immobilization process. To evaluate enzyme loading on phases accurately and sensitively, several methodologies are utilized, each tailored to specific experimental needs and contexts.

The enzyme-linked immunosorbent assay (ELISA) is a versatile method that has been adapted to quantitatively measure enzyme loading. This technique involves coating the solid surface with a substrate that reacts with the enzyme; the quantity of enzyme is then determined by the intensity of the colorimetric signal produced. For instance, Song et al. enhanced the sensitivity of such immunoassays through a cascade-amplifying system specifically for ochratoxin A detection, indirectly measuring enzyme loading through signal amplification[71].

Additionally, microfluidic devices offer precise control over enzyme and substrate volumes, allowing direct measurement of enzyme loading by observing reaction kinetics within the device's microchannels. This method was exemplified by Li et al., who employed a 3D-printed microfluidic

device in a one-step assay to measure enzyme kinetics, demonstrating the potential for direct assessments of enzyme loading[72].

Furthermore, polymer microarrays facilitate single-molecule detection by isolating individual enzyme molecules in microwells on solid surfaces. Detection is typically achieved using fluorescent markers or other visual indicators, enabling precise quantification at the molecular level. Duan et al. demonstrated this approach by using a polymer microarray to detect and quantify individual enzyme molecules, providing a highly accurate measure of enzyme loading[73].

These techniques collectively contribute to the optimization of enzyme immobilization processes, enhancing the effectiveness and efficiency of applications across various fields. Each method provides a unique set of advantages that, when appropriately applied, can yield detailed insights into enzyme loading dynamics on solid phases.

2.3.2 Recovered Activity

Post-immobilization, it is crucial to evaluate the extent to which the original enzymatic activity is retained, indicating the effectiveness of the immobilization technique. Several advanced methodologies provide comprehensive insights into the efficiency of enzyme immobilization techniques by directly measuring activity recovery.

One such method involves the simultaneous observation of both the structural orientation and enzymatic activity of immobilized enzymes on surfaces. This approach employs surface-sensitive techniques such as sum frequency generation (SFG) spectroscopy combined with fluorescence microscopy. For example, Jasensky et al. reported significant activity loss in β-glucosidase immobilized on a monolayer, providing vital data for understanding the enzyme functionality post-immobilization [74].

Calorimetric methods, including isothermal titration calorimetry (ITC) and differential scanning calorimetry (DSC), are also employed to assess the activity and stability of enzymes immobilized

on membranes or other supports. These techniques measure the heat change associated with the enzyme's reaction, thereby assessing its activity and stability under various conditions. Mason et al. demonstrated the effectiveness of these methods by using ITC and spectrophotometry to measure the activity of immobilized invertase, highlighting their applicability in evaluating the stability and reusability of membrane-immobilized enzymes[75].

Additionally, integrating an immobilized enzyme microreactor (IMER) with capillary electrophoresis allows for on-line enzyme assays, providing immediate feedback on recovered activity post-immobilization. This capillary electrophoresis-integrated approach was illustrated by Hu et al., who described its application for penicillinase, showcasing a rapid and efficient method for enzyme activity assays in complex real samples[76].

These diverse methods collectively contribute to a deeper understanding and improvement of enzyme immobilization processes, ensuring the recovered activity is maximized for industrial biocatalytic applications.

2.4 Magnetic nanoparticles as a carrier for immobilization

There are many types of magnetic nanoparticles, including alloys (e.g., Fe, Co, and Ni), iron oxides (Fe_3O_4, Fe_2O_3), and ferrites ($NiFe_2O_4$, $CuFe_2O_4$, $ZnFe_2O_4$). Among them, Fe_3O_4 has superparamagnetic properties and good dispersibility, and thus is widely used for enzyme immobilization.

2.4.1 Synthesis of Fe_3O_4 MNPs

Synthesis methods of Fe_3O_4 MNPs can be divided into chemical methods and physical methods. Physical methods include evaporative condensation and magnetron sputtering. Chemical methods include co-precipitation, microemulsion, hydrothermal, sol-gel and solvothermal methods.

The co-precipitation method is adding Fe^{2+} and Fe^{3+} in alkaline solution (NaOH or NH_3OH) and preparing Fe_3O_4 MNPs through the following oxidation-reduction reaction:

$$2Fe^{2+} + Fe^{3+} + 8OH^- = Fe_3O_4 + 4\ H_2O$$

This method is simple in operation, mild in conditions, high in yield and the produced Fe_3O_4 MNPs has superparamagnetic properties. However, the produced Fe_3O_4 MNPs are irregular in shape and has a wide particle size distribution range.[77,78]

Microemulsion method refers to adding Fe^{3+} and surfactant such as sodium dodecyl benzenesulfonate (NaDBS) $[CH_3(CH_2)_{11}(C_6H_4)SO_3]Na$ to form microemulsion in organic solvents. Microemulsion droplets collide with each other, grow, then add precipitant, such as NaOH, and finally form Fe_3O_4 MNPs within the droplets. The Fe_3O_4 MNPs synthesized by this method are small, tightly controlled particle size with narrow particle size distribution and therefore good dispersibility. However, it requires a large amount of organic solvents, and the yield is low.[79,80]

The hydrothermal method refers to use Fe^{3+} and aqueous system under high temperature and pressure to produce Fe_3O_4 MNPs. This method has the advantages of good dispersion and controllable particle size of Fe_3O_4 MNPs, but its requirements for the reaction conditions are high.[81]

Solvothermal method refers to the synthesis of Fe_3O_4 MNPs by mixing $FeCl_3 \cdot 6H_2O$, sodium acetate and ethylene glycol (as reductant) to form a clear solution and then seal the mixture in a Teflon-lined stainless-steel autoclave, heating and maintaining at 200 ℃ for a period of time. Then, after cooling to room temperature, Fe_3O_4 nanoparticles are separated and dried. The Fe_3O_4 MNPs synthesized by this method has good dispersibility and hydrophilicity, but the yield is low.[82] The comparison of different synthesis methods of Fe_3O_4 MNPs shown in Table 2-2.

Table 2-2 Comparison of synthesis methods for Fe_3O_4 MNPs

Name	Advantage	Shortage	Size	Reference
Co-precipitation	Simple and mild synthetic conditions	Irregular product shape and uneven size	5-15 nm	[77,78]
Microemulsion	Small and controllable size, good dispersion	Organic solvents and low yield	4-15 nm	[79,80]
Hydrothermal	Controllable size, good dispersion, high purity	Harsh reaction condition and long reaction time	varied size	[81]
Solvothermal	Controllable size, good dispersion, high purity	High reaction temperature, low yield	> 200 nm	[82]

2.4.2 Surface modification of Fe_3O_4 MNPs

Naked Fe_3O_4 MNPs have large surface-to-volume ratio with high Gibbs free energy and magnetic properties and are prone to agglomeration. In an aqueous suspension, they are easy to oxidize and therefore lose magnetism. In addition, the naked Fe_3O_4 MNPs lack sufficient functional groups to bind with enzymes. Therefore, surface modification of Fe_3O_4 MNPs is crucial for enzyme immobilization. According to the chemical composition of the modified material, the methodologies of MNP modification can be divided into inorganic and organic coating.

2.4.2.1 Inorganic coating

Coating with a layer of inorganic material can effectively improve the dispersibility and anti-oxidation ability of Fe_3O_4 MNPs. SiO_2, Au and Cu are the most commonly used inorganic coating materials for enzyme immobilization.

Karimi et al.[83] immobilized lipase on mesoporous magnetic nanoparticles coated with SiO_2. Different from the traditional Fe_3O_4 MNPs single coated with SiO_2. The results showed that there was a possibility that multiple Fe_3O_4 MNPs agglomerated together and were coated with SiO_2. After coating, the grafted amino groups were activated with glutaraldehyde, and then, used to immobilize *B. cepacia* lipase on its surface

2.4.2.2 Organic coating

Using organic molecules such as organic silane, citric acid, chitosan, and dopamine to modify the Fe_3O_4 MNPs can effectively reduce the surface energy of the Fe_3O_4 MNPs to prevent them from agglomerating. They also provide abundant functional groups for subsequent reactions compared with modified using inorganic materials.

2.5 Alcalase and immobilized alcalase

2.5.1 Source and applications of alcalase

Alcalase (EC 3.4.21.62) is a protease produced by *Bacillus lichenformis* with optimum pH and temperature of 8.2 and 60°C, respectively. Commercial alcalase has been successfully used in the detergent industry to remove protein-based stains such as blood, egg and faeces[84], and in the food industry[85], e.g., to hydrolyse egg white proteins to enhance the digestibility, stability, and solubility, and reduce the allergenicity of products. It has also be widely used to produce peptides from dairy (i.e., cheese whey)[86], agricultural (e.g., soymeal)[87] and fishery wastes[88] to enhance both the recovery of proteins and the value of products.

2.5.2 Structure and catalytic mechanism of alcalase

Alcalase (EC 3.4.21.62) is a serine-type none-specific endo-protease, which is a member of the subtilisin-like protease family with Asp, Ser and His catalytic triad that hydrolyses peptide bonds in multiple types of proteins[89]. The total molecular weight of alcalase is 27.41 kDa. As shown in Figure 2-2, alcalase has several exposed Lys residues, which offer $–NH_2$ functional group, and Glu and Aps residues, which offer –COOH group, on the surface. The immobilization of alcalase on PDA coated MNPs using GA or PEI as spacer very likely involves the Lys 12, Lys 15, Lys 136, Lys 237, and Lys 265. These residues all locate at the opposite side of the active site and therefore the immobilization of alcalase on the carrier via them will not block the active site. Lys 94 and Lys 170 are quite close to the active site, however, they both locate in the "valleys" and have much smaller probability to react with the spacer than other Lys residues on surface. Nonetheless, anchoring enzymes on a solid surface, i.e., the carrier surface, would restrict the enzyme molecules from colliding with substrate molecules via Brownian motions but instead require the diffusion of substrate protein from the bulk solution to the carrier surface. Since the diffusion of proteins, which are the substrates of alcalase and of large molecular weights, is very slow, the restriction of motion of enzyme molecules by immobilization could have significant impact on enzymatic activity[90]. Such negative impact could be partially relieved by using flexible spacers.

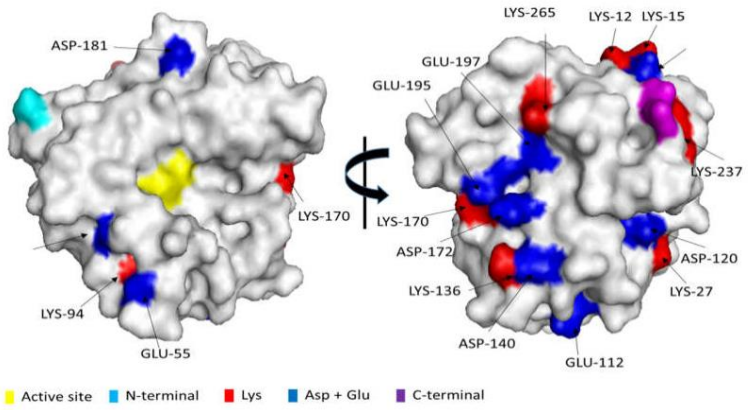

Figure 2-2 Structure models of alcalase (EC 3.4.21.62) (PDB 1SCA)

The catalytic mechanism of serine proteases hydrolysing peptide is shown in Figure 2-3 [89].

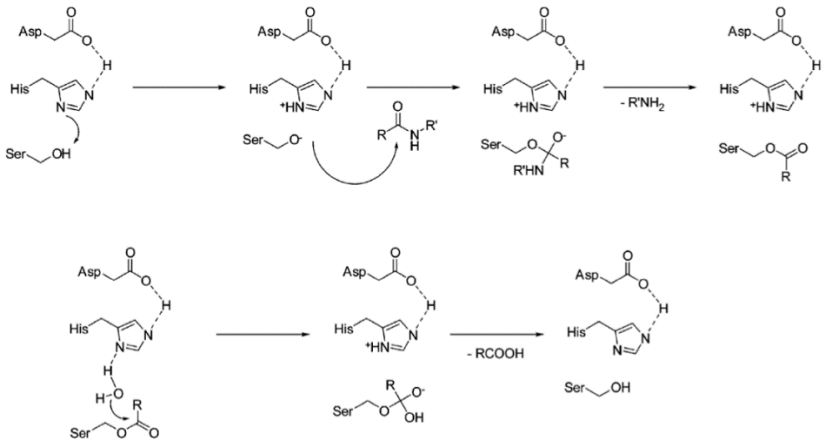

Figure 2-3 Schematic of the mechanism of peptide hydrolysis by serine protease

2.5.3 Immobilized alcalase and applications

Immobilization of alcalase can transfer alcalase into insoluble form that can be recovered for convenient reuse in industrial applications. Table 2-3 shows some commonly methods for immobilizing alcalase, their performance improvements and their applications.

Table 2-3 Different methods used to immobilize alcalase and their applications

Carrier	Reagent	Immobilization method	(Improved) Properties	Applications	Ref
Glass sol-gel matrices	Alkoxysilanes	Entrapment	1) Efficiency of immobilization 68-98%; 2) Amidation activity increased to 1.76 u/mol/h/mg gel. 3) Loading capacity 115mg/g. 4) resusability: 100% activity after 14 cycles. 5) Thermal stability: threefold at 70℃.	Synthesis of C-terminal peptide	91
Carboxyl functionalized magnetic beads	Carbodiimide	Covalent	1) Enzyme activity: 20.55 U/mg; 2) Enzyme loading: 925mg/g. 3) Improved thermal and storage stability. 4) Reusability: 55% activity after 10 cycles.	Hydrolyse egg white protein to reduce allergenicity	92
Chitosan microbeads	None	Adsorption, crosslinking, covalent	1) Highest activity: 23.6 U/mg. 2) Best enzyme loading: 340.2 mg/g (electrostatic extrusion). 3) Highest hydrolysis degree: 29.85 ± 0.967% after 180 min (covalent enzyme bonding)	Potential biocatalysts	93
Monoaminoethyl-N-aminoethyl (MANAE)-agarose beads	GA	Cooperation of covalent and ion exchange	1) Alcalase cannot be immobilized at high ionic strength. 2) Immobilization is relatively rapid at low ionic strength. 3) Using ions exchange theory explain how pH affects the immobilized alcalase stability: pH 9 has the highest activity.	Theoretical research	94
Magnetic chitosan nanoparticles	GA	Crosslinking	1) The activity of immobilized alcalase has been enhanced. 2) The optimum reaction temperature and pH value are 55℃ and 10, compared with the free enzyme, the optimum reaction temperature and pH range are broadened. 3) Thermal stability enhanced. 4) 86% immobilized alcalase activity retains after 10 times usage.	Soy protein isolates hydrolysis	95
Polymer-coated mesoporous silica nanoparticles	None	Adsorption	1) Highest activity for both immobilized and free alcalase at pH 9. 2) Immobilized alcalase more stable than free alcalase under high temperature. 3) Immobilized alcalase has more storage stability compared free alcalase.	A new carrier to immobilizes alcalase	96

Alcalase-inorganic hybrid nanoflowers	None	Mixing alcalase, PBS and $CaCl_2$ to synthesize a nanoflower	Activity of alcalase 1.57 folds higher than free enzyme.	A new method to immobilizes alcalase	97
Sol-gel matrices	None	Adsorption	1) The activity of immobilized alcalase to hydrolyze melinjo seed protein gradually decreased after 2h. 2) After 4 times use, the initial activity was retained.	Synthetic of antioxidant peptides from melinjo seed protein	98

2.6 Lipase

2.6.1 Source and application of lipase

Lipase (triacylglycerol acyl hydrolase EC 3.1.1.3) is a class of enzymes that can hydrolyze insoluble triacylglycerols. It can catalyze a variety of reactions such as hydrolysis, alcoholysis, transesterification, esterification and reverse synthesis of esters[99]. There are a variety of lipases, which can be classified into plant lipases, animal lipases and microbial lipases according to their sources. Plant lipases can be obtained from rapeseed, oats and castor seeds. Animal lipases are mainly derived from the pancreas of cattle, sheep and swine. Microbial lipases can be obtained from bacteria, fungi and yeasts[100,101] and are the main way to obtain lipases because they are easier to obtain than plant and animal lipases.

Lipases are widely used in production of biodiesel, food and pharmaceutical industries, not only for hydrolysis of oils and fats, but also for splitting of chiral compounds, synthesis of biodiesel, and synthesis of structural esters in non-aqueous phase.

2.6.1.1 Production of biodiesel

With the consumption of fossil fuels, the energy crisis is drawing attention. Biodiesel is a mixture of long-chain fatty acid monoesters obtained by transesterification or esterification of waste animal and vegetable oils and fats and broken-chain alcohols. Compared with traditional fossil fuels, the amount of hydrocarbons and fine dust emitted from the combustion of biodiesel is much lower, and the biodiesel has the advantages of being renewable and non-toxic. There are three main ways to synthesize biodiesel: bioenzymatic, acid and alkaline processes. Due to the fast reaction and low production cost, the alkaline method is more commonly used in the industry for biodiesel synthesis. The enzymatic method is gaining attention because of its mild reaction conditions and environmental protection.

2.6.1.2 Food industry

Lipase has a wide range of applications in dairy products, dough, and oil processing. The short-chain fatty acids released by lipase hydrolysis can be used to enhance the flavor of the food itself. By adding lipase to raw dough, the glycerol produced by lipid hydrolysis can improve the freezing resistance of yeast[102,103].

2.6.2 Structure and catalytic mechanism of lipase

The active site of most lipases is covered by a cap-like structure (AKA "lid"), the outer surface of the “lid” is relatively hydrophilic and the inner surface is relatively hydrophobic. However, when the lipase is at the water-oil interface, the "lid" is opened due to interfacial activation, which can expose the active site, resulting in the formation of the enzyme-substrate complex[104,105]. As an illustrative example, the structure of *R. miehei* lipase with the "lid" closed and open is shown in Figure 2-4[106].

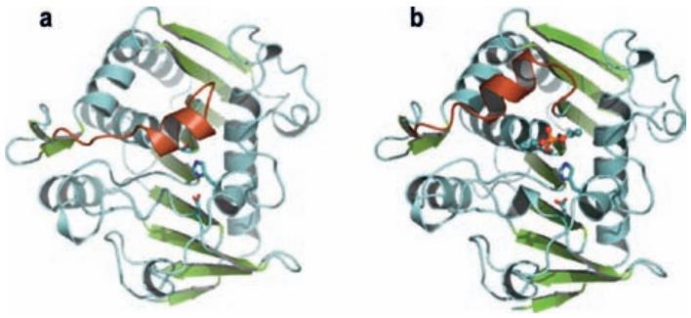

Figure 2-4 The lid closed (a) and open (b) conformation of *R. miehei* lipase (the lid is in brown)

2.6.3 Immobilization of lipase and application

Lipase immobilization is a powerful strategy to overcome the inherent incompatibility between aqueous and oil phases, a challenge that often limits the enzyme's catalytic efficiency in industrial applications. By anchoring lipase onto solid carriers, the enzyme can retain its active conformation and function at the interface of water and oil, effectively bridging the two phases[107]. This interfacial activation enhances lipase's catalytic performance in reactions such as hydrolysis, transesterification, and esterification, which frequently occur in biphasic systems. Additionally, immobilization provides benefits such as improved enzyme stability, reusability, and ease of separation from reaction mixtures, making it a highly practical approach for industrial processes in food, pharmaceuticals, and biofuels. The optimized immobilization process ensures that lipase achieves maximum activity and selectivity, unlocking its full potential in both aqueous and non-aqueous environments[108].

2.7 Dopamine (DA) and polydopamine (PDA) as functional agent

Although there are many methods to modify Fe_3O_4 MNPs, they all have some short comings, such as poor specificity and reduced magnetic property[109]. As a new type of modifying agent, dopamine

may solve these problems to some extent. Dopamine can modify Fe_3O_4 MNPs in two ways, i.e., dopamine (DA) directly modifying Fe_3O_4 MNPs and dopamine self-polymerizing (PDA) on the surface of Fe_3O_4 MNPs[110,111].

2.7.1 Dopamine (DA) as functional agent

Dopamine (DA) is a stable and efficient biomimetic adhesive with good biocompatibility so that it has wide applications in biomaterials[112]. The ortho-phenolic hydroxyl group in the dopamine structure can chelate with Fe ions on the surface of the magnetic nanoparticles, thereby directly link with the Fe_3O_4 MNPs [113,114], the schematic illustration of this mechanism is shown in Figure 2-5[110]. Chen et al. [115] reported that the bidentate enediol ligand in dopamine's structure can convert the surface-coordinated Fe into an octahedral crystal structure of oxygen-coordinated Fe, which enables dopamine to be immobilized on the surface of magnetic nanoparticles firmly.

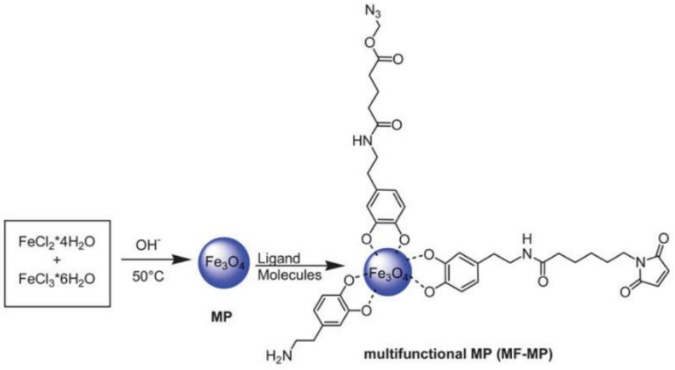

Figure 2-5 Schematic illustration of using different dopamine derivatives to functionalize Fe_3O_4 MNPs

2.7.2 Polydopamine (PDA) as coating agent

The formation of polydopamine (PDA) coating layer requires polymerization and deposition of dopamine molecules. Firstly, the dopamine molecules oxidize and self-polymerize to form PDA agglomerates. These PDA agglomerates can perform Brownian motion in the solution. When they

move to a suitable position, they rely on the interaction force between materials and PDA as the driving force to adhere to the surface of material to form a PDA coating layer.

However, the mechanism of PDA self-polymerization is not clear yet. It is generally believed that dopamine molecules are first oxidized to a quinone structure, and then, the primary amine undergoes intramolecular cyclization through a nucleophilic reaction, and then, undergoes an intramolecular rearrangement reaction to generate 5,6-dihydroxyindole, and finally occurs the polymerization[116–119]. This hypothetical process is shown in Figure 2-6 [120].

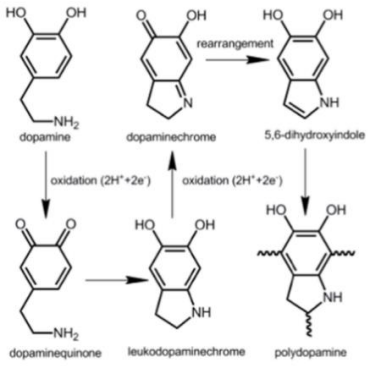

Figure 2-6 Schematic illustration of oxidative self-polymerization mechanism of dopamine

Since the formation mechanism of PDA is uncertain, the structure of PDA is also controversial. Buehler et al. [121], based on molecular dynamics and density functional simulation, proposed that PDA is mainly oligomers such as dimers, trimers and tetramers. Liebscher et al. [122] reported that the molecular chain of PDA is an oligomer formed by the C-C between benzene rings or indole structures, and there are uncyclized amino groups in the PDA. Nicola et al. [123] believed that dopamine will produce carboxyl derivatives during the oxidation process, so there will be carboxyl groups in the final structure of PDA. In conclusion, PDA contains many functional groups, such as amino, carboxyl, indole, and catechol. Precisely because of its complex molecular structure and abundant functional

groups, PDA has shown powerful ability of adhesion and post-functionalization capabilities.

PDA has strong ability of adhesion that generally is non-covalent interactions, such as hydrophobic interactions, chelating coordination interactions, hydrogen bonds, cation-π interactions and π-π interactions. For different materials, PDA could automatically match it using its different functional groups, which may be dominated by a kind of non-covalent force, or it may be a synergistic effect of multiple non-covalent forces. A lot of work has proved that PDA can adhere to the surface of Fe_3O_4 MNPs and form a coating layer, while it can immobilize differently. The two possible polymerization processes of PDA and their resulting products are shown in Figure 2-7.

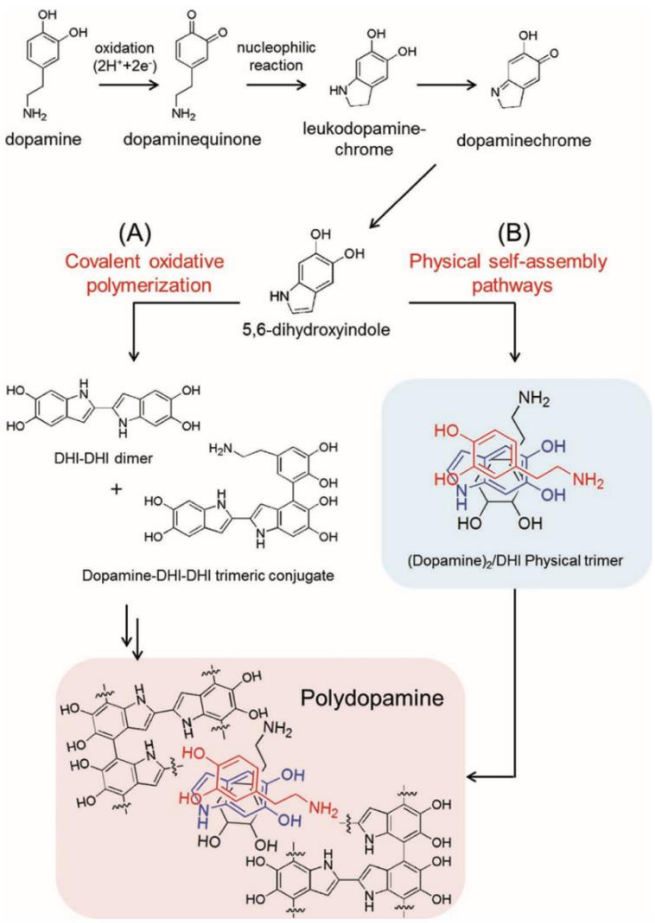

Figure 2-7 Schematic illustration of oxidative self-polymerization and physical self-assembly mechanism of dopamine

Peng et al. [124] used the one-pot chemical polymerization method to synthesise a multi-functional core-shell glucose oxidase-Au-polydopamine-Fe_3O_4 MNPs (GOx-Au-PDA-Fe_3O_4 MBNPs) that can be used as a biosensor to monitor the concentration of glucose. Bi et al.[125] successfully immobilized *Thermomyces lanuginosus* lipase on Fe_3O_4 MNPs that was coated with PDA. They found the immobilized *Thermomyces lanuginosus* lipase showing broader temperature and pH tolerance and, at the meanwhile, better stability compared with free *Thermomyces lanuginosus* lipase. Zhang[126] et al. mixed laccase, DA

and Fe_3O_4 MNPs together to immobilize laccase on Fe_3O_4 MNPs, which can be used for removal 4-chlorophenol. In this research, PDA was not likely playing a role as a coating agent, but more likely as a linking agent. Through this method, the pH range, thermostability, storage ability and relative activity were enhanced compared with free laccase. In summary, because PDA can provide abundant functional groups, strong adhesion ability to Fe_3O_4 MNPs and a simple synthesis method, it can be used as a coating agent, or a linking reagent to immobilize different enzymes on the surface of Fe_3O_4 MNPs.

2.8 Polyethylenimine (PEI) as spacer

2.8.1 PEI as spacer

Polyethyleneimine (PEI) is formed by iminoethylene units and is a kind of widely used cationic polymer, which has a high density of primary (25%), secondary (50%) and tertiary (25%) amino groups[127,128]. Through different synthetic methods, PEI can form linear, branched, network and other structures in different molecular weights, which can affect its physical and chemical properties[129]. The structural formula of iminoethylene and how iminoethylene units to produce branched-PEI via ring-open polymerization are shown in Figure 2-8 [130].

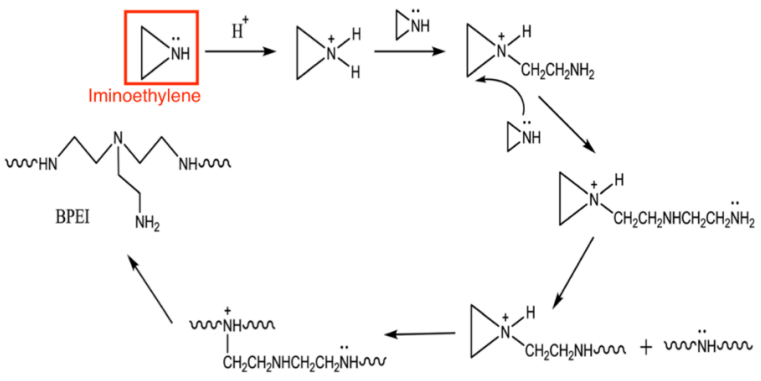

Figure 2-8 Iminoethylene units and standard synthetic route to produce branched-PEI via ring-open polymerization

PEI has a wide range of applications in immobilizing enzymes. First, it can activate the carrier that is used to immobilize enzymes. Secondly, PEI can also immobilize multilayers of enzymes through repeating cross-linking and immobilization reactions several times. In addition, PEI can also improve the physical stability of the ionic polymer carrier[130]. In this proposal, PEI will be used as a length controllable spacer to connect Fe_3O_4 MNPs modified by PDA and enzymes.

Motevalizadeh[131] et al. used PEI-modified Fe_3O_4 MNPs chelated with three different metal ions to immobilize lipase and found that Fe_3O_4@PEI chelated by Co^{2+} is more suitable for immobilizing lipase. Compared with the free enzyme, the storability of the immobilized lipase is improved, and the relative activity is retained at a wider temperature and pH.

Xia[132] et al. used glutaraldehyde (GA) as a cross-linking reagent to graft PEI on the surface of amine-functioned Fe_3O_4 MNPs, and then immobilize iminodiacetic acid (IDA)-Cu^{2+} groups to the Fe_3O_4@PEI, and then studied its adsorption model on bovine hemoglobin (BHb) and bovine serum albumin (BSA). It proves that Fe_3O_4@PEI@ Cu^{2+} has the potential ability to adsorpt proteins[133]. Based on this, she compared the loading capacity of Fe_3O_4@NH_2@PEI@Cu^{2+} and Fe_3O_4@NH_2@Cu^{2+} when immobilizing laccase, and found that using PEI as spacer-arms can increase the loading amount and the enzymatic activity of laccases[134]. How the PEI chain

immobilize laccases via chelated with metal ions is shown in Figure 2-9[134]. She further used Fe_3O_4@NH_2@PEI@Cu^{2+} with different PEI molecular weights to immobilize laccase and explored the best PEI molecular weight under an alternating magnetic field, and then she found that when the molecular weight of PEI is 1200, it has the best enzymatic performance in the bioreactor under alternating magnetic field compared with other molecular weights and under mechanical steering condition.

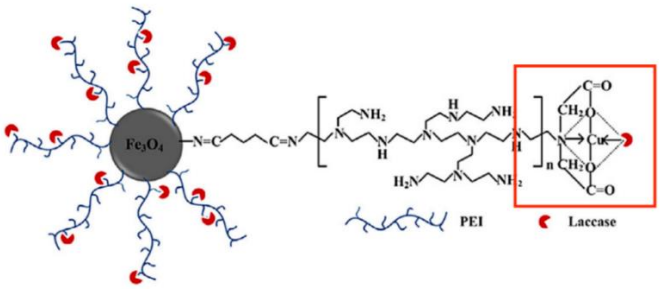

Figure 2-9 Laccase immobilized on PEI chain via chelated with Cu^{2+}

In a series of reported studies, researchers need to firstly modify the surface of Fe_3O_4 MNPs before grafting PEI, the surface modifying reagent that have been proven to be applicable to here are poly (methacrylic acid) (PMAA)[135,136], divinyl sulfone[137] and polyamidoamine (PAMAM) dendrimers[138], and then, through chelation with mental ions to immobilize enzymes. From these works, grafting PEI to Fe_3O_4 MNPs can increase the loading density of enzymes and improve the enzymatic performance.

2.8.2 PEI linked with PDA

PDA as a coating agent can modify the surface of MNPs with functional groups, which help MNPs to link with spacers, such as PEI. In Liu's[139] work, the PEI chain was successfully grafted to the carrier surface that is modified by PDA, which provided the possibility for the research of this proposal. The PEI could crosslink PDA through Michael addition reaction or Schiff base reaction

under oxidizing conditions. In this case, the three-dimensional hierarchical structure of fibrils coated with PDA changed a lot due to the conjugation of PEI. In Zhang's[140] work, it also proved that the PEI can react with PDA, through Michael addition reaction or Schiff base reaction.

2.8.3 PEI grafted on PDA modified Fe_3O_4 MNPs

In referenced research work, there is still no research on grafted PEI branch chains on PDA modified Fe_3O_4 MNPs, and based on it, this thesis will explore immobilizing enzymes on it and test its' enzymatic performance.

2.9 References

1. Bolivar, J. M., Woodley, J. M. & Fernandez-Lafuente, R. Is enzyme immobilization a mature discipline? Some critical considerations to capitalize on the benefits of immobilization. *Chem. Soc. Rev.* **51**, 6251–6290 (2022).
2. Brady, D. & Jordaan, J. Advances in enzyme immobilisation. *Biotechnol. Lett.* **31**, 1639–1650 (2009).
3. Jesionowski, T., Zdarta, J. & Krajewska, B. Enzyme immobilization by adsorption: a review. *Adsorption* **20**, 801–821 (2014).
4. Biodiesel production by lipases co-immobilized on the functionalized activated carbon. *Bioresour Technol Rep* **7**, 100248 (2019).
5. Pore size effect in the amount of immobilized enzyme for manufacturing carbon ceramic biosensor. *Microporous Mesoporous Mater.* **247**, 95–102 (2017).
6. Holyavka, M. G., Kondratyev, M. S., Lukin Anatoly N and Agapov, B. L. & Artyukhov, V. G. Immobilization of inulinase on KU-2 ion-exchange resin matrix. *Int. J. Biol. Macromol.* **138**, 681–692 (2019).
7. A versatile strategy for enzyme immobilization: Fabricating lipase/inorganic hybrid nanostructures on macroporous resins with enhanced catalytic properties. *Biochem. Eng. J.* **139**, 101–108 (2018).
8. Improved immobilization yields by addition of protecting agents in glutaraldehyde-induced immobilization of protease. *J. Biosci. Bioeng.* **89**, 377–379 (2000).
9. Maghraby, Y. R., El-Shabasy, R. M. & Ibrahim Ahmed H and Azzazy, H. M. Enzyme Immobilization Technologies and Industrial Applications. *ACS Omega* **8**, 5184–5196 (2023).
10. Rueda, N. *et al.* Chemical Modification in the Design of Immobilized Enzyme Biocatalysts: Drawbacks and Opportunities. *Chem. Rec.* **16**, 1436–1455 (2016).
11. Gan, J. *et al.* Covalent organic frameworks as emerging host platforms for enzyme immobilization and robust biocatalysis - A review. *Int. J. Biol. Macromol.* **167**, 502–515 (2021).
12. Aghaei, H., Mohammadbagheri, Z., Hemasi, A. & Taghizadeh, A. Efficient hydrolysis of starch by α -amylase immobilized on cloisite 30B and modified forms of cloisite 30B by adsorption and covalent methods. *Food Chem* **373**, 131425 (2022).

13. Bahlawan, R. & Karboune, S. The preparation of two immobilized levansucrase biocatalysts and their application for the synthesis of lactosucrose. *Process Biochemistry* **122**, 248–262 (2022).
14. Mortazavi, S. & Aghaei, H. Make proper surfaces for immobilization of enzymes: Immobilization of lipase and α-amylase on modified Na-sepiolite. *Int J Biol Macromol* **164**, 1–12 (2020).
15. Hu, Y. *et al.* Lipase Immobilization on Macroporous ZIF - 8 for Enhanced Enzymatic Biodiesel Production. 6–11 (2021) doi:10.1021/acsomega.0c05225.
16. Wang, Z. *et al.* Efficient Immobilization of Enzymes on Amino Functionalized MIL-125-NH2 Metal Organic Framework. *Biotechnology and Bioprocess Engineering* **27**, 135–144 (2022).
17. Zhou, J. *et al.* Anti-VEGFR2-labeled enzyme-immobilized metal-organic frameworks for tumor vasculature targeted catalytic therapy. *Acta Biomater* **141**, 364–373 (2022).
18. Bahri, S., Homaei, A. & Mosaddegh, E. Zinc sulfide-chitosan hybrid nanoparticles as a robust surface for immobilization of Sillago sihama α-amylase. *Colloids Surf B Biointerfaces* **218**, 112754 (2022).
19. Cui, J., Cui, L., Jia, S., Su, Z. & Zhang, S. Hybrid Cross-Linked Lipase Aggregates with Magnetic Nanoparticles: A Robust and Recyclable Biocatalysis for the Epoxidation of Oleic Acid. (2016).
20. Wan, W., Lin, Y., Prakash, A. & Zhou, Y. Three-dimensional carbon-based architectures for oil remediation: from synthesis and modification to functionalization. *J. Mater. Chem. A Mater. Energy Sustain.* **4**, 18687–18705 (2016).
21. Barbosa, O. *et al.* Glutaraldehyde in bio-catalysts design: a useful crosslinker and a versatile tool in enzyme immobilization. *RSC Adv.* **4**, 1583–1600 (2013).
22. Purification of a thermostable laccase from Leucaena leucocephala using a copper alginate entrapment approach and the application of the laccase in dye decolorization. *Process Biochem.* **49**, 1196–1204 (2014).
23. Koklukaya, S. Z., Sezer, S., Aksoy, S. & Hasirci, N. Polyacrylamide-based semi-interpenetrating networks for entrapment of laccase and their use in azo dye decolorization. *Biotechnol. Appl. Biochem.* **63**, 699–707 (2016).
24. Muhammad Nasir Iqbal, H. & Asgher, M. Decolorization applicability of sol-gel matrix immobilized manganese peroxidase produced from an indigenous white rot fungal strain Ganoderma lucidum. *BMC Biotechnol.* **13**, 56 (2013).

25. Imam, H. T., Marr, P. C. & Marr, A. C. Enzyme entrapment, biocatalyst immobilization without covalent attachment. *Green Chem.* **23**, 4980–5005 (2021).
26. Immobilization of laccase on phase-change microcapsules as self-thermoregulatory enzyme carrier for biocatalytic enhancement. *Chem. Eng. J.* **405**, 126695 (2021).
27. Encapsulation and immobilization of ficin extract in electrospun polymeric nanofibers. *Int. J. Biol. Macromol.* **118**, 2287–2295 (2018).
28. Mooney, K. E., Jennifer A. Nelson, A. & Wagner*, M. J. Superparamagnetic Cobalt Ferrite Nanocrystals Synthesized by Alkalide Reduction. (2004).
29. Franssen, M. C. R., Steunenberg, P., Scott Elinor L and Zuilhof, H. & Sanders, J. P. M. Immobilised enzymes in biorenewables production. *Chem. Soc. Rev.* **42**, 6491–6533 (2013).
30. Improvement of enzyme activity, stability and selectivity via immobilization techniques. *Enzyme Microb. Technol.* **40**, 1451–1463 (2007).
31. Food enzymes immobilization: novel carriers, techniques and applications. *Curr Opin Food Sci* **43**, 27–35 (2022).
32. Recent advances in enzyme immobilization based on novel porous framework materials and its applications in biosensing. *Coord. Chem. Rev.* **459**, 214414 (2022).
33. Design of composite nanosupports and applications thereof in enzyme immobilization: A review. *Colloids Surf. B Biointerfaces* **217**, 112602 (2022).
34. Magner, E. Immobilisation of enzymes on mesoporous silicate materials. *Chem. Soc. Rev.* **42**, 6213–6222 (2013).
35. Recent advances in nano-carrier immobilized enzymes and their applications. *Process Biochem.* **92**, 464–475 (2020).
36. Ali, M., Husain, Q., Alam, N. & Ahmad, M. Enhanced Catalytic Activity and Stability of Ginger Peroxidase Immobilized on Amino-Functionalized Silica-Coated Titanium Dioxide Nanocomposite: A Cost-Effective Tool for Bioremediation. *Water Air Soil Pollut. Focus* **228**, 1–11 (2016).
37. Dudczig, S., Veres, D., Aneziris, C., Skiera, E. & Steinbrech, R. Nano- and micrometre additions of SiO2, ZrO2 and TiO2 in fine grained alumina refractory ceramics for improved thermal shock performance. *Ceram. Int.* **38**, 2011–2019 (2012).
38. Saengdee, P. *et al.* Surface modification of silicon dioxide, silicon nitride and titanium oxynitride for lactate dehydrogenase immobilization. *Biosens. Bioelectron.* **67**, 134–138 (2015).

39. Progress and perspective of enzyme immobilization on zeolite crystal materials. *Biochem. Eng. J.* **172**, 108033 (2021).
40. Bolivar, J. M., Gascon, V., Marquez-Alvarez Carlos and Blanco, R. M. & Nidetzky, B. Oriented Coimmobilization of Oxidase and Catalase on Tailor-Made Ordered Mesoporous Silica. (2017).
41. Ding, Y. *et al.* Well-oriented bioarchitecture for immobilization of chloroperoxidase on graphene oxide nanosheets by site-specific interactions and its catalytic performance. *J. Mater. Sci.* **52**, 10001–10012 (2017).
42. Graphene and graphene oxide: Functionalization and nano-bio-catalytic system for enzyme immobilization and biotechnological perspective. *Int. J. Biol. Macromol.* **120**, 1430–1440 (2018).
43. Ratanapongleka, K. & Punbut, S. Removal of acetaminophen in water by laccase immobilized in barium alginate. *Environ. Technol.* (2018).
44. Virkutyte, J., Varma, R. S. & Jegatheesan, V. *Treatment of Micropollutants in Water and Wastewater*. (IWA Publishing, 2010).
45. Verma, M. L., Kumar, S., Das, A., Randhawa, J. S. & Chamundeeswari, M. Chitin and chitosan-based support materials for enzyme immobilization and biotechnological applications. *Environ. Chem. Lett.* **18**, 315–323 (2019).
46. Kamdem Tamo, A. *et al.* Biodegradation of Crystalline Cellulose Nanofibers by Means of Enzyme Immobilized-Alginate Beads and Microparticles. *Polymers (Basel)* **12**, 1522 (2020).
47. Wang, Z., Wan, L. & Xu, Z. Immobilization of catalase on electrospun nanofibrous membranes modified with bovine serum albumin or collagen: Coupling site-dependent activity and protein-dependent stability. *Soft Matter* **5**, 4161–4168 (2009).
48. Pore size of macroporous polystyrene microspheres affects lipase immobilization. *J. Mol. Catal. B Enzym.* **66**, 182–189 (2010).
49. Song, M., Yu, H., Gu, J., Ye, S. & Zhou, Y. Chemical cross-linked polyvinyl alcohol/cellulose nanocrystal composite films with high structural stability by spraying Fenton reagent as initiator. *Int. J. Biol. Macromol.* **113**, 171–178 (2018).
50. Ma, L. *et al.* Combination of biochar and immobilized bacteria accelerates polyacrylamide biodegradation in soil by both bio-augmentation and bio-stimulation strategies. *J. Hazard. Mater.* (2020).

51. Casalini, T. *et al.* A Systematic Experimental and Computational Analysis of Commercially Available Aliphatic Polyesters. *NATO Adv. Sci. Inst. Ser. E Appl. Sci.* (2019).
52. Ye, N. *et al.* Metal-Organic Frameworks: A New Platform for Enzyme Immobilization. *Chembiochem* **21**, (2020).
53. Nadar, S. S. & Rathod, V. Magnetic-metal organic framework (magnetic-MOF): A novel platform for enzyme immobilization and nanozyme applications. *Int. J. Biol. Macromol.* **120 Pt B**, 2293–2302 (2018).
54. Aslani, E., Abri, A. & Pazhang, M. Immobilization of trypsin onto Fe3O4@SiO2 -NH2 and study of its activity and stability. *Colloids Surf. B Biointerfaces* **170**, 553–562 (2018).
55. Dedisch, S. *et al.* Matter-tag: A universal immobilization platform for enzymes on polymers, metals, and silicon-based materials. *Biotechnol. Bioeng.* **117**, 49–61 (2020).
56. Fopase, R., Paramasivam, S., Kale, P. & Paramasivan, B. Strategies, challenges and opportunities of enzyme immobilization on porous silicon for biosensing applications. *J Environ Chem Eng* **8**, (2020).
57. He, J. *et al.* Thermostable enzyme-immobilized magnetic responsive Ni-based metal-organic framework nanorods as recyclable biocatalysts for efficient biosynthesis of S-adenosylmethionine. *Dalton Trans. J. Inorg. Chem.* **48 6**, 2077–2085 (2019).
58. Bilal, M., Zhao, Y., Rasheed, T. & Iqbal, H. M. N. Magnetic nanoparticles as versatile carriers for enzymes immobilization: A review. *Int. J. Biol. Macromol.* **120 Pt B**, 2530–2544 (2018).
59. Hosseini, S., Hosseini, S. A., Zohreh, N., Yaghoubi, M. & Pourjavadi, A. Covalent Immobilization of Cellulase Using Magnetic Poly(ionic liquid) Support: Improvement of the Enzyme Activity and Stability. *J. Agric. Food Chem.* **66 4**, 789–798 (2018).
60. Lee, C., Lee, S., Ha, J.-H., Lee Jongman and Song, I. & Moon, K. The Effects of a Zirconia Addition on the Compressive Strength of Reticulated Porous Zirconia-Toughened Alumina. *NATO Adv. Sci. Inst. Ser. E Appl. Sci.* (2021).
61. Mussavi Rizi, S. M. & Ghatee, M. A study of mechanical properties of alumina–zirconia composite films prepared by a combination of tape casting and solution impregnation method. *J. Aust. Ceram. Soc.* **56**, 167–174 (2020).
62. Khan, R. S. *et al.* Recent trends using natural polymeric nanofibers as supports for enzyme immobilization and catalysis. *Biotechnol. Bioeng.* **120**, 22–40 (2022).

63. Wang, J. *et al.* Preparation of magnetic polyacrylamide hydrogel with chitosan for immobilization of glutamate decarboxylase to produce γ-aminobutyric acid. *Prep. Biochem. Biotechnol.* 1–12 (2023).
64. Weng, Y., Dunn, C. B., Qiang, Z. & Ren, J. Immobilization of Protease K with ZIF-8 for Enhanced Stability in Polylactic Acid Melt Processing and Catalytic Degradation. *ACS Appl. Mater. Interfaces* (2023).
65. Samadian, H. *et al.* A tailored polylactic acid/polycaprolactone biodegradable and bioactive 3D porous scaffold containing gelatin nanofibers and Taurine for bone regeneration. *Sci. Rep.* **10**, (2020).
66. Hata, Y., Sawada, T., Sakai, T. & Serizawa, T. Enzyme-Catalyzed Bottom-Up Synthesis of Mechanically and Physicochemically Stable Cellulose Hydrogels for Spatial Immobilization of Functional Colloidal Particles. *Biomacromolecules* **19 4**, 1269–1275 (2018).
67. Maroufi, L. Y. *et al.* Recent Advances of Macromolecular Hydrogels for Enzyme Immobilization in the Food Products. *Adv Pharm Bull* **12**, 309–318 (2021).
68. Erdal, M. & Güngör, S. Electrospun Nanofibers as Carriers in Dermal Drug Delivery. 139–163 (2020).
69. Rather, A. H., Khan, R. S., Wani, T. U., Beigh, M. A. & Sheikh, F. A. Overview on immobilization of enzymes on synthetic polymeric nanofibers fabricated by electrospinning. *Biotechnol. Bioeng.* **119**, 33–39 (2021).
70. Characterization and evaluation of immobilized enzymes for applications in flow reactors. *Curr Opin Green Sustain Chem* **25**, 100349 (2020).
71. Song, Z. *et al.* Dramatically Enhancing the Sensitivity of Immunoassay for Ochratoxin A Detection by Cascade-Amplifying Enzyme Loading. *Toxins (Basel)* **13**, (2021).
72. Li, X., He, Z., Li, C. & Li, P. One-step enzyme kinetics measurement in 3D printed microfluidics devices based on a high-performance single vibrating sharp-tip mixer. *Anal. Chim. Acta* **1172**, (2021).
73. Duan, B. K., Cavanagh, P. E., Li, X. & Walt, D. Ultrasensitive Single-Molecule Enzyme Detection and Analysis Using a Polymer Microarray. *Anal. Chem.* **90 5**, 3091–3098 (2018).
74. Jasensky, J. *et al.* Simultaneous Observation of the Orientation and Activity of Surface-Immobilized Enzymes. *Langmuir* **34 31**, 9133–9140 (2018).

75. Mason, M. *et al.* Calorimetric Methods for Measuring Stability and Reusability of Membrane Immobilized Enzymes. *J. Food Sci.* **83 2**, 326–331 (2018).
76. Hu, X., Yang, J., Chen, C., Khan Habib and Guo, Y. & Yang, L. Capillary electrophoresis-integrated immobilized enzyme microreactor utilizing single-step in-situ penicillinase-mediated alginate hydrogelation: Application for enzyme assays of penicillinase. *Talanta* **189**, 377–382 (2018).
77. On, I. T. IEEE Transactions on Multimedia. *IEEE Transactions on Signal Processing* **54**, 4856–4856 (2006).
78. Wu, S. *et al.* Fe3O4 magnetic nanoparticles synthesis from tailings by ultrasonic chemical co-precipitation. *Mater Lett* **65**, 1882–1884 (2011).
79. Lu, T. *et al.* Surfactant effects on the microstructures of Fe3O4 nanoparticles synthesized by microemulsion method. *Colloids Surf A Physicochem Eng Asp* **436**, 675–683 (2013).
80. Gupta, A. K. & Gupta, M. Synthesis and surface engineering of iron oxide nanoparticles for biomedical applications. *Biomaterials* **26**, 3995–4021 (2005).
81. Wang, X., Zhuang, J., Peng, Q. & Li, Y. A general strategy for nanocrystal synthesis. *Nature* **437**, 121–124 (2005).
82. Deng, H. *et al.* Monodisperse magnetic single-crystal ferrite microspheres. *Angewandte Chemie - International Edition* **44**, 2782–2785 (2005).
83. Karimi, M. Immobilization of lipase onto mesoporous magnetic nanoparticles for enzymatic synthesis of biodiesel. *Biocatal Agric Biotechnol* **8**, 182–188 (2016).
84. Anwar, A. & Saleemuddin, M. Alkaline proteases: A review. *Bioresour Technol* **64**, 175–183 (1998).
85. Yang, A. *et al.* Enzymatic characterisation of the immobilised Alcalase to hydrolyse egg white protein for potential allergenicity reduction. *J Sci Food Agric* **97**, 199–206 (2017).
86. Jung, T. H. *et al.* Hydrolysis by alcalase improves hypoallergenic properties of goat milk protein. *Korean J Food Sci Anim Resour* **36**, 516–522 (2016).
87. Wang, Z. *et al.* Reduction of the allergenic protein in soybean meal by enzymatic hydrolysis. *Food Agric Immunol* **25**, 301–310 (2014).
88. Guérard, F., Dufossé, L., De La Broise, D. & Binet, A. Enzymatic hydrolysis of proteins from yellowfin tuna (Thunnus albacares) wastes using Alcalase. *J Mol Catal B Enzym* **11**, 1051–1059 (2001).
89. Margelefsky, E. L., Zeidan, R. K. & Davis, M. E. Cooperative catalysis by silica-supported organic functional groups. *Chem Soc Rev* **37**, 1118–1126 (2008).

90. Hussain, F. *et al.* Further stabilization of alcalase immobilized on glyoxyl supports: Amination plus modification with glutaraldehyde. *Molecules* **23**, 1–15 (2018).
91. Corîci, L. N. *et al.* Sol-gel immobilization of Alcalase from Bacillus licheniformis for application in the synthesis of C-terminal peptide amides. *J Mol Catal B Enzym* **73**, 90–97 (2011).
92. Yang, A. *et al.* Enzymatic characterisation of the immobilised Alcalase to hydrolyse egg white protein for potential allergenicity reduction. *J Sci Food Agric* **97**, 199–206 (2017).
93. Žuža, M. G. *et al.* Design and characterization of alcalase–chitosan conjugates as potential biocatalysts. *Bioprocess Biosyst Eng* **40**, 1713–1723 (2017).
94. Ait Braham, S. *et al.* Cooperativity of covalent attachment and ion exchange on alcalase immobilization using glutaraldehyde chemistry: Enzyme stabilization and improved proteolytic activity. *Biotechnol Prog* **35**, 1–4 (2019).
95. Wang, S. nan *et al.* Immobilized alcalase alkaline protease on the magnetic chitosan nanoparticles used for soy protein isolate hydrolysis. *European Food Research and Technology* **239**, 1051–1059 (2014).
96. Özbek, B. & Ünal, Ş. Preparation and characterization of polymer-coated mesoporous silica nanoparticles and their application in Subtilisin immobilization. *Korean Journal of Chemical Engineering* **34**, 1992–2001 (2017).
97. Memon, A. H., Ding, R., Yuan, Q., Wei, Y. & Liang, H. Facile synthesis of alcalase-inorganic hybrid nanoflowers used for soy protein isolate hydrolysis to improve its functional properties. *Food Chem* **289**, 568–574 (2019).
98. Siswoyo, T. A., Matra, N. F., Safiera, A. A. & Supriyadi, A. Synthesis of antioxidant peptides from Melinjo (Gnetum gnemon) seed protein isolated using sol-gel immobilized alcalase. *Int J Adv Sci Eng Inf Technol* **7**, 1315–1321 (2017).
99. Villeneuve, P., Muderhwa, J. M., Graille, J. & Haas, M. J. Customizing lipases for biocatalysis: A survey of chemical, physical and molecular biological approaches. *J Mol Catal B Enzym* **9**, 113–148 (2000).
100. Choudhury, P. & Bhunia, B. Review Article Industrial Application of Lipase : a Review. *Biopharm Journal* **1**, 41–47 (2015).
101. Singh, A. K. & Mukhopadhyay, M. Overview of fungal lipase: A review. *Appl Biochem Biotechnol* **166**, 486–520 (2012).
102. Izawa, S., Sato, M., Yokoigawa, K. & Inoue, Y. Intracellular glycerol influences resistance to freeze stress in Saccharomyces cerevisiae: Analysis of a quadruple mutant

in glycerol dehydrogenase genes and glycerol-enriched cells. *Appl Microbiol Biotechnol* **66**, 108–114 (2004).

103. Yadav, D. N., Patki, P. E., Khan, M. A., Sharma, G. K. & Bawa, A. S. Effect of freeze-thaw cycles and additives on rheological and sensory properties of ready to bake frozen chapaties. *Int J Food Sci Technol* **43**, 1714–1720 (2008).
104. Schrag, J. D. *et al.* The open conformation of a Pseudomonas lipase. *Structure* **5**, 187–202 (1997).
105. Cygler, M. & Schrag, J. D. Structure and conformational flexibility of Candida rugosa lipase. *Biochim Biophys Acta Mol Cell Biol Lipids* **1441**, 205–214 (1999).
106. Angkawidjaja, C. & Kanaya, S. Family I.3 lipase: Bacterial lipases secreted by the type I secretion system. *Cellular and Molecular Life Sciences* **63**, 2804–2817 (2006).
107. Asaduzzaman, F. & Salmon, S. Enzyme immobilization: polymer-solvent-enzyme compatibility. *Mol Syst Des Eng* **7**, 1385–1414 (2022).
108. Ismail, A. R. & Baek, K. H. Lipase immobilization with support materials, preparation techniques, and applications: Present and future aspects. *Int J Biol Macromol* **163**, 1624–1639 (2020).
109. Xu, C. *et al.* Dopamine as a robust anchor to immobilize functional molecules on the iron oxide shell of magnetic nanoparticles. *J Am Chem Soc* **126**, 9938–9939 (2004).
110. Mazur, M. *et al.* Iron oxide magnetic nanoparticles with versatile surface functions based on dopamine anchors. *Nanoscale* **5**, 2692–2702 (2013).
111. Deng, Y. *et al.* Preparation of iron-based MIL-101 functionalized polydopamine@Fe3O4 magnetic composites for extracting sulfonylurea herbicides from environmental water and vegetable samples. *J Sep Sci* **41**, 2046–2055 (2018).
112. Goldmann, A. S. *et al.* Biomimetic mussel adhesive inspired clickable anchors applied to the functionalization of Fe3O4 nanoparticles. *Macromol Rapid Commun* **31**, 1608–1615 (2010).
113. Pawar, S. P., Marathe, D. A., Pattabhi, K. & Bose, S. Electromagnetic interference shielding through MWNT grafted Fe3O4nanoparticles in PC/SAN blends. *J Mater Chem A Mater* **3**, 656–669 (2015).
114. Yuen, A. K. L., Hutton, G. A., Masters, A. F. & Maschmeyer, T. The interplay of catechol ligands with nanoparticulate iron oxides. *Dalton Transactions* **41**, 2545–2559 (2012).

115. Chen, L. X., Liu, T., Thurnauer, M. C., Csencsits, R. & Rajh, T. Fe2O3 nanoparticle structures investigated by X-ray absorption near-edge structure, surface modifications, and model calculations. *Journal of Physical Chemistry B* **106**, 8539–8546 (2002).
116. Bernsmann, F. *et al.* Dopamine-melanin film deposition depends on the used oxidant and buffer solution. *Langmuir* **27**, 2819–2825 (2011).
117. Ding, Y. *et al.* Insights into the Aggregation/Deposition and Structure of a Polydopamine Film. *Langmuir* **30**, 12258–12269 (2014).
118. Jiang, J., Zhu, L., Zhu, L., Zhu, B. & Xu, Y. Surface characteristics of a self-polymerized dopamine coating deposited on hydrophobic polymer films. *Langmuir* **27**, 14180–14187 (2011).
119. Hong, S. *et al.* Non-covalent self-assembly and covalent polymerization co-contribute to polydopamine formation. *Adv Funct Mater* **22**, 4711–4717 (2012).
120. Yang, H. C., Luo, J., Lv, Y., Shen, P. & Xu, Z. K. Surface engineering of polymer membranes via mussel-inspired chemistry. *J Memb Sci* **483**, 42–59 (2015).
121. Chen, C. T., Martin-Martinez, F. J., Jung, G. S. & Buehler, M. J. Polydopamine and eumelanin molecular structures investigated with ab initio calculations. *Chem Sci* **8**, 1631–1641 (2017).
122. Liebscher, J. *et al.* Structure of polydopamine: A never-ending story? *Langmuir* **29**, 10539–10548 (2013).
123. Della Vecchia, N. F. *et al.* Building-block diversity in polydopamine underpins a multifunctional eumelanin-type platform tunable through a quinone control point. *Adv Funct Mater* **23**, 1331–1340 (2013).
124. Peng, H. P., Liang, R. P., Zhang, L. & Qiu, J. D. Facile preparation of novel core-shell enzyme-Au-polydopamine-Fe3O4 magnetic bionanoparticles for glucose sensor. *Biosens Bioelectron* **42**, 293–299 (2013).
125. Bi, Y. *et al.* Improved catalytic properties of Thermomyces lanuginosus lipase immobilized onto newly fabricated polydopamine-functionalized magnetic Fe3O4 nanoparticles. *Processes* **8**, (2020).
126. Zhang, D., Deng, M., Cao, H., Zhang, S. & Zhao, H. Laccase immobilized on magnetic nanoparticles by dopamine polymerization for 4-chlorophenol removal. *Green Energy and Environment* **2**, 393–400 (2017).
127. Brissault, B. *et al.* Synthesis of linear polyethylenimine derivatives for DNA transfection. *Bioconjug Chem* **14**, 581–587 (2003).

128. Samal, S. K. *et al.* Cationic polymers and their therapeutic potential. *Chem Soc Rev* **41**, 7147–7194 (2012).
129. Yang, Q. & Runge, T. Polyethylenimines as Homogeneous and Heterogeneous Catalysts for Glucose Isomerization. *ACS Sustain Chem Eng* **4**, 6951–6961 (2016).
130. Virgen-Ortíz, J. J. *et al.* Polyethylenimine: A very useful ionic polymer in the design of immobilized enzyme biocatalysts. *J Mater Chem B* **5**, 7461–7490 (2017).
131. Motevalizadeh, S. F. *et al.* Lipase immobilization onto polyethylenimine coated magnetic nanoparticles assisted by divalent metal chelated ions. *J Mol Catal B Enzym* **120**, 75–83 (2015).
132. Xia, T. T., Lin, W., Liu, C. Z. & Guo, C. Improving catalytic activity of laccase immobilized on the branched polymer chains of magnetic nanoparticles under alternating magnetic field. *Journal of Chemical Technology and Biotechnology* **93**, 88–93 (2018).
133. Xia, T. *et al.* Synthesis of polyethylenimine modified Fe3O4 nanoparticles with immobilized Cu2+ for highly efficient proteins adsorption. *Colloids Surf A Physicochem Eng Asp* **443**, 552–559 (2014).
134. Xia, T. T., Liu, C. Z., Hu, J. H. & Guo, C. Improved performance of immobilized laccase on amine-functioned magnetic Fe3O4 nanoparticles modified with polyethylenimine. *Chemical Engineering Journal* **295**, 201–206 (2016).
135. Zhang, L., Wang, B., Wang, S. & Zhang, W. Recyclable trypsin immobilized magnetic nanoparticles based on hydrophilic polyethylenimine modification and their proteolytic characteristics. *Analytical Methods* **10**, 459–466 (2018).
136. Cao, Y. P. *et al.* PEI-crosslinked lipase on the surface of magnetic microspheres and its characteristics. *Colloids Surf B Biointerfaces* **189**, 110874 (2020).
137. Bezerra, R. M. *et al.* A new heterofunctional support for enzyme immobilization: PEI functionalized Fe3O4 MNPs activated with divinyl sulfone. Application in the immobilization of lipase from Thermomyces lanuginosus. *Enzyme Microb Technol* **138**, 109560 (2020).
138. Zhao, P. *et al.* Effect of the Structure and Length of Flexible Chains on Dendrimers Grafted Fe3O4@SiO2/PAMAM Magnetic Nanocarriers for Lipase Immobilization. *ACS Sustain Chem Eng* **4**, 6382–6390 (2016).
139. Liu, M. *et al.* Fast and robust lead (II) removal from water by bioinspired amyloid lysozyme fibrils conjugated with polyethyleneimine (PEI). *Chemical Engineering Journal* **390**, 124667 (2020).

140. Zhang, S., Jiang, Z., Zhang, W., Wang, X. & Shi, J. Polymer-inorganic microcapsules fabricated by combining biomimetic adhesion and bioinspired mineralization and their use for catalase immobilization. *Biochem Eng J* **93**, 281–288 (2015).

Chapter 3 Immobilization of alcalase on polydopamine modified magnetic particles[#]

Xinyue Wang, Hongying Zhou, Zitong Xu, Huan Wu, Jason Zhang, Christopher Q. Lan*

Department of Chemical and Biological Engineering

University of Ottawa

The content of this chapter was published as a peer-reviewed articlel: X. Wang, H. Zhou, Z. Xu, H. Wu, J. Zhang, C. Q. Lan. Immobilization of alcalase on polydopamine modified magnetic particles, *Biochem Eng J*. 207 (2024) 109310

3.1 Abstract

Enzymes play a crucial role in medicine, industry, and agriculture. Alcalase, a protease, has found wide-ranging applications in both the detergent and food industries. Immobilizing enzymes has gained prominence as a technology to enhance enzyme stability and reusability, and magnetic particles (MP) have emerged as promising carriers for enzyme immobilization due to their magnetic properties and ease of synthesis. In our study, we propose a novel approach that utilizes polydopamine-modified magnetic particles (MPP) as carriers for immobilizing alcalase. The immobilization process entails modifying the magnetic particles with polydopamine and functionalizing them with glutaraldehyde (GA). We conducted experiments to determine the optimal conditions for alcalase immobilization. These conditions were identified as a pH of 7.5, a GA concentration of 0.23 μg/mL, an alcalase concentration of 6.1 mg/mL, and an immobilization time of 4 hours. The immobilized alcalase significantly improved its temperature and pH stability. Furthermore, kinetic studies of the immobilized enzyme were conducted, revealing that while the Michaelis constant ($K_{m)}$ remained unaffected, there was a decrease in the maximum velocity (V_{max}). After 14 repeated uses, it retained 78.66% of its relative activity. This innovative strategy not only enhances our understanding of enzyme immobilization techniques but also offers new avenues for leveraging enzymes in a multitude of applications.

Key Words: Alcalase, enzyme immobilization, polydopamine, glutaraldehyde, cross-linker

Graphic Abstract

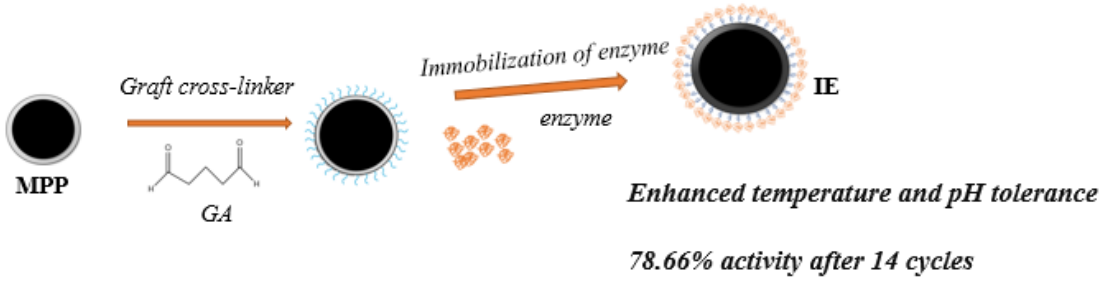

3.2 Introduction

Enzyme immobilization has been established as a technology that could vastly enhance the performance of enzymes. Immobilized enzymes (IE) offer some unique advantages such as better stability, operability, and convenient separation from the reaction system, which enables reuse of enzymes and precise control of the extent of reaction[1]. There are two types of enzyme immobilization methods: self cross-linking and carrier-based immobilization, with the latter being much more versatile and widely adopted. Among the numerous carriers used for enzyme immobilization[2], magnetic particles (MP) have gained popularity since they enable convenient separation of IE from reaction system[3] and can be acquired by relatively cost-effective synthesis methods at the desired particle size, providing flexibility to suit the requests of process control[4].

Immobilization of enzymes onto magnetic materials requires the modification of MP to introduce functional groups on to MP surface. This is commonly achieved using agents such as SiO_2[5], organic silanes[6], citric acid[7], chitosan[8], and polydopamine (PDA)[9]. Among them, PDA has minimal impact on the magnetic properties of magnetic particles, good biocompatibility, and excellent adhesion capability. It contains multiple functional groups, such as amino, carboxyl, indole, and catechol and has shown versatile post-functionalization capabilities [10, 11, 12].

Alcalase is a protease that has been successfully employed in a large variety of different fields including the detergent industry to remove protein-based stains and the food industry[13,14,15] for hydrolysis of proteins to enhance productivity, digestibility, stability, and solubility as well as reduced allergenicity of products. For instance, it has been used to produce peptides from wastes from dairy (i.e., cheese whey)[16], agricultural (e.g., soymeal)[17] and fishery sources[18] to enhance both the recovery and the value of the products.

Owning to its commercial significance, a variety of surface modification approaches have been investigated for the immobilization of alcalase onto MP, including aminopropyl trimethoxysilane,

Jeffamine, and chitosan[19,20]. However, to our best knowledge, no studies have been reported on the use of PDA modified MP for alcalase immobilization, even though it has been adopted for many other enzymes[23]. In this research, we employed for the first time a straightforward approach to immobilize alcalase on PDA-coated MP and investigated the effects of a few key conditions, including immobilization time, temperature, pH, and initial enzyme concentration, on the effectiveness of this approach. The carriers at different stages and the IE were characterized in terms of morphology, surface chemistry, and enzymatic performance.

3.3 Materials and methods

3.3.1 Materials

Alcalase 2.4 L (protease from *Bacillus licheniformis*), Azo-casein and Bradford reagent were purchased from Sigma-Aldrich Inc., St. Louis, MO. Bovine serum albumin (BSA) was purchased from Thermo-Scientific, Rockford, IL. Glutaraldehyde solution (25%) was obtained from Electron Microscopy Sciences, Hatfield, PA. Sodium acetate anhydrous were obtained from VWR Life science, Solon, Ohio. Iron (III) chloride hexahydrate, ethylene glycol, Tris-base and phosphate buffered saline (10× solution) were purchased from Fisher Scientific.

3.3.2 Immobilization of alcalase on magnetic particles

As shown in Figure 3-1, the immobilization of alcalase was carried out in the following steps, i.e., 1) coating the PDA layer onto the MPs surface to produce PDA modified MPs (MPPs); 2) grafting cross linking agent glutaraldehyde (GA) on to the functionalized surface of MPP as spacer to produce MPP grafted with glutaraldehyde (MPPG); and 3) immobilizing alcalase onto MPPG through Schiff reaction between the amino groups of alcalase and the aldehyde groups of GA residues to produce the IEs.

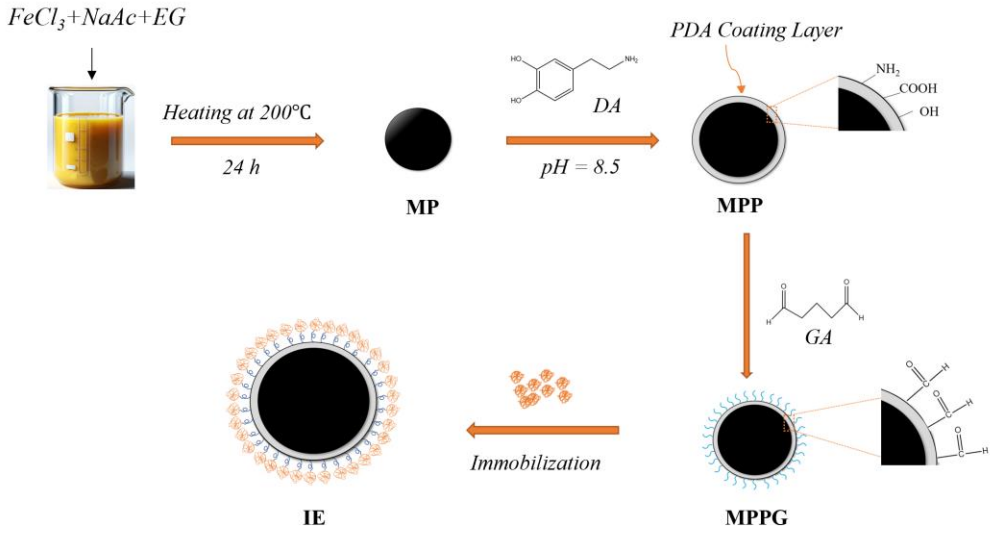

Figure 3-1 Enzyme immobilization process

3.3.2.1 Synthesis of magnetic particle (MP)

The MPs were synthesized using the modified classic solvothermal reduction method and co-precipitation method[21]. For the solvothermal reduction method, $FeCl_3 \cdot 6H_2O$（2.7 g）was dissolved in 80 ml ethylene glycol and stir for 30 minutes to form a yellow opaque solution. Then 3.6 g of sodium acetate was added to the solution and continue to stir for 30 minutes to form a yellow homogeneous solution, which was transferred into a 100 ml Teflon-lined stainless-steel autoclave and heated 200 °C for 24 h to synthesis MPs. The mixture was cooled to room temperature and washed it for 3 times with anhydrous alcohol, then dried it under vacuum at 40°C, and stored at 4°C.

3.3.2.2 MP coated with polydopamine (MPP)

The MPPs were prepared by self-polymerization of dopamine onto the MP surface. Briefly, 2 g of the MPs obtained in the above experiment, were washed twice using Tris-HCl (pH 8.5, 20 mM) solution, suspended in 80 ml Tris-HCl (pH 8.5, 20 mM) solution, and homogenized using an ultra-

sonification bath (model, manufacturer) for 30 min[22]. Then, 20 m of 10 mg/ml dopamine stock solution was added into the MP suspension and homogenized again before being incubated at 25°C for 18 h. The coated MPs, i.e., MPPs, were separated by centrifugation at 13000 rpm and washed three times with deionized water and dried in a vacuum oven at 40 ºC overnight. The dried MPPs were stored at 4°C for later use.

3.3.2.3 MPP grafted with GA (MPPG)

MPPs (0.01g) were weighed and transferred to a 2 ml tube where 1 mL of 10 mM PBS (pH 7.4) was added, and the solution was ultrasonicated for 30 min to disperse the particles. After dispersion, the appropriate amount of GA (25% wt)was added, the solution was mixed, and incubated on a shaker at 250 rpm and room temperature (20°C) for 3 h. The MPPGs were centrifuged and washed with deionized water 3 times and then store the MPPG in deionized water at 4 ºC for later use.

3.3.2.4 Immobilization of alcalase on MPPG to produce IE

For the immobilization of alcalase, 10 mg MPPGs were mixed with 1 mL alcalase solution and incubated for 4 hours at 250 rpm and 40°C. Then, the mixture was centrifuged at 13000 rpm for solid-liquid separation. The supernatant was drained and collected, and the particles were repeatedly washed with 10 mM PBS solution until no protein could be detected in the supernatant. All supernatants obtained from the washing of the immobilized enzyme (IE) were collected and then stored in a fridge at 4°C for further analysis of protein concentration.

3.3.2.5 Characterizations of MP and MPP

The crystallographic structure and surface chemistry of the synthesized MPs were characterized by powder X-ray diffraction (XRD). The morphologies of MPs and IE were examined using scanning

electron microscopy (SEM, model JSM-7500F) and the diameter of particles determined by analyzing the SEM micrographs using Image J software. Fourier Transform Infra-Red spectroscopy (FT-IR, Agilent Cary 630 FT-IR spectrometer) was used to investigate the functional groups on the surface of the MPs and MPPs. The magnetization of MP and MPP was characterized at room temperature with a vibrating sample magnetometer (VSM).

3.3.3 Determination of protein concentration, enzyme loading density, enzyme activity and kinetic parameters

3.3.3.1 Protein concentration

Protein concentration was determined using Bradford method with BSA as the standard[23].

Deionized water was used to prepare BSA standard solution with a concentration range of up to 2.0 mg/mL as stock. 20 uL of each BSA standard was mixed with 1 mL of Coomassie Brilliant Blue G-250 solution, incubating the mixture at room temperature for 5 minutes, and then measure the absorbance at 595 nm using spectrophotometer. The convert factor was determined to be 2.522 mg BSA/L per OD_{595} unit.

3.3.3.2 Loading density of enzymes

The Bradford method as described above was used to determine the loading density of enzymes onto the MPPs. Briefly, 20 µL samples diluted appropriately were mixed with 1 ml of Coomassie Brilliant Blue G-250 solution. OD_{595} was measured after incubation for 5 minutes at room temperature. The loading density of IE was calculated by the following equation：

$$q = \frac{(C_0V_0 - CV)}{m} \qquad (1)$$

where q is the mass of enzyme per unit mass of IE (mg/g), C_0 (mg/mL) and V_0 (mL) the initial enzyme concentration and volume of the enzyme solution used in immobilization, V (mL) and C (mg/mL) represent the total volume of the supernatant collected during the washing steps of the IE

and the protein concentration determined using the Bradford method, respectively, and *m* the mass of MPPs (g).

3.3.3.3 Assay of enzyme activity

The activity of free alcalase and IE was determined using azo-casein as the substrate for enzymatic hydrolysis[24]. Azo-casein, which is casein protein conjugated with azo dye, liberates soluble chromogenic peptides with azo (-N=N-) bonds upon hydrolysis by alcalase. The absorbance of these peptides can be measured by a spectrophotometer. By monitoring the change in absorbance at a specific wavelength, the protease activity can be quantitatively analyzed. The measurement steps are as follows: Initially, 1 mL of 6 wt% azo-casein buffered in 0.1 M PBS at pH 8.5 was mixed with either 10 μL of free enzyme solution or 10 mg of IE and then incubated for 30 minutes at 40°C on a shaker at 250 rpm. Subsequently, 0.5 mL of 10% trichloroacetic acid solution was added to quench the reaction by denaturing the unhydrolyzed azo-casein, which was then separated from the supernatant by centrifugation at 13000 rpm for 10 minutes. The absorbance of the chromogenic peptides in the supernatant was measured, and the activity of the tested alcalase was determined by comparing it to a standard curve. The standard curve was established by measuring alcalase of known activity. The supernatant was subject to measurement of optical density at 430 nm (i.e., OD_{430}). The enzymatic activity per gram of IE was calculated using the following equations:

$$Activity\ (AU/g) = \frac{OD_{430}}{0.0263 \times m} \qquad (2)$$

where 0.0263 is a conversion factor, which was pre-determined as the slope of the linear section of a standard curve, and *m* (mg) the mass of IE.

The specific enzymatic activity of free enzymes and IE were calculated using the following equations:

For FE:

$$Specific\ activity\ (AU/mg) = \frac{Activity}{C \times V} \qquad (3)$$

where *C* is the concentration of enzymatic proteins in sample and *V* the volume of enzyme solution. For IE:

$$Specific\ activity\ \left(\frac{AU}{mg}\right) = \frac{Activity}{Loading\ density} \qquad (4)$$

Activity retention refers to the percentage of the specific activity of alcalase that was retained after immobilization. It quantifies how much of the enzyme's initial catalytic capability was preserved following the immobilization process. The activity retention was calculated using the following formula:

$$Activity\ Rentention\ (\%) = (\frac{Specific\ Activity\ of\ IE}{Specfic\ Activity\ of\ FE}) \times 100 \qquad (5)$$

This formula compares the specific activity (activity per unit mass of enzyme) of the immobilized alcalase to that of the free enzyme, providing a percentage that represents the efficiency of the immobilization technique in retaining the enzyme's functional activity.

3.3.3.4 Kinetics of enzymatic reaction

Kinetic studies involved using azo-casein as the substrate, with concentrations of 2.5, 5.0, 10, 15, 20, 30, and 40 g/L, in a 0.2 M Tris-HCl buffer, incubating the IEs at 40°C and measuring the initial enzymatic reaction velocities. For each substrate concentration, four samples were prepared so that the velocity could be measured at four time intervals, i.e., 1, 2, 3, and 4 minutes, one sample for each sampling time. The kinetic data were collected and fitted to the Michaelis-Menten equation to determine the Michaelis constant (*Km*) and the maximum velocity (*Vmax*).

$$V = \frac{V_{max} \cdot S}{K_m + S} \qquad (6)$$

Where V is the enzymatic reaction velocity ($mM \cdot min^{-1}$), which is characterized by the rate of increase in azo-casein concentration in the reaction mixture as a function of substrate concentration (S, mM).

3.3.4 Characterizations

3.3.4.1 Optimum temperature and pH range of FE and IE

To determine the influence of temperature on the enzymatic activity, the activities of both the FE and IE were tested at temperatures ranging from 20 to 60℃ at pH 7.5. To characterize the pH adaptation and stability, enzymatic activity was assayed at different pH ranging from 6.5 to 10.5 at 40^{o}C. The highest activities of both FE and IE within the tested temperature and pH range used to normalize the data, and the optimal pH and temperature ranges were determined by comparing the variations in relative activity values within this tested temperature and pH range.

3.3.4.2 Thermal stability, storage stability and reusability of FE and IE

To test the thermal stability of the immobilized alcalase and free alcalase, the two types of enzymes were stored at different temperatures (20, 30, 40, 50, 60, 70℃) for 48 h before determining their enzymatic activities. The initial enzymatic activities of both IE and FE, represented by the highest values observed in the results, were set as 100%. To evaluate storage stability, FE and IE were stored at their respective optimal conditions (pH 8.5) and temperatures for 2, 4, 8, and 10 hours. Samples were then collected at these time intervals to measure their residual enzymatic activities. The initial activity of each enzyme was defined as 100%. The storage stability over time was expressed as a series of relative activity values, calculated as the measured activity of IE and FE at each time point divided by their respective initial activity values. These relative activity values were used to track changes in storage stability as a function of storage duration.

The reusability of IEs was investigated by repeat use of the IEs synthesized under optimal conditions for up to 14 cycles. To initiate the first cycle, 1 mL azo-casein was incubated with 10 mg IE at 40 ºC for 30 min at 250 rpm. The IE was magnetically recovered and washed with 1 mL PBS and then being incubated with fresh 1 mL azo-casein solution for the next cycle. The absorbance (430 nm) of the supernatant from the end of each cycle was measured to determine the enzyme activity. The initial activity of IE was set to be 100% and the activity of IE from each cycle was normalized to the initial activity to obtain the relative activity of IE after each cycle.

3.4 Results and Discussions

3.4.1 Characterization of carrier

3.4.1.1 XRD pattern of MP surface

The XRD pattern of the Fe_3O_4 MP synthesized via the solvothermal method is shown in Figure 3-2. Six characteristic peaks were found at 2θ=30.1, 35.4, 43.1, 53.4, 57 and 62.5°, which are assigned to the crystal plane: (2 2 0), (3 1 1), (4 0 0), (4 2 2), (5 1 1) and (4 4 0).These peaks align with the standard pattern for Fe_3O_4, indicating that the Fe_3O_4 cubic spinel structure was successfully synthesized[25].

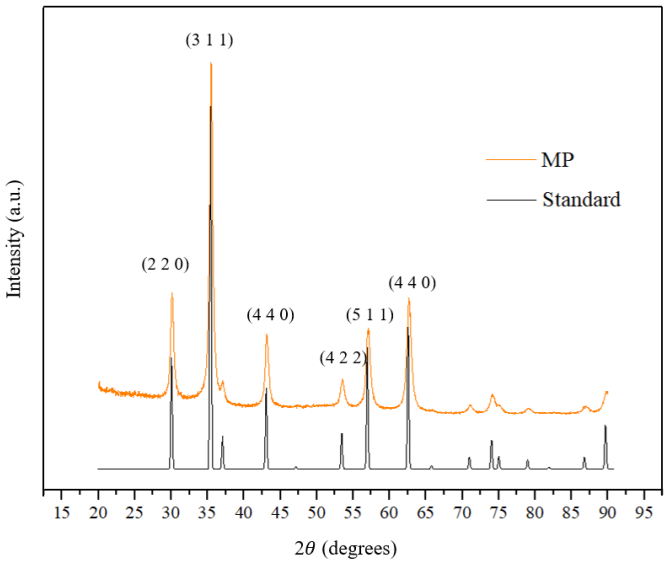

Figure 3-2 XRD pattern of Fe_3O_4 MP surface

3.4.1.2 Magnetic property

Magnetic properties of MP and MPP were studied using a vibrating sample magnetometer (VSM). As shown in Figure 3-3, the S-shaped magnetization curves with zero coercivity and remanent magnetization confirm the superparamagnetic nature of the synthesized MP and MPP. Furthermore, due to the PDA coating enveloping the surface of MP, the functionalization at the magnetic nanoparticle surface resulted in a reduction in the saturation magnetization values, with the naked MP and MPP exhibiting saturation magnetization values of 83.3 and 62.1 emu/g, respectively. This finding aligns with the results from previous studies. For instance, Oroujeni et al. [26] modified MPs with PDA and 6-thio-β-cyclodextrin, resulting in saturation magnetization values of 76 and 66 emu/g for bare MPs and modified MPs, respectively. Ghani et al. [27] reported the saturation magnetization values of the bare MPs and MPPs as 60 and 20 emu/g, respectively. While the saturation magnetization values of MPs may differ in studies due to factors such as synthesis methods, particle size, chemical properties and thickness of coating, lattice defects, and impurities,

a common observation is that the presence of the PDA coating layer consistently results in reduced saturation magnetization values.

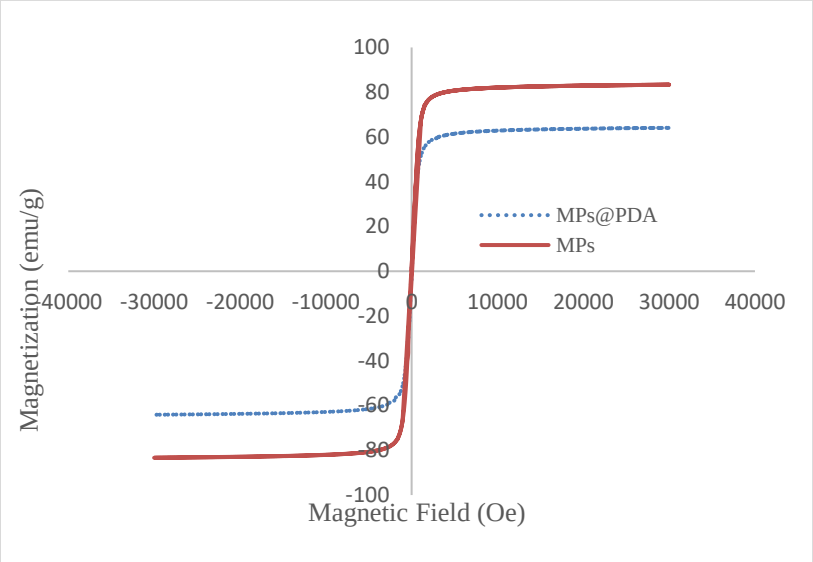

Figure 3-3 VSM analysis of MP and MPP

3.4.1.3 Morphology of MP

Figure 3-4 shows the SEM images of Fe_3O_4 particles synthesized using two different methods, the co-precipitation method and the solvothermal method, as well as MPP immobilized with alcalse. The Fe_3O_4 particles synthesized using the co-precipitation method had irregular shape and uneven size (Figure 3-4a) while the particles obtained by the solvothermal methods were spheres with an average size of about 660 nm (Figure 3-4b). These results are compatible with those in the literature [21, 28]. The more uniform Fe_3O_4 particles synthesised by the solvothermal method was used as carrier in this paper. The morphological characterization of the enzyme immobilized on MPPG is shown in Figure 3-4c. The average diameter of the MPPs immobilized with alcalase was determined to be 663 nm, which is very close to that of the original MPs. In the meantime, the IE maintained a smooth and regular spherical shape, indicating that immobilizing alcalase does not alter the morphology of the MPs carriers.

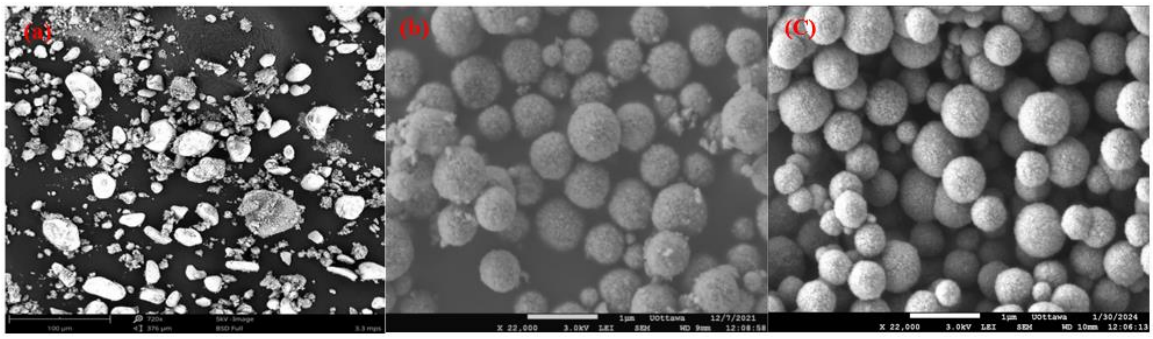

Figure 3-4 SEM images of MPs synthesized by (a) co-precipitation method; (b) solvothermal method, and (c) with alcalase immobilized on surface (IE).

3.4.1.4 Materials chemical composition (FT-IR)

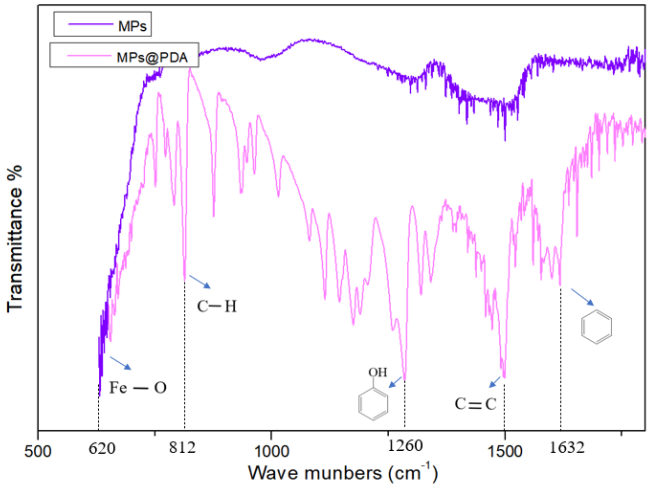

Figure 3-5 FT-IR spectra of the MPs (Fe_3O_4) and the MPs coated with PDA (MPP)

Figure 3-5 shows the FT-IR spectra of the bare MP and MPP between wavenumbers 620-1800 (cm^{-1}). MP and MPP exhibit a strong absorption at 620 cm^{-1}, attributed to the vibration of the Fe–O functional group[29,30]. In comparison to naked MP, the spectrum of PDA@Fe_3O_4 exhibited multiple peaks, including those near 1632 cm^{-1}, 1500 cm^{-1}, 1260 cm^{-1}, and 812 cm^{-1}. These absorption peaks are attributed to the benzene ring skeleton vibration, C=C bending, phenolic hydroxyl group

stretching mode, and C-H bending vibration, respectively[31]. This indicates the successful coating of PDA onto the MP.

3.4.2 Effects of key conditions on alcalase immobilization

The effects of the concentrations of alcalase and GA, immobilization pH, as well as immobilization time were evaluated with regard to enzyme protein loading density, enzymatic activity, and reaction kinetics.

3.4.2.1 Effects of alcalase concentration

As shown in Figure 3-6, the loading density increased first with the increase of enzyme concentration in the immobilization mixture and plateaued at 208.83 mg/g with an alcalase concentration of 30.5 mg/ml. However, the enzymatic activity per gram of IE initially increased but then decreased after reaching a peak value of 0.39 AU/mg, which was achieved at alcalase concentration 6.1 g/ml. As shown in Figure 3-6 (b), an increase in alcalase concentration in immobilization buffer led to a rapid decrease in specific activity at the low concentration range, dropping from 7.07 U/mg at 0.51 mg/L to 3.45 U/mg at 3.05 mg/L and reaching 1.75 U/mg at 12.20 mg/L and beyond. Given that the activity is usually the preferred evaluation criterion, the optimal alcalase concentration is identified as 6.1 mg/ml. Glomm et al. [32] studied the immobilization of protease subtilisin A using three different linkers, i.e., aminopropyl trimethoxy-silane, chitosan, and Jeffamine coating. They reported linear increase of loading density with enzyme concentration in buffer in the tested range and observed a similar decrease of specific enzyme activity with increasing loading densities.

It is expected that loading density would increase with the concentration of the enzyme in the buffer when using the same mass of MP as carriers were used since more enzymes would be available for the same mass of MP. On the other hand, the rapid decrease of specific enzymatic activity of the

IEs could be tentatively attributed two possible reasons: 1) “crowded” monolayer enzymes immobilized on carrier surface may partially block each other, causing increased resistance to the mass transfer of substrates and/or products to and/or from the active sites of enzymes; and 2) “overcrowded” enzymes may form additional layers on carrier surface, via adsorption or cross linking, preventing enzymes beneath from accessing substates. From the economic perspective, free enzymes are one of the major contributors to the costs of IEs. It is therefore imperative to carefully select the appropriate enzyme concentration in buffer to avoid unnecessary waste and resource utilization inefficiencies[33]. Conversely, excessively low enzyme concentrations may lead to suboptimal utilization of the carrier material and diminished enzymatic activity per gram MP. Striking the right balance in the enzyme solution concentration is crucial for achieving efficient immobilization and maximizing enzymatic performance.

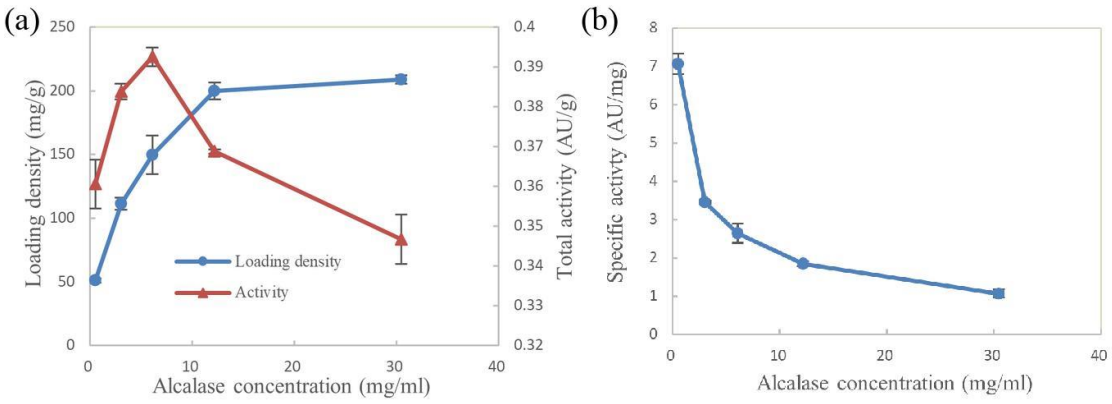

Figure 3-6 Effect of enzyme concentration on (a) loading density, activity per milligram MP, (b) specific activity

3.4.2.2 Effects of GA concentration

As shown in Figure 3-7a, the loading density increased continuously when the GA concentration increased in the tested range, i.e., 0.025-0.416 μg/L GA, with the loading density increasing from

53.47 to 386.97 mg/g. The activity per gram IE, however, increased rapidly from 0.253 AU/g at 0.025 μg/mL GA to a peak of 0.354 AU/g at 0.23 μg/mL GA. As shown in Figure 3-7b, the specific activity of IE decreased continuously in the tested range with increasing GA concentration, but the rate of decrease declined with GA concentration increase. This phenomenon could be tentatively explained by the following hypothesis.

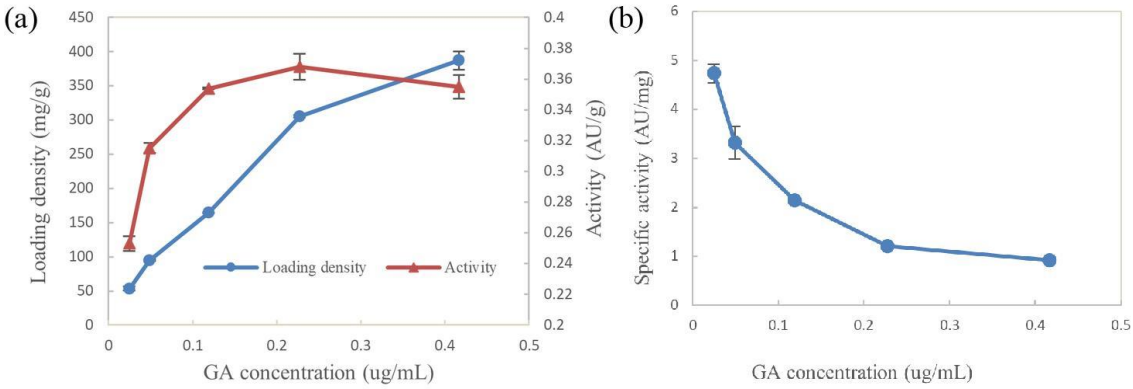

Figure 3-7 Effect of GA concentration on (a) loading density and activity per milligram MP; as well as (b) specific activity

As a cross-linker, GA possesses two aldehyde groups capable of reacting with the amino and hydroxyl groups of the PDA layer on MPP surface and those on alcalase surface. At low GA concentration, the MP surface did not have sufficient spacer sites for enzyme protein immobilization. Therefore, both the loading density and enzymatic activity per gram MP increased with GA concentration. Although the specific enzymatic activity decreased more rapidly in the low concentration range with the increase of GA concentration, the increase of loading density was greater than that required to compensate for the decrease of specific activity. Conversely, increasing GA concentration can lead to GA residue density increased on MPPs surface, which in turn

increases the opportunity of connecting multiple GA residues with the amino groups and hydroxyl groups on alcalase surface. The multi-point cross-linking on the enzyme's surface could potentially alter its conformation and render it inactive[34].

3.4.2.3 Effects of immobilization pH

Figure 3-8 depicts the effects of immobilization buffer pH. The enzyme loading density increased from 166.3 mg/g at pH 7.5 to 181.3 mg/g at pH 8.5 and then increased slightly to 189.4 mg/g at pH 11.5. As for the enzymatic activity per gram MPs, it decreased slightly from 0.327 AU/g at pH 7.5 to 0.322 AU/g at pH 9.5 and then significantly to 0.278 AU/g at pH 11.5. As shown in Figure 3-8b, the specific activity of IE decreased gradually from 2.3 AU/mg at pH 7.5 to 1.7 AU/mg at pH 11.5. Buffer pH 7.5 is considered to be the optimal.

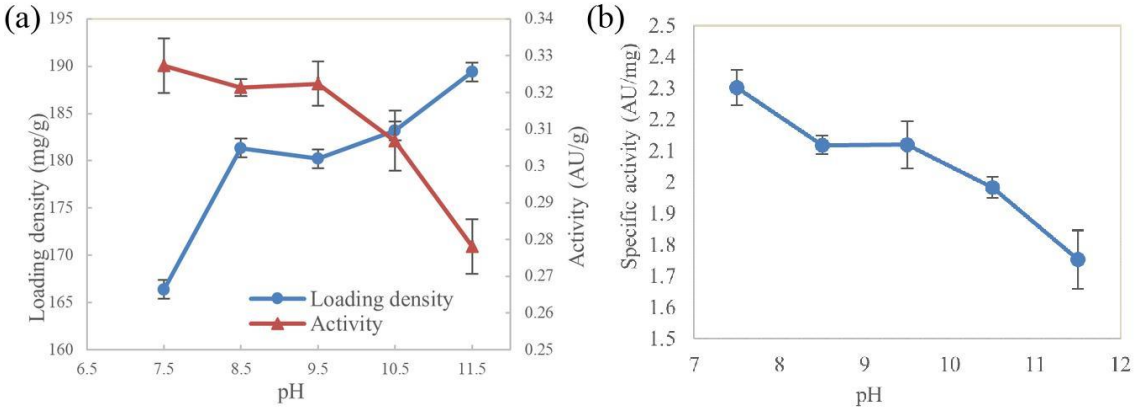

Figure 3-8 Effects of immobilization pH on (a) loading density, activity per gram MP and (b) specific activity

During the immobilization process, excessive acidity or alkalinity in the solution could affect the protonation/deprotonation of functional groups on enzymatic protein surface and therefore impact its surface charge and configuration. Consequently, they could affect the interaction between the

functional groups of the enzyme and GA[35]. Therefore, the immobilization buffer pH may have strong effects on the loading density of enzymatic proteins on to carrier surfaces and the specific activity of IEs.

3.4.2.4 Effect of immobilization time

The influence of immobilization time on immobilization efficiency is depicted in Figure 3-9. The loading density increased with immobilization time, reaching its plateau at 4 hours. Concurrently, the activity per gram IE also reached its maximum at 4 hours but decreased with longer immobilization times. These findings are consistent with the work conducted by Flores[36]. who found that 14 hours was the most efficient immobilization time. In our work, we determined 4 hours as the optimal immobilization time.

The impact of immobilization time on specific activity is particularly evident, as shown in Figure 3-9b. When the immobilization time was 1 hour, the specific activity reached 6.04 AU/mg. However, as the immobilization time gradually increased, there was a sharp decline in specific activity. This reduction in activity may be due to the formation of multi-point attachment and conformational changes in the enzyme's tertiary structure, which might negatively affect the stability of enzyme conformation and ultimately led to activity reduction or even deactivation[36]. Comparatively, among other immobilization conditions, it is apparent that immobilization time exerted a significant influence on specific activity.

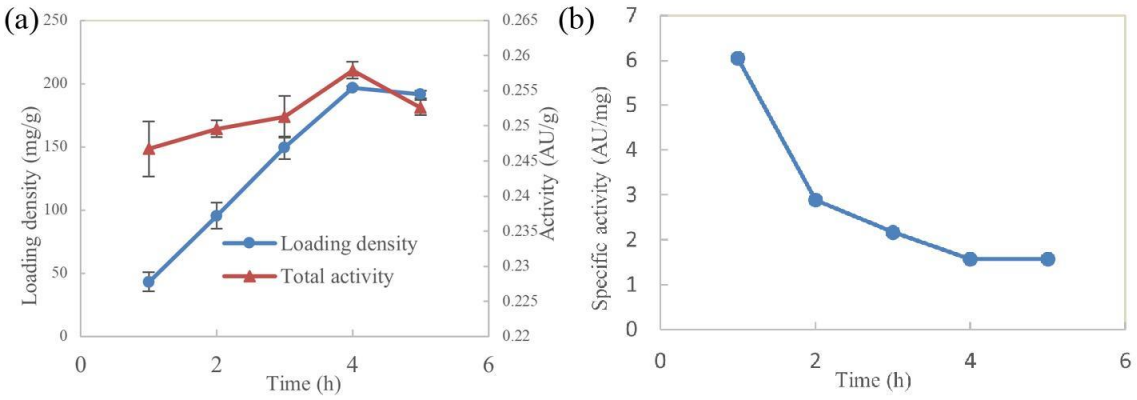

Figure 3-9 Effect of immobilization time on loading density, activity per gram MP and specific activity

3.4.2.5 Enzymatic reaction kinetics and activity retention

The kinetic parameters of both FE and IE are listed in Table 3-1. The Michaelis constant (K_m) for immobilized alcalase was slightly lower (0.701 mM) compared to that of free alcalase (0.716 mM), suggesting that the affinity of alcalase towards its substrate remained largely unchanged post-immobilization. Conversely, the maximum velocity (V_{max}) of the immobilized alcalase (0.2289 $mM \cdot min^{-1}$) exhibited a 37% reduction relative to the free alcalase (0.3584 $mM \cdot min^{-1}$). This reduction highlights a diminished availability of active sites on the immobilized enzyme, attributable to steric hindrance and a partial reduction in conformational flexibility upon anchoring the enzyme to the carrier's surface. The observed 62.8% activity retention further supports this assertion.

Table 3-1 Kinetic parameters and activity retention of free and immobilized alcalase

Alcalase	K_m （mM)	V_{max} (mM ·min^{-1})	Activity Retention (%)
Free	0.7159	0.3584	–
Immobilized	0.7009	0.2289	62.8

3.4.3 Characterization of IE

3.4.3.1 Optimum temperature range

As shown in Figure 3-10, the free alcalase had a very narrow optimum of temperature, i.e., 50-55℃ and the enzymatic activity dropped sharp outside of this range. On the other hand, the immobilized alcalase had a much wide optimal temperature range of 45-60 ºC, in which the relative activity was above 90%.

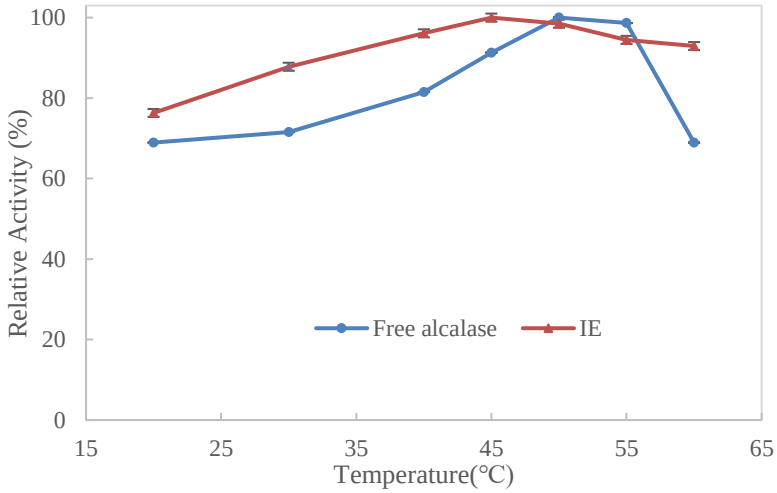

Figure 3-10 FE and IE optimum temperature range

The broadened temperature optima of IEs in comparison to their free counterparts have been widely reported for different IEs, including alcalase. For instance, Zhu et al. immobilized alcalase onto MP modified with tannic acid and polyethyleneimine[37]. They observed that the immobilized alcalase exhibited better temperature tolerance compared to the free alcalase, with both immobilized and free alcalase showing an optimal temperature of 50℃. This result is similar to our findings. This phenomenon can be explained by the fact that the increase in temperature enhances the collision frequency between the substrate and the enzyme, thereby facilitating the enzyme-substrate interaction and increasing the reaction rate. On the other hand, the anchoring effects of carrier surface on to the immobilized enzyme might help stabilizing configuration of enzymatic protein and therefore enhance its thermal stability. However, it should be noted that excessively high temperatures can lead to protein denaturation.[38].

3.4.3.2 Optimum pH range

As shown in Figure 3-11, the optimum pH of free alcalase was 8.5, and that of immobilized alcalase rose to 9.5. The IE also had the better pH tolerance because the relative activity of IE was less affected during the change of pH. These data are compatible with literature data[39]. For instance, Zhu et al. observed that the IE exhibited enhanced pH tolerance compared to the free alcalase, with the optimal pH for free alcalase being 10, while the IE displayed an increased optimal pH of 11. This trend can be explained by the fact that pH is an important factor affecting enzyme activity since it can change the ionization state of both the substrate molecule and the enzyme molecule, which can subsequently affect the configuration of the enzyme molecule, especially that of the active site of enzyme. Since the glutaraldehyde binds with the amino groups of alcalase, reducing the positive charges at alcalase surface, it led to a pH optimum shift towards the alkaline side[40].

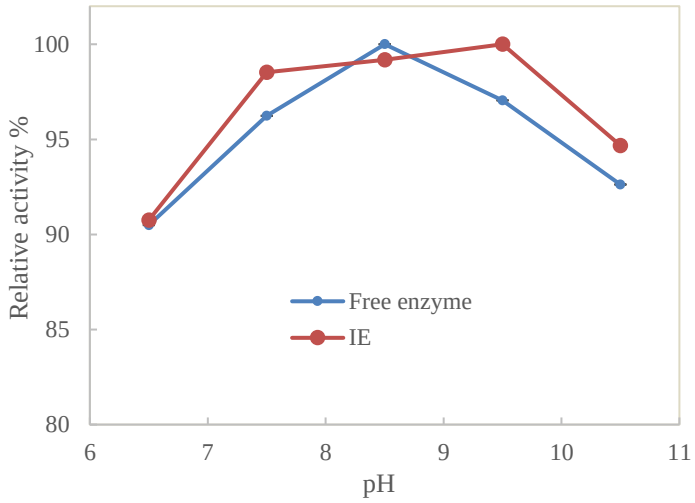

Figure 3-11 FE and IE optimum pH range

3.4.3.3 Thermal stability

In the thermal stability study, free and immobilized alcalase stored at different temperatures, ranging from 20 to 70 ℃, for 24 h, then had their enzymatic activities were tested under standard assay conditions. As shown in Figure 3-12, both FE and IE had the highest activity when stored at 20℃. In the temperature range from 20 to 50 ℃, their relative activity decreased continuously from 100% to 80%. When the storage temperature was greater than 50 ℃, the trend was more obvious. At a storage temperature of 70 ℃, they lost almost all their activity. It is important to note that IE had better thermal stability than free alcalase throughout this range. It can be explained since the conformation of alcalase could be protected through immobilization, due to the restriction of the conformational mobility from the immobilization, which help mitigate the thermal denaturation. This trend was also reported by Silveira's study[38].

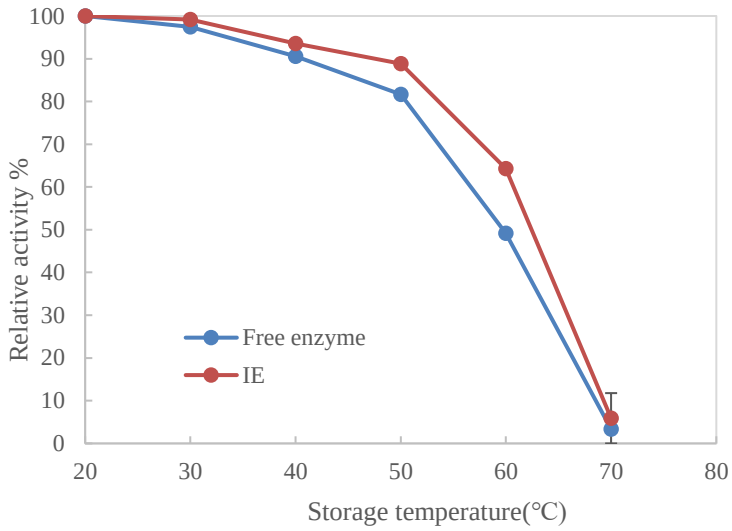

Figure 3-12 FE and IE thermal stability

3.4.3.4 Reusability

The reusability of immobilized alcalase is shown in Figure 3-13. After 14 reaction-magnetic separation-PBS washing cycles, the relative activity of IE was maintained at 78.66%, which is higher or comparable with the results reported in the literature. For instance, Zhu et al.[39] reported the retention of 61% activity after 10 cycles of reuse for alcalase immobilized on tannic acid/polyethyleneimine modified magnetic particles. the decrease of the relative activity of the IE with the increased recycled use times could be due to the enzyme leakage from the carrier or the slow enzyme inactivation during multiple uses[39].

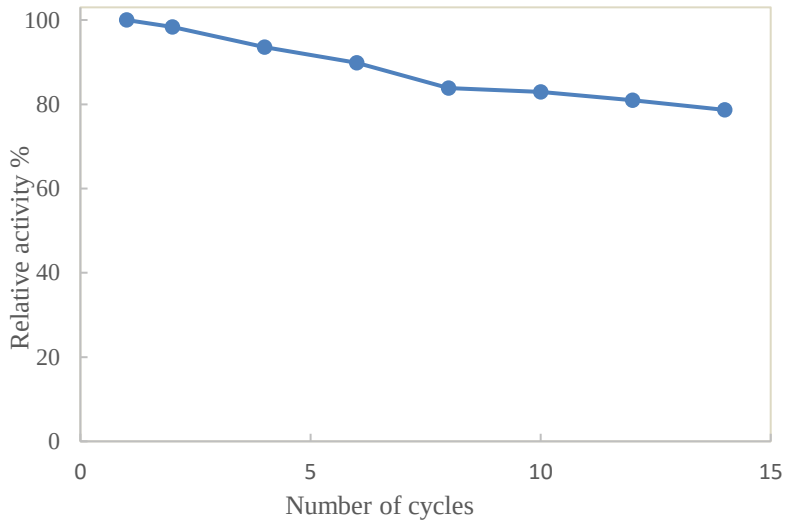

Figure 3-13 Reusability of IE

3.4.3.5 Comparison of results of this study with literature data

Table 3-2 Comparison of different functionalization agents for alcalase immobilization onto MP surface and with GA as spacer

Surface functionalization agent	Reduction of Saturation Magnetization	pH Optimum	Temperature Optimum	Specific activity decrease	Activity Retention (%) /Cycles of Use	Ref.
Chitosan	-	8	55-65	-	65%/5	[41]
Chitosan	-	9-10	50-60	-	85%/10	[42]
APTES	-	8.5	50	-	-	[43]
APTES	33%	7.5-8.5	65	46%	50.1%/10	[44]
PDA	25%	7.5-9.5	45-60	37.2%	79%/14	This study

Table 3-2 lists the key performance parameters of reports on immobilization of alcalase on to MP surface functionalized using different agents, including chitosan, 3-aminopropyl-triethoxysilane (APTES), and PDA, from literature data and this study. All used GA as the spacer. While all parameters are comparable, using PDA as the surface modification agent as in this study generally offered a smaller reduction of saturation magnetization of modified MP, a broader pH and temperature range, lower reduction of specific enzyme activity, and better reusability.

3.5 Conclusions

The synthesis of MP through a solvothermal method yielded spherical particles with an average diameter of 633 nm. Coating these MPs with PDA led to a moderate decrease in their magnetic responsiveness. Optimal enzymatic activity per unit mass of MP was achieved under specific conditions: a GA concentration of 0.23 μg/mL, an immobilization pH of 7.5, an alcalase concentration of 6.1 mg/mL, and an immobilization duration of 4 hours. When compared to its free form, the immobilized alcalase exhibited enhanced tolerance and stability against variations in temperature and pH. Kinetic analysis revealed a decrease in V_{max}, while K_m remained largely unchanged. Despite an initial activity retention of 62.8% following immobilization, the IEs maintained 78.66% of its activity after 14 cycles of enzymatic reactions. These results indicate that magnetic particles coated with polydopamine, and MPPG are an effective carrier for the immobilization of alcalase, significantly improving the enzyme's reusability, stability, and overall performance. Furthermore, this research provides new opportunities for industrial applications, particularly within the food and pharmaceutical sectors, where the enhanced stability and reusability of enzymes can contribute to greater process efficiency and cost-effectiveness.

This study demonstrates that PDA-modified MP could be an effective carrier for alcalase immobilization. This method, notable for its simplicity and effectiveness, significantly improves alcalase' s operational stability and reusability. These developments play a crucial role in promoting sustainable and efficient bioprocesses, marking a notable progress in development of IEs for the applications in diverse industrial sectors.

3.6 References

1. Ashkan, Z. *et al.* International Journal of Biological Macromolecules Immobilization of enzymes on nanoinorganic support materials : An update. *Int J Biol Macromol* **168**, 708–721 (2021).
2. Bolivar, J. M., Woodley, J. M. & Fernandez-lafuente, R. Chem Soc Rev Is enzyme immobilization a mature discipline ? Some critical considerations to capitalize on the benefits of immobilization. 6251–6290 (2022) doi:10.1039/d2cs00083k.
3. Zhang, Q., Yang, X. & Guan, J. Applications of Magnetic Nanomaterials in Heterogeneous Catalysis. *ACS Appl Nano Mater* **2**, 4681–4697 (2019).
4. Bilal, M., Zhao, Y., Rasheed, T. & Iqbal, H. M. N. Magnetic nanoparticles as versatile carriers for enzymes immobilization: A review. *Int J Biol Macromol* **120**, 2530–2544 (2018).
5. Lu, J., Li, Y., Zhu, H. & Shi, G. SiO2-Coated Fe3O4Nanoparticle/Polyacrylonitrile Beads for One-Step Lipase Immobilization. *ACS Appl Nano Mater* **4**, 7856–7869 (2021).
6. Rana, S. *et al.* Fabrication and characteristic studies of doped metal oxide - silane magnetic nanocomposite for enhancement of stability of α - amylase. *Applied Physics A* **128**, 1–10 (2022).
7. Patel, U., Chauhan, K. & Gupte, S. Synthesis , characterization and application of lipase - conjugated citric acid - coated magnetic nanoparticles for ester synthesis using waste frying oil. *3 Biotech* **8**, 1–12 (2018).
8. Lira, R. *et al.* International Journal of Biological Macromolecules Fructo-oligosaccharides production by an Aspergillus aculeatus commercial enzyme preparation with fructosyltransferase activity covalently immobilized on Fe 3 O 4 – chitosan-magnetic nanoparticles. *Int J Biol Macromol* **150**, 922–929 (2020).
9. Yang, Y. *et al.* Enhanced reusability and activity: DNA directed immobilization of enzyme on polydopamine modified magnetic nanoparticles. *Biochem Eng J* **137**, 108–115 (2018).
10. Chen, C. T., Martin-Martinez, F. J., Jung, G. S. & Buehler, M. J. Polydopamine and eumelanin molecular structures investigated with ab initio calculations. *Chem Sci* **8**, 1631–1641 (2017).

11. Liebscher, J. *et al.* Structure of polydopamine: A never-ending story? *Langmuir* **29**, 10539–10548 (2013).
12. Della Vecchia, N. F. *et al.* Building-block diversity in polydopamine underpins a multifunctional eumelanin-type platform tunable through a quinone control point. *Adv Funct Mater* **23**, 1331–1340 (2013).
13. Mechri, S. *et al.* Identification of a novel protease from the thermophilic Anoxybacillus kamchatkensis M1V and its application as laundry detergent additive. *Extremophiles* **23**, 687–706 (2019).
14. Ling, Z. *et al.* Food Hydrocolloids Fabrication egg white gel hydrolysates-stabilized oil-in-water emulsion and characterization of its stability and digestibility. *Food Hydrocoll* **102**, 105621 (2020).
15. Weng, Z. *et al.* Food Chemistry : X Assessment the flavor of soybean meal hydrolyzed with Alcalase enzyme under different hydrolysis conditions by E-nose , E-tongue and HS-SPME-GC – MS. *Food Chem X* **12**, 100141 (2021).
16. Ceruti, R. J., Marino, F., Mammarella, E. J. & Ricardo, M. In fl uence of the degree of hydrolysis on the bioactive properties of whey protein hydrolysates using. **72**, (2019).
17. Wang, Z. *et al.* Reduction of the allergenic protein in soybean meal by enzymatic hydrolysis. *Food Agric Immunol* **25**, 301–310 (2014).
18. Sica, J. A. P. & Márquez, C. C. M. C. Enzymatic Hydrolysis of Fish Waste as an Alternative to Produce High Value - Added Products. *Waste Biomass Valorization* **12**, 847–855 (2021).
19. Wang, S. nan *et al.* Immobilized alcalase alkaline protease on the magnetic chitosan nanoparticles used for soy protein isolate hydrolysis. *European Food Research and Technology* **239**, 1051–1059 (2014).
20. Glomm, W. R. *et al.* Immobilized protease on magnetic particles for enzymatic protein hydrolysis of poultry by-products. *Lwt* **152**, 112327 (2021).
21. Deng, H. *et al.* Monodisperse magnetic single-crystal ferrite microspheres. *Angewandte Chemie - International Edition* **44**, 2782–2785 (2005).
22. Deng, Y. *et al.* Preparation of iron-based MIL-101 functionalized polydopamine@Fe3O4 magnetic composites for extracting sulfonylurea herbicides from environmental water and vegetable samples. *J Sep Sci* **41**, 2046–2055 (2018).
23. Reagent, B., Description, P., Used, A. F. & Number, C. Bradford Protocol. 3–8 (2011).

24. Kimberle, P. dos S., Carolina, M. S., Ana, I. S. B. & Luciana, R. B. G. Modifying alcalase activity and stability by immobilization onto chitosan aiming at the production of bioactive peptides by hydrolysis of tilapia skin gelatin. *Process Biochemistry* **97**, 27–36 (2020).
25. Wang, S. nan *et al.* Immobilized alcalase alkaline protease on the magnetic chitosan nanoparticles used for soy protein isolate hydrolysis. *European Food Research and Technology* **239**, 1051–1059 (2014).
26. Oroujeni, M., Kaboudin, B., Xia, W., Jönsson, P. & Ossipov, D. A. Progress in Organic Coatings Conjugation of cyclodextrin to magnetic Fe 3 O 4 nanoparticles via polydopamine coating for drug delivery. *Prog Org Coat* **114**, 154–161 (2018).
27. Ghani, M., Jafari, Z., Maleki, B. & Chamani, M. Magnetic solid-phase extraction of warfarin and gemfibrozil in biological samples using polydopamine-coated magnetic nanoparticles via core-shell nanostructure. *J Sep Sci* **46**, (2023).
28. Jafari Eskandari, M. & Hasanzadeh, I. Size-controlled synthesis of Fe3O4 magnetic nanoparticles via an alternating magnetic field and ultrasonic-assisted chemical co-precipitation. *Mater Sci Eng B Solid State Mater Adv Technol* **266**, 115050 (2021).
29. Yang, F., Dong, Y. & Guo, Z. Facile fabrication of core shell Fe3O4@polydopamine microspheres with unique features of magnetic control behavior and special wettability. *Colloids Surf A Physicochem Eng Asp* **463**, 101–109 (2014).
30. Hemmati, S., Zangeneh, M. M. & Zangeneh, A. CuCl2 anchored on polydopamine coated-magnetic nanoparticles (Fe3O4@PDA/Cu(II)): Preparation, characterization and evaluation of its cytotoxicity, antioxidant, antibacterial, and antifungal properties. *Polyhedron* **177**, 114327 (2020).
31. Bi, Y. *et al.* Improved catalytic properties of Thermomyces lanuginosus lipase immobilized onto newly fabricated polydopamine-functionalized magnetic Fe3O4 nanoparticles. *Processes* **8**, (2020).
32. Glomm, W. R. *et al.* Immobilized protease on magnetic particles for enzymatic protein hydrolysis of poultry by-products. *Lwt* **152**, 112327 (2021).
33. Al-Duri, B. & Yong, Y. P. Lipase immobilisation: An equilibrium study of lipases immobilised on hydrophobic and hydrophilic/hydrophobic supports. *Biochem Eng J* **4**, 207–215 (2000).

34. Silveira, T. R. *et al.* An efficient decolorization of methyl orange dye by laccase from Marasmiellus palmivorus immobilized on chitosan-coated magnetic particles. *Biocatal Agric Biotechnol* **30**, 1–10 (2020).
35. de Andrades, D. *et al.* Immobilization and stabilization of different β-glucosidases using the glutaraldehyde chemistry: Optimal protocol depends on the enzyme. *Int J Biol Macromol* **129**, 672–678 (2019).
36. Flores, E. E. E. *et al.* Influence of reaction parameters in the polymerization between genipin and chitosan for enzyme immobilization. *Process Biochemistry* **84**, 73–80 (2019).
37. Zhu, S. *et al.* Production of Cardamine violifolia selenium-enriched peptide using immobilized Alcalase on Fe3O4 modified by tannic acid and polyethyleneimine. *RSC Adv* **12**, 22082–22090 (2022).
38. Silveira, T. R. *et al.* An efficient decolorization of methyl orange dye by laccase from Marasmiellus palmivorus immobilized on chitosan-coated magnetic particles. *Biocatal Agric Biotechnol* **30**, 1–10 (2020).
39. Zhu, S. *et al.* Production of Cardamine violifolia selenium-enriched peptide using immobilized Alcalase on Fe3O4 modified by tannic acid and polyethyleneimine. *RSC Adv* **12**, 22082–22090 (2022).
40. Sangeetha, K. & Emilia Abraham, T. Preparation and characterization of cross-linked enzyme aggregates (CLEA) of Subtilisin for controlled release applications. *Int J Biol Macromol* **43**, 314–319 (2008).
41. Liu, Y. & Dave, D. Beyond processing waste: Extraction of oil from Atlantic salmon (Salmo salar) by-products using immobilized Alcalase on chitosan-coated magnetic nanoparticles. *Aquaculture* **548**, (2022).
42. Wang, S. nan *et al.* Immobilized alcalase alkaline protease on the magnetic chitosan nanoparticles used for soy protein isolate hydrolysis. *European Food Research and Technology* **239**, 1051–1059 (2014).
43. Li, H. *et al.* Milk protein hydrolysates obtained with immobilized alcalase and neutrase on magnetite nanoparticles: Characterization and antigenicity study. *J Food Sci* **87**, 3107–3116 (2022).
44. Hu, T. G., Cheng, J. H., Zhang, B. B., Lou, W. Y. & Zong, M. H. Immobilization of alkaline protease on amino-functionalized magnetic nanoparticles and its efficient use for preparation of oat polypeptides. *Ind Eng Chem Res* **54**, 4689–4698 (2015).

Chapter 4 Effects of spacer chemistry and length on immobilization of lipase on polydopamine modified magnetic microparticles

Xinyue Wang[1], Xiao Hong[2], Freeman Lan[3], Jason Zhang[1], Christopher Q. Lan[1]*

[1] *Department of Chemical and Biological Engineering, University of Ottawa, 161 Louis Pasteur Private, Ottawa, Ontario, Canada, K1N 6N5*

[2] *Department of Cellular and Molecular pharmacology, University of California, San Francisco, 600 16th street, N316, San Francisco, California, USA, 94158*

[3] *Biomedical Engineering Institute, the University of Toronto, 164 College St., Toronto, ON, Canada*

The content of this chapter was submitted to Bioresource Technology

4.1 ABSTRACT

Lipase is pivotal in multiple sectors, including food, pharmaceutical and biofuels production. Immobilized enzyme (IE) offers several advantages over their free forms, such as enhanced stability, easy separation, and reusability. Among the different methods of enzyme immobilization, the use of magnetic microparticles as carriers has gained significant attention due to their unique properties, including convenient separation using an external magnetic field. In this research, we present the immobilization of lipase on polydopamine (PDA)-modified magnetic microparticles using different spacers, including different types, i.e., branched polyethyleneimine (PEI) and glutaraldehyde (GA) and the same molecule but of different length, i.e., PEI of three different molecular weights. Through analyses of the surface of the 3D structure of the lipase, immobilization will not affect the active site by 3D modeling when either PEI or GA is used as the spacer and that PEI is potentially a more effective spacer than GA, both of which were confirmed by experimental results. For this purpose, we defined atom ratio as the benchmark for identification of valley amino acid residues. Results showed that PEI-600 Da exhibited optimal efficiency in lipase immobilization, whereas PEI-1800 Da maintained the highest specific enzymatic activity. We then determined the optimal immobilization conditions as follows: lipase concentration 4.25 mg/ml, pH 6, immobilization time 5 hours, and immobilization temperature of 10°C. In comparison to the free lipase, the IE had wider pH and temperature optima as well as better thermal, storage, and operational stabilities. The IE maintained 50% of its activity after 10 cycles of usages.

Key Words: immobilized enzyme, lipase, PDA, PEI, GA, magnetic particle

4.2 Introduction

Lipase triacylglycerol eater hydrolases, EC 3.1.1.3, is an enzyme that catalyzes the hydrolysis of triglycerides into free fatty acids, diacylglycerol, monoacylglycerol, and glycerol[1]. Due to its efficiency in various reactions such as esterification, alcoholises, and ester exchange, it finds extensive industrial applications in food manufacturing, cosmetics processing, pharmaceuticals, and biodiesel production[2–4]. Enzymes exhibit high activity and selectivity, operating under mild experimental and environmental conditions. Nevertheless, its high cost has remained a significant challenge in industrial applications[5]. To mitigate production costs, immobilization techniques are commonly employed, fixing the lipase onto suitable carriers for repeated use. Immobilization is a widely adopted method, offering separability and hence reusability, and enhancing the stability of lipase. Common immobilization techniques include physical adsorption, covalent bonding, crosslinking, and entrapment on solid support materials[6].

Magnetic particle materials, known for their excellent magnetic responsiveness, simple synthesis process, controllable size, large surface area, low cost, and modifiability, find wide application as supports for enzyme immobilization[7]. These materials can be utilized for enzyme immobilization through direct physical adsorption or by modification. Enzymes directly immobilized via physical adsorption may suffer from weaker forces, potentially leading to inadequate immobilization and potential enzyme leakage[8,9]. Moreover, enzyme clustering on the carrier's surface could shield active sites, resulting in reduced enzyme activity[10]. Therefore, further in-depth research is required to investigate surface modification of magnetic microparticles through grafting specific spacers. This aims to overcome the steric hindrance, allowing the immobilized enzyme to maintain its activity effectively by addressing issues related to the shielding of the active centers. Glutaraldehyde is a short spacer cross-linking agent that contains aldehyde groups at each end. These groups allow it to react with the functional groups on the carrier surface and the enzyme surface, facilitating the immobilization of the enzyme on the carrier surface[11]. ^{206}PEI

(Polyethyleneimine) is a branched long-chain polymer that varies in length according to its molecular weight. It possesses numerous amino groups in its structure, enabling it to react with the carboxyl and hydroxyl groups on the enzyme surface, thereby allowing the enzyme to be immobilized on the PEI [12]. A considerable amount of research indicates that both GA and PEI can immobilize lipase on carriers. However, there is a lack of experimental evidence to simultaneously compare the immobilization effects of GA and PEI on lipase, as well as to investigate the suitability of different lengths of PEI for immobilizing lipase.

In this investigation, we explored the immobilization of lipase on MPP using two distinct spacers: glutaraldehyde (GA) and polyethyleneimine (PEI) of three different molecular weights (600, 1800, and 10,000) under varied conditions, including MP functionalization, temperature, enzyme concentration, and contact time of enzyme immobilization. The selected molecular weights of PEI were strategically chosen to assess their influence on immobilization performance. Low molecular weight PEI (PEI-600) may provide high mobility and low viscosity, facilitating the formation of thin, minimally obstructive layers that enhance substrate accessibility to the enzyme's active site. Medium molecular weight PEI (PEI-1800) may balance mobility and the availability of amine groups, optimizing the trade-off between enzyme activity and stability. High molecular weight PEI (PEI-10,000) can form robust three-dimensional structures with increased amine group density, enhancing structural stability and operational durability.

Additionally, by introducing a novel definition of atom ratio, we systematically classified the surface amino acid residues of a lipase into valley and peak residues using surface analysis. This approach provided a deeper understanding of how different spacers influence enzyme immobilization and the interactions between the enzyme and the carrier surface. This study offers insights into optimizing lipase immobilization and expanding its practical applications.

4.3 Materials and methods

4.3.1 Materials

Lipase, i.e., *Candida antarctica* Lipase B, 4-nitrophenyl palmitate, triton X-100, dopamine hydrochloride, and Bradford reagent were procured from Sigma-Aldrich Inc., St. Louis, MO. bovine serum albumin (BSA), PEI with branched molecular weights of 600, 1800, and 10000, were purchased from Thermo-Scientific, Rockford, IL. Glutaraldehyde (25% solution) was sourced from Electron Microscopy Sciences, Hatfield, PA. Sodium acetate was obtained from VWR Life Science, Solon, Ohio. Iron (III) chloride hexahydrate, ethylene glycol, Tris-base, and phosphate buffered saline (10× solution) were procured from Fisher Scientific.

4.3.2 Preparation of PDA-modified magnetic particles (MPP)

The synthesis of magnetic microparticles (MPs) was conducted using an adapted variant of the conventional solvothermal reduction method[13]. In brief, 2.7 g of $FeCl_3 \cdot 6H_2O$ were weighed and subsequently dissolved in 80 ml of ethylene glycol, followed by stirring the mixture for 30 minutes to yield a yellow opaque solution. Next, 3.6 g of sodium acetate was introduced into the solution, continuing the stirring process for an additional 30 minutes to obtain a homogeneous yellow solution. This solution was then transferred into a 100 ml Teflon-lined stainless-steel autoclave and subjected to a heating process at 200 °C for 24 hours to facilitate the synthesis of the magnetic particles (MP). Post-synthesis, the product was allowed to naturally cool to room temperature (20°C). Subsequently, it was washed thrice with 99% alcohol and dried under vacuum at 40°C overnight. The synthesized MP were then stored at 4°C.

The polydopamine coating layer on the MPs was prepared through the surface polymerization of dopamine, with the experimental procedure delineated as follows: Initially, 2 g of the MP, procured from the aforementioned synthesis process, were weighed and washed twice with 30 ml of Tris-HCl (pH 8.5, 20 mM) solution. Subsequently, these were suspended in 80 ml of Tris-HCl (pH 8.5, 20 mM) solution and subjected to ultrasonic mixing for 30 minutes to ensure thorough dispersion

within the solution[14]. Prepare 10 mg/ml dopamine solution 20 mL and stock it. Upon the completion of dispersion of the MP solution, it is mixed with the stocked 20 mL dopamine solution, and the mixture is then placed on a shaker set at 25°C and agitated at a speed of 150 rpm to react for 18 hours. Subsequently, the resultant product, MPP, was washed three times with deionized water and dried under a vacuum at 40°C overnight. Finally, the product is stored at 4°C.

4.3.3 Functionalization of MPP with GA or PEI to prepare MPPG and MPPP

To prepare particles modified with either GA (MPPG) or PEI (MPPP) as spacers, the process is as follows: Initially, 10 mg of MPP is weighed and placed into a 2 ml tube, then added to 2 mL of pH 7.4 PBS buffer solution for rinsing. Subsequently, a series of solutions with varying concentrations are prepared using 25% glutaraldehyde and 99% PEI solutions with different molecular weights. Subsequently, 1 ml of the above spacers solutions is transferred into tubes, and the MPs are subjected to ultrasonic treatment for 30 minutes to ensure full dispersion. Then, they are placed in a shaker at 25°C with a speed of 250 rpm for a reaction duration of 3 hours. After the reaction, the products are washed three times with 1 mL of pH 7.4 PBS solution to remove residual chemicals.

4.3.4 Lipase immobilization to prepare immobilized enzymes (IE)

Prepare the lipase solution by diluting the purchased lipase solution with PBS to intended concentrations for subsequent use. Then, transfer 1 mL of the lipase solution into the test tube containing pre-set amount of MPPG or MPPP, place the mixture on a shaker, and incubate at 250 rpm and 40°C for 18 hours. After the reaction, drain the supernatant and then wash three times with pH 7.4 PBS solution to ensure the removal of any residual free enzymes from particle surfaces.

4.3.5 Characterizations of MP, MPP and IE

The crystallographic structure and chemical composition of the synthesized MPs, MPP, and IE were characterized using powder X-ray diffraction (XRD). The morphology of MPs, MPP, and IE was examined utilizing scanning electron microscopy (SEM, model JSM-7500F). X-ray

Photoelectron Spectroscopy (XPS) was utilized to analyze the types of surface elements present in the MPs, MPP, and IE.

4.3.6 Surface analysis of Lipase

The primary amino acid sequence of the lipase was retrieved from the National Center for Biotechnology Information (NCBI) database (https://www.ncbi.nlm.nih.gov/), and the crystal structure of the lipase (5GV5) was obtained from the Protein Data Bank (RCSB PDB). A comprehensive analysis of the primary sequence of the lipase was conducted to determine the number and proportion of amino acid residues (AAR) carrying functional groups that could form covalent bond with PEI or GA. Subsequently, the PyMOL molecular virtualization system (PyMOL | pymol.org) was employed to examine the three-dimensional structure and generate visual representation of the enzyme surface applying a solvent-accessible surface area (SASA) cutoff of 2.5 Å² (the resolution of the PDB file is 2.89 A°). While this cutoff is empirical, it is consistent with previously reported SASA thresholds used to define the enzyme's molecular surface[15,16,17]. An in-depth analysis was then conducted to quantify the number and proportion of these reactive surface residues and depict their distribution on the lipase surface by the PyMOL script 'FindSurfaceResidue.py' (http://pymolwiki.org/index.php/FindSurfaceResidues). Following that, the relative per-residue solvent accessible surface area (RSA) of individual reactive AAR was calculated by the PyMOL function 'get_sasa_relative', based on the equation: RSA = SASA/MaxSASA, where SASA is solvent accessible surface area of an AAR in the 3D structure of the enzymatic protein and MaxSASA the maximum SASA of the AAR, which was retrieved from the literature[18].

4.3.7 Determination of protein loading and enzyme activity

In this study, three key parameters are employed to evaluate the efficiency of immobilization: loading density, activity-IE, and specific activity. Loading density is the mass of enzymatic proteins immobilized per unit mass of IE. It quantifies the number of enzymes that can be bound per unit

mass of the carrier, serving as a measure of immobilization capacity of carrier under certain conditions. Activity-IE is defined as the enzymatic activity displayed by the immobilized enzymes on a unit mass of carrier. It represents the activity of all immobilized enzymes in unit carrier and is of practical significance. On the other hand, specific activity focuses on the intrinsic activity possessed by each unit of enzyme, being them free or immobilized on the carrier. It is determined by dividing the activity-IE by the loading density of the IE. Specific activity provides insights into the relative efficiency and performance of the immobilized enzymes and holds relevance for theoretical analysis.

4.3.7.1 Protein concentration and loading density of enzymes

The determination of protein concentration and loading density followed the methods described in my previous research report[19]. Briefly, the enzyme loading density is defined as the mass of enzyme immobilized per unit mass of carrier, was measured using the Bradford method with BSA as the standard. To create a standard curve, prepare BSA solutions (0.25 - 2 mg/mL). Mix 20 μL of each BSA solution (or 20 μL PBS as the blank) with 1 mL of Coomassie Brilliant Blue G-250. Incubate for 5 minutes at room temperature, then measure absorbance at 595 nm. The conversion factor was 2.522 mg BSA/L per OD_{595} unit.

For determining the enzyme loading density on carrier, mix 20 μL of appropriately diluted samples with 1 mL Coomassie Brilliant Blue G-250. Measure OD_{595} after 5 minutes of incubation at room temperature. Calculate the loading density of IE (q, mg/g), which was defined as the mass of enzymatic proteins immobilized per unit mass of IE using the following equation:

$$q = \frac{(C_0V_0 - CV)}{m} \qquad (1)$$

where q is the mass of enzymatic proteins per unit mass of IE (mg/g), C_0 (mg/mL) and V_0 (mL) the initial enzyme concentration and volume of the enzyme solution used in immobilization, V (mL) and C (mg/mL) represent the total volume of the supernatant collected during the washing steps of

the IE and the protein concentration determined using the Bradford method, respectively, and m the mass of IE (mg).

4.3.7.2 Assay of enzyme activity

(1) Activity assay

The enzymatic activity was assessed using a modified Zhu's method[20]. Briefly, the cleavage of p-nitrophenol palmitate (p-NPP) produced p-nitrophenol (p-NP). To prepare the substrate solution, 50 mg of p-NPP was dissolved in 10 mL of isopropanol and then diluted 10 times with PBS, with Triton X-100 as a surfactant. One milliliter of substrate was added to 10 mg IEs, followed by sonication for 5 minutes and incubation on a shaker at 220 rpm and 40℃ for 15 minutes. The mixture was then centrifuged, and 200 μL of the supernatant was transferred to 1 mL of 95% ethanol, and the absorbance was measured at 405 nm. The activities of free and immobilized lipase were determined using a standard curve. One unit of enzyme activity (U) was defined as the amount of enzyme required for producing 1 μmol p-NP per minute at 40℃ and the specific activity IE (SA_{IE}, U/g), which is defined as the enzymatic activity per gram of IE, was calculated using the following equation:

$$SA_{IE} = \frac{A_{405}}{k \times t \times m} \qquad (2)$$

where A_{405} is the light absorbance at 405 nm wavelength; k the slope of the p-NP standard curve, which is 0.0014 OD/μM, and t the reaction time (15 min).

The specific activity (SA), which is defined as the enzymatic activity per milligram of enzymatic protein, is calculated as follows:

For free enzyme in solution,

$$SA\left(\frac{U}{mg}\right) = U/C \qquad (3)$$

where *U* is enzymatic activity of enzyme solution (U/mL) and *C* the concentration of enzymatic proteins of the enzyme solution (mg/mL).

For IE,

$$SA\ \left(\frac{U}{mg}\right) = SA_{IE}/q \quad (4)$$

4.3.8 Features of immobilized lipase

4.3.8.1 Optimum temperature

To compare the optimal temperature of free and immobilized lipase, the enzymes were combined with a substrate solution prepared from p-nitrophenol palmitate (p-NPP) and incubated in a shaker at temperatures ranging from 10℃ to 60℃ under identical conditions. Following the reaction, centrifugation was employed for solid-liquid separation, and the optical density (OD) of the supernatant was measured. The relative activity is defined as the activity value at a specific temperature divided by the highest activity value obtained across all temperatures tested. This metric is utilized to illustrate the variation in activity value in relation to temperature, with the maximum activity designated as 100%.

4.3.8.2 Optimum pH range of free and immobilized lipase

To compare the optimum pH range of free and immobilized lipase, a series of n-NPP solutions with a pH range of 6 to 10 were prepared. The enzymes were then mixed with these n-NPP solutions, and the mixture was incubated on a shaker at 40°C with a speed of 250 rpm for 30 minutes. After the reaction, centrifugation was used for solid-liquid separation, and the optical density (OD) of the supernatant was measured. The relative activity at different pH conditions was calculated. The relative activity is defined as the activity value at a specific pH, divided by the highest activity value obtained across all pH levels tested. This measure is utilized to illustrate how the activity value fluctuates with changes in pH, setting the maximum activity as 100%.

4.3.8.3 Thermal storage stability and reusability

The thermal storage stability of the free and immobilized lipases will be evaluated by incubating them at temperatures ranging from 10 to 60°C for 24 hours. Following incubation, an activity assay will be conducted. The relative activity will then be calculated to compare the impact of different storage temperatures on the activity of the two forms of lipase. The relative activity is a measure of the enzyme activity at a specific temperature relative to the highest activity observed, providing insights into how the lipase activity is influenced by storage temperature.

To evaluate the reusability of the immobilized lipase, the enzymes will undergo 10 consecutive reaction cycles, with their activities being quantified after each cycle. The activity recorded in the initial cycle will serve as the baseline, designated as 100%. The relative activity for each subsequent cycle will then be calculated in comparison to this initial value, providing a measure of the enzyme's activity retention and stability over multiple uses.

4.4 Results and Discussions

4.4.1 Characterization of MP and IE

4.4.1.1 XRD of MP, MPP, and IE

The X-ray diffraction (XRD) pattern of the Fe_3O_4 magnetic particles (MP) synthesized via the solvothermal method is depicted in Figure 4-1. Six distinctive peaks were observed at 2θ values of 30.1°, 35.4°, 43.1°, 53.4°, 57°, and 62.5°, corresponding to the crystallographic planes: (2 2 0), (3 1 1), (4 0 0), (4 2 2), (5 1 1), and (4 4 0). These peaks are consistent with the standard pattern for Fe_3O_4, confirming the successful synthesis of the cubic spinel structure of Fe_3O_4[21]. Comparative analysis of the XRD patterns of the immobilized enzyme (IE) and magnetic particles (MPs) reveals identical peak positions, indicating that the immobilization of lipase does not alter the lattice structure of the carrier.

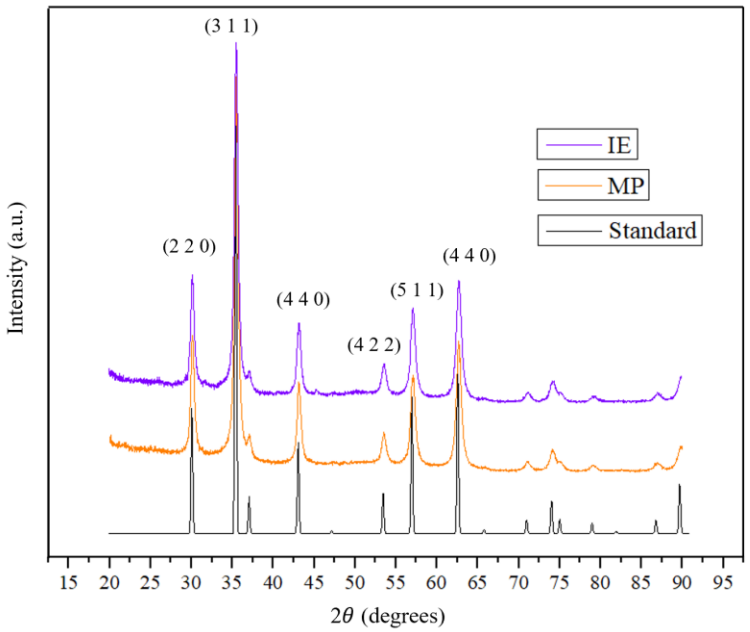

Figure 4-1 XRD pattern of Fe_3O_4 MNPs

4.4.1.2 Morphology of MP, MPP and IE

Figure 4-2 presents the Scanning Electron Microscopy (SEM) images of microparticles (MP) synthesized via the solvothermal method, the MP coated with PDA referred to as MPP, and the immobilized lipase IE. Figures 4-2A, 4-2C, and 4-2E are the micrographs of the MP, MPP, and IE under 5000 magnifications, respectively. These micrographs reveal that the majority of the particles are regular spheroids with an average diameter of 800 nm. It is worth noting that, as highlighted in the two red cycles in Figure 4-2C, there are lumps of particles in the individual particles. These lumps are probably formed due to the self-polymerization of PDA that trapped multiple particles in the matrices of PDA networks rather than coating the surfaces of individual particles. Furthermore, Figures 4-2B, 4-2D, and 4-2F are zoomed out of version of Figures 4-2A, 4-2C, and 4-2E, respectively (the scale bar in Figure 4-2F is 100 nm, distinctive from that of the 1-micron scale bars of the other micrographs). Most particles in Figure 4-2D have areas on their surfaces that are distinctive from the rest of the surface, as shown on the particles in the red cycle marked as ‘a’.

These distinctive areas are absent from the surfaces of the MP as shown in Figure 4-2B and are therefore might be related to the polymerization of PDA on the MP surface that does not cover the surface uniformly. Concurrently, it is observed that some particles do not have such distinctive areas, e.g., the one in the red circle marked ‘b’, which might be a MP particle that does not have PDA coating. These observations suggest that the coating suspension was not homogenous during the reaction and further steps, such as enhanced agitation, might be required to improve the process. As shown in Figure 4-2F, it is apparent that the immobilization of lipase on the MPP surface resulted in a pronounced change of the surface morphology and the distinctive areas on surface of MPP particles are not visible on the IE particles. These observations might indicate that the enzymes anchored onto the PDA coating on MPP surfaces are able to cover the surfaces completely to give a rather uniform surface morphology of IE.

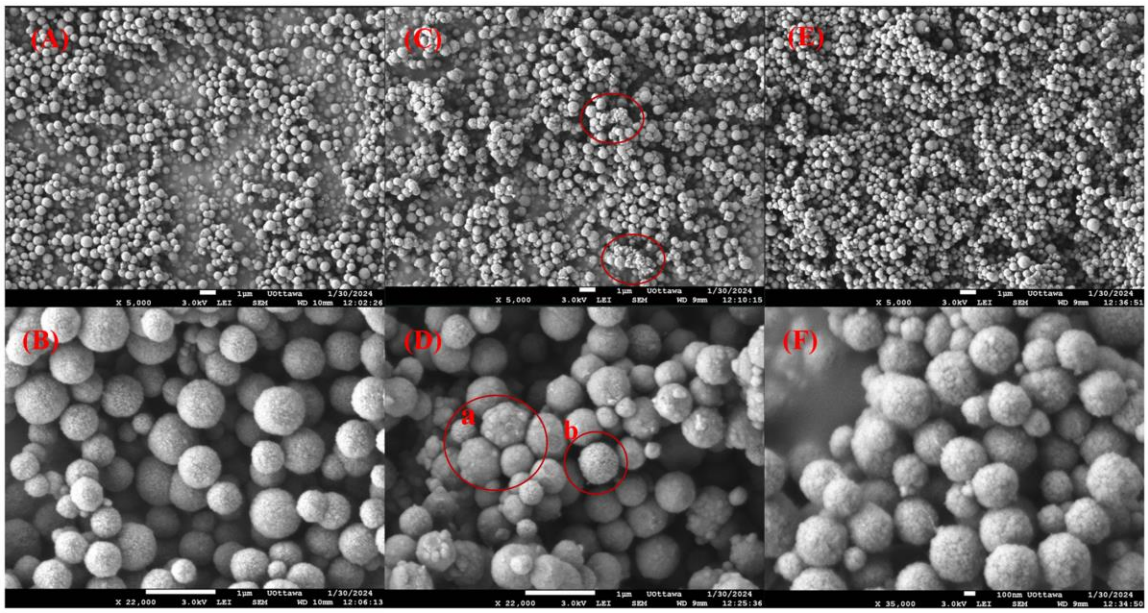

Figure 4-2 Scanning Electron Microscopy (SEM) images 5000× – original and zoom-out views of MP (A & B), MPP (C & D), and IE (E & F)

4.4.1.3 X-ray Photoelectron Spectroscopy (XPS) of MP, MPP and IE

To further confirm the successful immobilization of PDA and lipase onto the carrier surface, surface elemental analysis of MP, MPP, and IE was conducted using XPS. As shown in Figure 4-3(a), the surface of MP exhibited two prominent peaks corresponding to Fe 2p at a binding energy of 705 eV and O 1s at 528 eV. By comparing the XPS spectra of MPP and MP, it was observed that MPP contained additional elements, C and N, corresponding to binding energies of 280 eV and 396 eV, respectively. These peaks were attributed to the amino groups contributed by PDA. Meanwhile, the peak areas of Fe 2p at 705 eV and O 1s at 528 eV decreased significantly after PDA coating, indicating a reduction in the signals of Fe and O due to the formation of a shell-like structure by PDA on the surface of MP[22]. The deconvoluted N 1s spectrum, as illustrated in Figure 4-3 (b), demonstrates three chemically distinct species within the N 1s region, exhibiting binding energies at 399.0, 399.8, and 400.7 eV, which corresponded to N single bond H, CNC and $NH4^+$ species present on the surface[23]. By comparing the XPS spectra of IE and MPP, although the peaks did not increase, the peak areas of the C and N peaks were enhanced. The displacement of these C and N peaks can be attributed to lipase, indicating the successful immobilization of lipase onto the carrier[24].

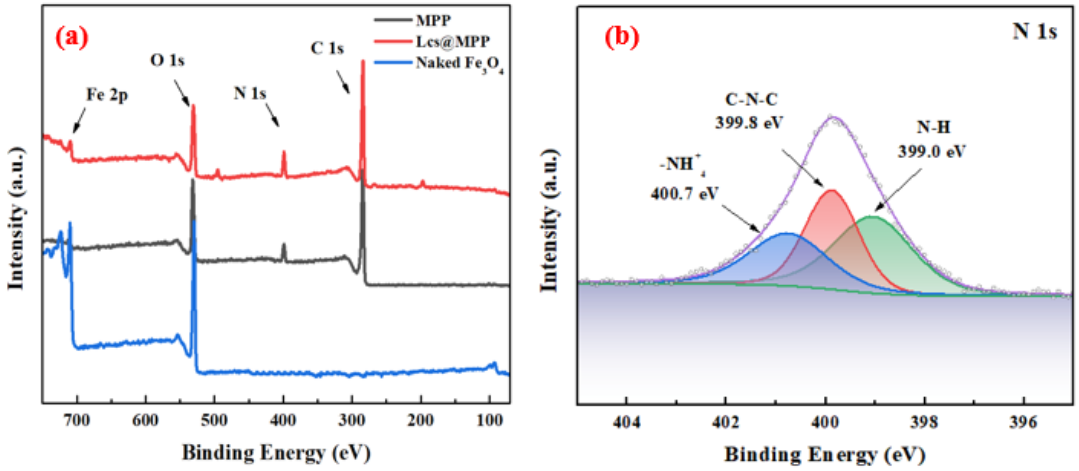

Figure 4-3 XPS spectra of (a) MP, MPP, and IE; (b) deconvolution of N 1s after coated with PDA

4.4.1.4 Structural analysis of lipase

The effectiveness of two spacer molecules, i.e., GA and PEI, are compared in this study. The aldehyde groups at the two ends of GA can react with the amino groups of lysine (Lys) residues and the hydroxyl groups of threonine (Thr), serine (Ser), and tyrosine (Tyr) residues. The amino groups of polyethyleneimine (PEI) can react with the carboxyl groups of aspartic acid (Asp) and glutamic acid (Glu) residues as well as the hydroxyl groups of threonine (Thr), serine (Ser), and tyrosine (Tyr) residues.

The lipase used in this study was *Candida antarctica* Lipase B. It is an octamer composed of 2,536 amino acid residues, with each monomer consisting of 317 amino acid residues. From Table 4-1, it can be observed that the residues capable of reacting with GA constitute 26.82% of the composition of lipase AAR, while those capable of reacting with PEI make up 23.97%.

However, knowing the composition of all ARR with functional groups capable of reacting with spacer molecules is not sufficient as the enzyme protein's folded configuration does not allow all these active groups to be fully exposed for reactions. Therefore, it is necessary to conduct an analysis of the distribution of these active groups to determine their accessibility for reactions that would lead to enzyme immobilization by covalent boding. For this purpose, we defined the surface AAR with an atom exposure level less than its **atom ratio** as "valley" residues and the surface AAR having an exposure level equal to or higher than 50% as “peak” residues. Furthermore, we define the **atom ratio** as the ratio between the number of atoms of the functional group and the total number of atoms of an AAR. For instance, the Glu molecule ($C_5H_9NO_4$) has 19 atoms and the Glu residue in a peptide has 16 atoms, whereas the functional group of the Asp residue, i.e., the carboxyl group (-COOH), has 4 atoms. The atom ratio of Glu residue is therefore 4/16, i.e., 25%. Accordingly, all the surface Glu residues with an exposure less than 25% were referred to as valley Glu residues and highlighted in blue in Figure 4-4. Similarly, all surface Glu residues with an

exposure of 50% or higher were referred to as peak Glu residues and highlighted in red in Figure 4-4.

According to our definitions, all valley residues would have at least part of their functional group inaccessible for chemical reactions and are therefore not likely to react with reagents such as the spacer molecules without substrate interference. This is reinforced by the fact that in the determination of RSA, the max SASA of an AAR, which would be substantially smaller than total surface area of all the atoms of the AAR. On the other hand, as shown in Table 4-1, Asp has the largest atom ratio of 30.8% among all the reactive AAR, and it is substantially smaller than 50%. Therefore, a peak residue is likely to have its functional group fully exposed to the attacks of other reagents and therefore participate in reactions that would lead to the immobilization of an enzyme molecule on the carrier surface through a spacer molecule, either PEI or GA. It should be noticed that however, the choice of atom ratio as the benchmark to distinguish valley residues from other surface residues assumes that all atoms have the same surface area. A modification of the benchmark to account for the surface areas of individual atoms may lead to further improvement of this approach.

Table 4-1 Peak and valley residues of reactive amino acids on the lipase surface

Functional Group	AAR	AR	Surface	Valley	Peak
Carboxyl	Asp	30.8	112	51	14
	Glu	25.0	32	22	12
	Subtotal	**NA**	**144**	**73**	**26**
Amino	Lys	14.3	72	2	11
	Subtotal	**NA**	72	2	11
Hydroxyl	Thr	14.3	216	96	33
	Ser	18.2	248	122	85

	Tyr	9.5	72	33	8
	Subtotal	**NA**	536	285	126

As shown in Table 4-1, there are in combination 126 Thr, Ser, and Tyr residues, which have hydroxyl as their functional group that could react with both the amino group of PEI and the aldehyde group of GA. More importantly, the lipase has 26 peak Glu and Asp, which have a carboxyl group that could form covalent bond with the amino group of PEI, and 11 peak Lys residues, which have an animo group that could form covalent bond with the aldehyde group of GA. Furthermore, the aldehyde group of GA is more reactive with the amino group of Lys than with the hydroxyl group of Thr, Ser, and Tyr, and the amino group of PEI is more reactive with the carboxyl groups of Glu and Asp than with the hydroxyl groups of Thr, Ser, and Tyr. It seems to be reasonable to predict that that PEI would have higher efficiency as a spacer than GA.

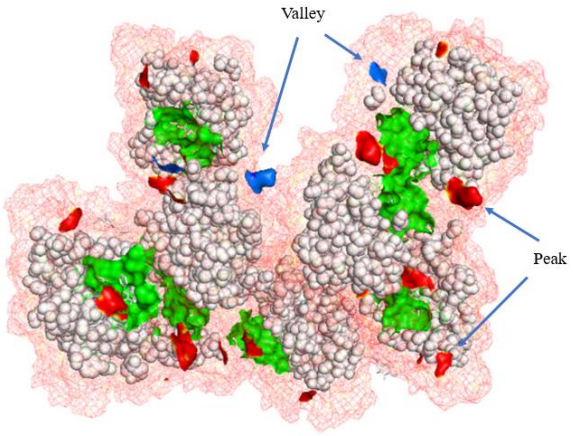

Figure 4-4 The distribution of Glu residues (carboxyl groups) on the molecular surface of lipase. (Peak Glu, valley Glu, and the active sites are labeled in red, blue, and green, respectively) [Created by Pymol]

The active sites of the lipase, which is Lipase B from *Candida antarctica* expressed by recombinant *Aspergillus niger*, includes Asp and Ser[25]. Results of the RSA analysis indicate that they are all valley residues. In other words, while they will be accessible during enzymatic reaction due to the specific configuration change induced by substate molecules, they are not accessible in reactions with the spacer molecules in immobilization due to the absence of substrate. Furthermore, Figure 4-5 illustrates the distribution of peak reactive residues, including one Glu, two Asp, and one Lys, on the same side of the active site of a monomer of the octamer lipase. It is clear that all these reactive surface AAR are well away from the active site. Therefore, the immobilization of the lipase through either PEI or GA as the spacer should not directly affect the active site.

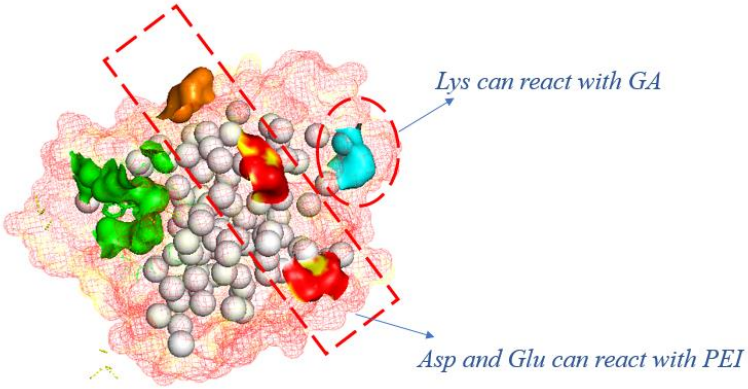

Figure 4-5 The distribution of peak Asp, Glu (carboxyl groups) and Lys (amino group) residues on the molecular surface of chain A in lipase. (Asp is labelled in red, Glu labelled in brown, Lys in blue, and active site in green)

4.4.2 Effects of key factors on lipase immobilization

The effects of factors such as spacer properties and immobilization conditions including lipase concentration, buffer pH, temperature, and time have significant impacts on the results of immobilization on efficiency of enzymatic protein loading, enzymatic activity, and specific enzymatic activity were studied.

4.4.2.1 Effect of spacer: a protein structural perspective

Two different spacers, i.e., GA and PEI, were tested in this study. GA is a cross-linking agent that possesses two aldehyde groups (Figure 4-6), which enable it to react with amino group of Lys and the hydroxyl group of Thr, Ser, and Thr residues on the surface of enzymatic proteins. This allows for the covalent anchoring of enzyme using GA as a short spacer, facilitating immobilization onto desired carriers. PEI has a branched structure that provides numerous amino groups that can react with the hydroxyl groups of Thr, Ser, and Tyr residues, and carboxyl groups of Glu and Asp residues, on the enzyme surface. Furthermore, a large variety of PEI molecules of different molecular weights are available, allowing the convenient exploration on the effects of spacer length on the efficiency of enzyme immobilization in terms of both enzymatic protein loading density and performance of IE.

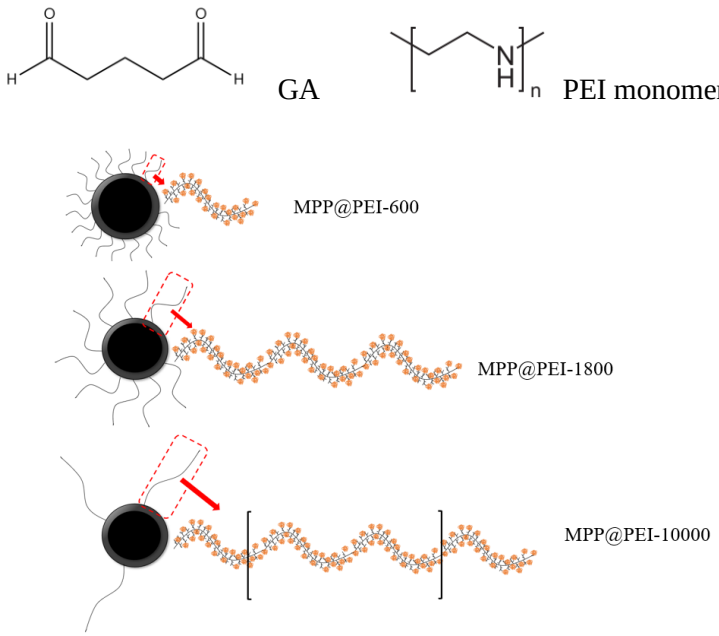

Figure 4-6 Molecular structures of GA and PEI and schematics of MPP with different PEI of different molecular weights

As shown in Figure 4-7A, the loading density of lipase was 25.05 mg/g without GA, indicating that the functional groups of the PDA coating on MPP could also immobilize lipase. Furthermore,

immobilizing lipase on to MPPG with GA concentration of 3.13 mg/mL in the grafting buffer resulted in a much higher loading density of 35.18 mg/g, which further increased to 47.57 mg/g when the GA in grafting buffer increased to 12.5 mg/mL. These results indicate MPPG had more available bonding sites, i.e., functional groups, for enzyme immobilization in comparison to MPP, which further increased when GA concentration increased from 2.5 mg/mL to 12.5 mg/mL. As the concentration of GA increased from 0 mg/mL to 12.5 mg/mL, the enzymatic activity per unit of magnetic particles (MP) increased from 0.19 to 0.25 U/mg. This trend aligns with findings reported in the literature, where low GA concentrations are associated with low loading density and activity[26]. However, in terms of specific activity, a decreasing trend was observed as the GA concentration increased, as shown in Figure 4-7B. A hypothetic explanation of this observation is that GA residues on MPPG surface might be able to bind to multiple AAR on enzyme surface, which in turn alters the enzyme's configuration, leading to the reduction of either the accessibility or affinity of the active sites of enzyme to substrate molecules or both[27].

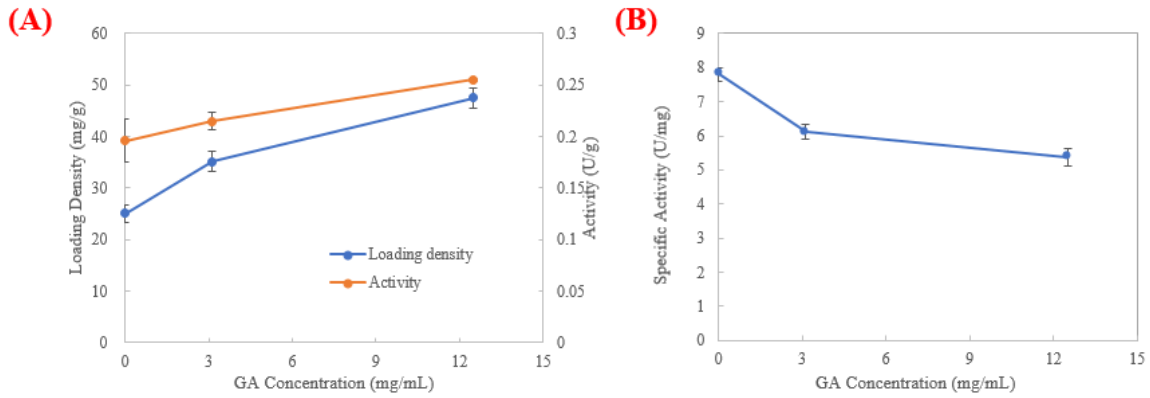

Figure 4-7 Effect of GA concentration on (A) loading density and specific activity IE (U/g), and (B) specific activity.

The results of immobilizing lipase using three different lengths of PEI are presented in Figure 4-8. As shown in Figure 4-8(A), the loading density of any of the three PEIs increased with increasing

PEI concentration until plateaued at a maximum loading density, which was 104, 70, and 60 mg/g for PEI-600, PEI-1800, and PEI-10000, respectively. The decrease in maximum loading density with increasing molecular weight (Mw) of PEI might be due to the entanglement of PEI on the carrier surface, which reduces the number of PEI molecules that could be grafted on to a unit MP surface area. Interestingly, Figures 4-8B and 4-8C show that PEI-18000 had the highest specific activity IE (enzymatic activity per unit mass of IE) and specific activity when compared with PEI-600 and PEI-10000. When the immobilization buffer contains 5%wt PEI, the specific activity IE reached 1.85 U/g. Additionally, IE with PEI-1800 also exhibited the highest specific activity, which was 28.4 U/mg. The specific activities of the free enzyme (FE) and immobilized enzymes (IEs) using GA and three different lengths of PEI are presented in Table 4-2. As indicated in Table 4-2, immobilization with PEI-1800 retained 66% of the specific activity.

The results also indicate that increasing the loading density enhances the quantity of immobilized enzymes on the carrier surface. However, excessive loading density can lead to enzyme crowding and steric hindrance, thereby impeding substrate binding and catalytic efficiency. Thus, achieving an optimal balance between loading density and activity is crucial. Moreover, an appropriate spacer length facilitates favorable interactions between immobilized enzymes and substrates, thereby improving the accessibility of active sites.

As shown in Figure 4-8 (A), the loading density, which was defined as the mass of lipase loading on to per unit mass of MP, of all three PEI spacers, i.e., PEI-600, PEI-1800, and PEI-10000, increased rapidly in the spacer concentration range of 0-2.5 wt% and plateaued beyond 2.5 wt% spacer. The data show that excessive PEI did not result in the continuous increase in loading density or enzymatic activity per unit mass of MP, which are compatible with literal data[28]. These could be attributed to either or both of the following two reasons: 1) when the number of PEI molecules per unit MPP surface increased beyond certain threshold, the amino groups on the side chains of PEI residues became less accessible for enzyme immobilization due to steric hindrance; and 2) the

number of PEI residues on MPP stop increasing with PEI concentration in the grafting buffer beyond certain threshold due to limited biting sites on the MP surface. It is worth noting that the loading density of all three PEI plateaued approximately the same mass concentration, i.e., 2.5 wt% of PEI. Given that the Mw of the three PEI are vastly different, it means they plateaued at hugely different molar concentration, in other words, number of PEI molecules available per unit mass of MP. This is probably related to the fact that PEI molecules are branched polymers of ethylamine ($CH_3CH_2NH_2$), which contain a large number of side amino groups. Therefore, the same mass of PEI may have approximately the same number of amino groups even though the number of molecules would vary with their Mw. This observation suggests that lipase is capable of loading not only to the end amino group but also to various side amino groups of the branched PEI molecules (Figure 4-6).

As shown in Figure 4-8B, PEI-1800 had the highest specific activity IE, making it the best choice among the three PEIs in terms of practical application while the loading densities of PEI-1800 and PEI-10000 were quite close to each other, indicating that the loading density was strongly dependant on PEI molecular weight in the range of 600-1800 Da but relative independent of PEI Mw beyond 1800 Da. Figure 4-8C shows that PEI-600 had the lowest specific activity while PEI-1800 had the highest with PEI-10000 coming as a close second highest. This phenomenon could be tentatively attributed to the self-entanglement of PEI on the carrier surface.

Comparing the results of immobilizing lipase using GA (Figure 4-7) or PEI as the spacer (Figure 4-8), it is evident that all three PEI molecules are better than GA as the spacers as with drastically higher loading density and specific activities. The large loading density of PEI may be attributed to 1) the branched structure of PEI residues on the surface of MPPP could provide vastly more sites for lipase binding than GA residues on MPPG surface; and 2) there are 26 peak AAR containing carboxyl group are likely reactive with the amino groups of PEI residues on the surface of MPPP

but only 11 peak AAR containing amino group that is highly reactive with the aldehyde group of GA residues on the MPPG surface (Table 4-1).

Furthermore, the large specific activity of PEI-spaced IE in comparison to that of GA-spaced might be hypothetically explained by the long PEI residues providing more flexibility to the anchored lipase for easy access to substrates; and 2) the different bonding sites for PEI versus that for GA (Figure 4-5) might affect the configuration of lipase in a way that enhanced the activity of enzyme.

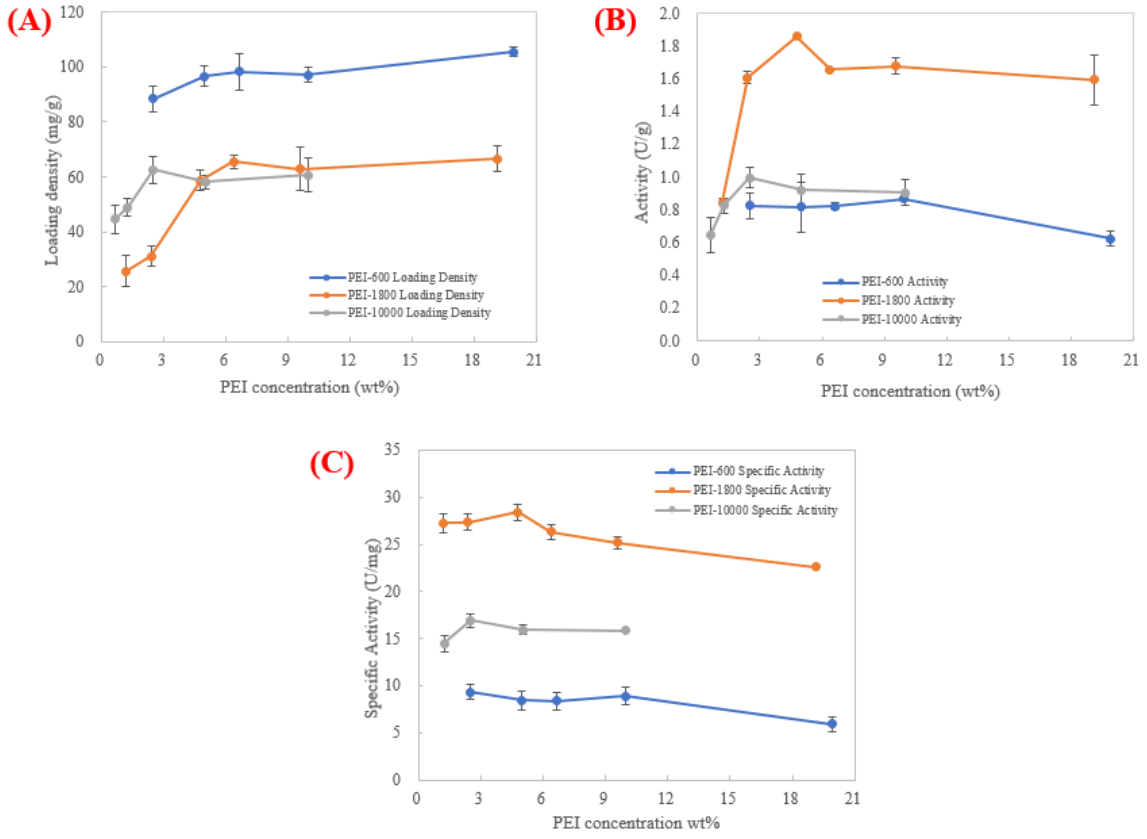

Figure 4-8 Effect of PEI length and concentration on loading density (A), activity (B), and specific activity (C) of immobilized lipase

Table 4-2 Immobilization results of IEs and SA of FE

Carrier	LD (mg/g)	SA*IE* (U/g)	SA (U/mg)
FE	-	-	42.68
MPP	25.05	0.19	7.8
MPP-GA	47.57	0.25	6.10
MPPP-600	105.43	0.87	9.34
MPPP-1800	65.42	1.86	28.40
MPPP-10000	62.47	0.99	16.90

4.4.2.2 Effects of lipase concentrations

From Figure 4-9, it can be observed that the loading density increases with the increase of lipase initial concentration. The maximum loading density was achieved when the lipase concentration was 8.91 mg/ml. Similarly, the enzymatic activity also increased with increasing initial lipase concentration and reached a plateau. The maximum activity is achieved at a lipase concentration of 4.45 mg/ml, which is 1.44 U/g. Simultaneously, with an increase in lipase concentration, there is a gradual decrease in specific activity. This is because the sites available for enzyme attachment on the carrier surface are fixed. As the initial enzyme concentration increases, these sites become progressively occupied until the surface-bound enzyme reaches saturation. Simultaneously, with the increase in the enzyme, total activity also gradually rise. However, due to the accumulation of the enzyme on the carrier surface, the active sites of the enzyme become shielded, resulting in a declining trend in specific activity. This trend is consistent with the findings of previous studies, including the work conducted by Yao et al[29].

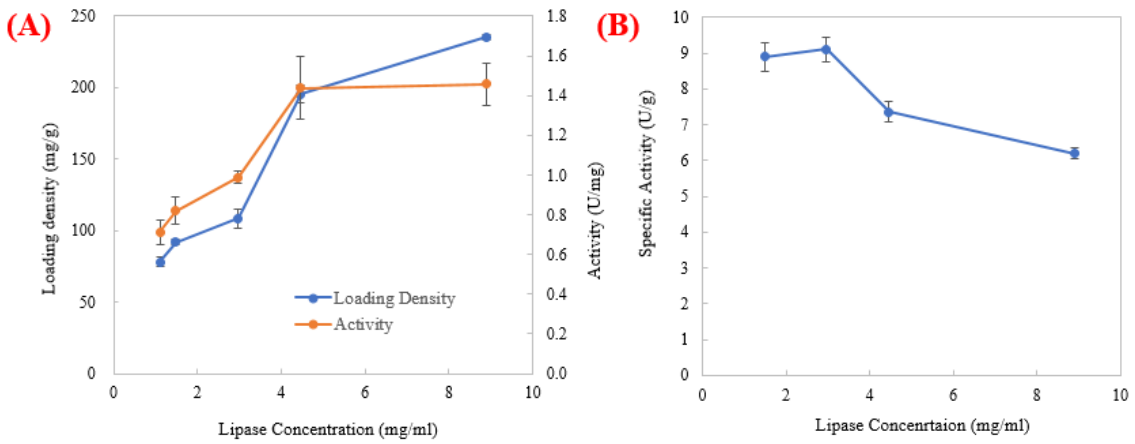

Figure 4-9 Effect of lipase concentration on loading density, total activity and specific activity

4.4.2.3 Effects of pH

During the immobilization process, pH is a critical influencing factor. Our data show that pH had a minor impact on loading density (Figure 4-10A) but a significant effect on the specific activity of the enzyme (Figure 4-10B). These data are compatible with those reported by Panzavolta et al.[30] This is due to the varying degrees of enzyme ionization under different pH conditions. At an appropriate pH, it assists in maintaining the enzyme's conformation. Regarding lipase, following the "pH memory" theory, when transitioning from the aqueous phase to the organic phase, the lipase retains its ionized state, thus preserving the configuration of the enzyme. Hence, there is a need to investigate the optimal pH value for immobilizing lipase in the aqueous phase. To determine the optimal pH for immobilizing lipase, the pH was varied from 5 to 10, and the changes in loading density and total activity were observed in Figure 4-10. Under other constant conditions, the loading density does not vary significantly with the change of pH, while the total activity decreases as the pH increases. As depicted in Figure 4-11, there is a notable variation in specific activity with changes in pH. When the pH transitions from 5 to 6, there is a significant increase in specific activity. However, as the pH continues to increase, there is a gradual decline in specific activity.

The optimal pH for immobilization was found to be pH 6. This trend aligns with previous findings reported in literature.[30,31].

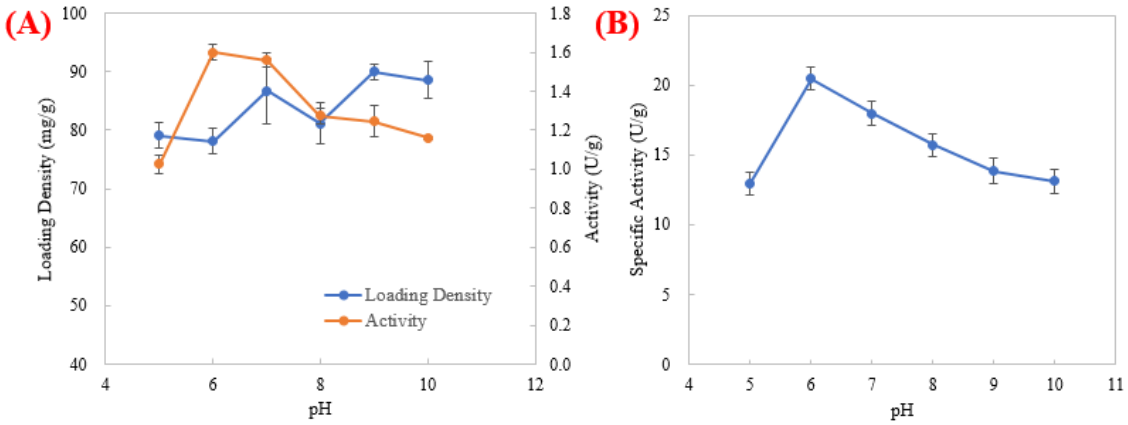

Figure 4-10 Effect of immobilization pH on (A) loading density, activity and (b) specific activity

4.4.2.4 Effect of immobilization time

The immobilization time is also a crucial factor influencing the immobilization results. During the immobilization process, an excessively long duration will cease to change the loading density, whereas may lead to inadequate immobilization. Therefore, we examined the effects of immobilization time ranging from 5 to 20 hours on the loading density, total activity, and specific activity of the immobilized enzyme. The effect of immobilization time on the immobilization efficiency is shown in Figure 4-11 (A). The results demonstrate that the loading density increases with immobilization time and reaches its maximum at 15 hours before stabilizing. However, the total activity observed maximum at 5 hours and decreases with longer immobilization time. The impact of immobilization time on specific activity is most obviously, as illustrated in Figure 4-11 (b). When the immobilization time is 5 hours, the specific activity can reach 314.86 U/mg. However, as the immobilization time increases gradually, there is a sharp decline in specific activity. This result is consistent with that reported by Badoei-dalfard et al.[32]. They explain this phenomenon as

follows: with an increase in the immobilization duration, the accumulation of lipase on the carrier surface grows, resulting in increased steric hindrance among them. This increased hindrance enhances the resistance to substrate diffusion, making it challenging for the substrate to bind and react at the enzyme's active sites. Consequently, this diminishes both the total activity and specific activity.

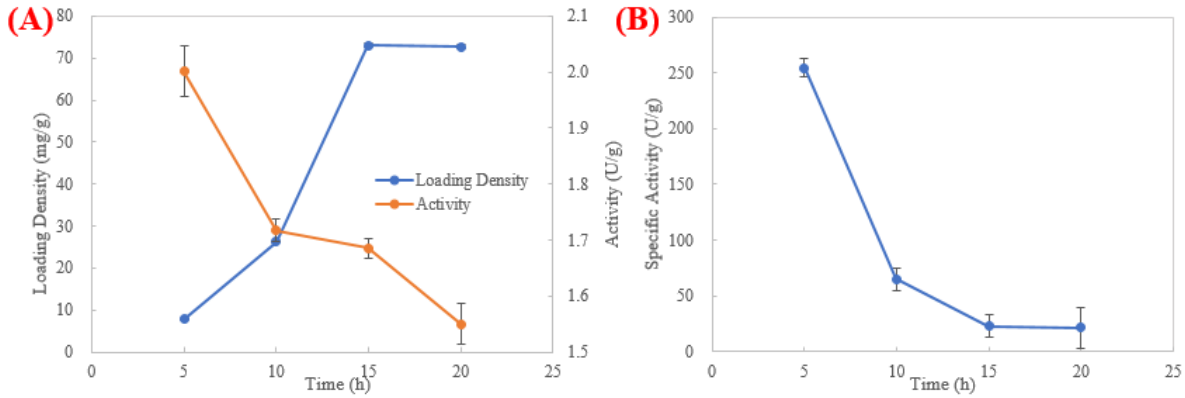

Figure 4-11 Effect of immobilization time on (A) loading density, activity; and (B) specific enzyme activity

4.4.2.5 Effect of temperature

The temperature of enzyme immobilization significantly influences the outcome. A low temperature might lead to insufficient activation of the enzyme protein and reaction groups on the carrier surface, resulting in slower reaction rates. Conversely, higher temperatures facilitate increased contact between the enzyme and spacer in the system, thus accelerating the immobilization process. However, excessively high temperatures may cause enzyme denaturation and deactivation[33]. To investigate the impact of temperature on immobilization, we separately examined the effects of temperatures ranging from 5 to 65 ℃ on the loading density, total activity, and specific activity.

As shown in Figures 4-12, within the temperature range of 5 to 40 ℃, there is a gradual increase in the activation of reaction groups as the temperature rises, leading to a corresponding increase in the loading density. During the 5-10 ℃ range, there is a slight increase in total activity, with the immobilized lipase displaying the maximum total activity at 10 ℃. However, as the temperature continues to increase beyond this point, the activity notably decreases. In terms of specific activity, its value consistently diminishes with the rising temperature.

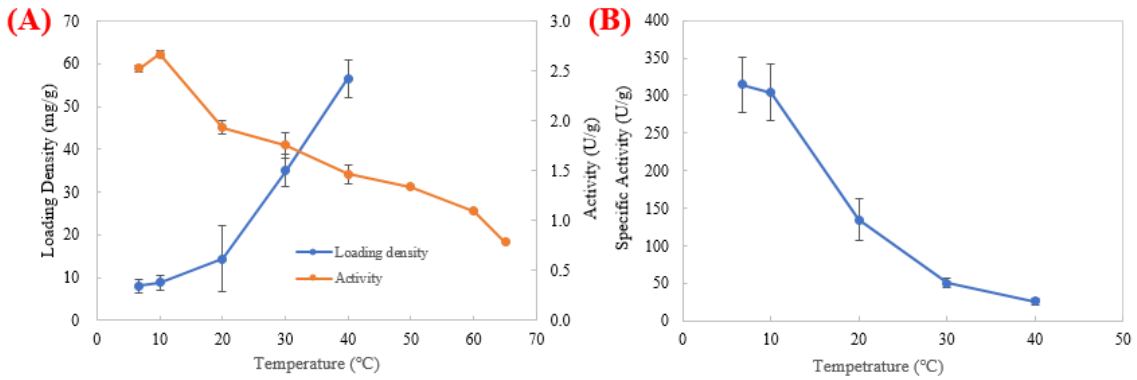

Figure 4-12 Effect of immobilization temperature on (A) loading density, activity and (B) specific activity

4.4.3 Performance of immobilized lipase

4.4.3.1 Optimum temperature range

After immobilization, the optimum temperature range of lipase can change. Typically, enzyme immobilization can provide a stable microenvironment for the enzyme, making it less likely to undergo protein denaturation and thus lose activity at high temperatures. However, immobilization can increase the diffusion resistance of substrates to reach the active site, and with increasing temperature, the possibility of collisions between substrate and enzyme molecules also increases, which can accelerate the enzymatic reaction rate[34]. Therefore, considering these three factors, it is necessary to consider the changes in the optimum reaction temperature and temperature range after

immobilizing the enzyme using different lengths of spacers. In this part, the optimum temperature range of free lipase and immobilized lipase with three different lengths (PEI-600,1800 and 1000) were compared from the temperature range from 10-60℃.

In Figure 4-13 (A), within the temperature range of 10 to 50 ℃, the relative activity of both free and three types of immobilized lipases increases with increasing temperature. In the temperature range of 50 to 60 ℃, the relative activity of free lipase decreases significantly, while no significant change is observed for the immobilized lipases. Between 40 and 60 ℃, the relative activity of all three immobilized lipases remains above 90%. These suggests that immobilized lipase exhibits better resistance to temperature effects compared to free lipase. For the lipase immobilized using three different lengths of spacers, the relative activity of the lipase immobilized with PEI-600 was consistently higher than the other two, indicating that the lipase immobilized with PEI-600 has better temperature stability. The immobilization process can enhance the protein's structural "rigidity," rendering the immobilized lipase more stable compared to its free form. Among the three spacers, PEI-600 is a shorter spacer, allows the immobilized lipase to experience relatively less "swaying" in solution than the lipase immobilized on longer spacers. This reduced swaying exposes the immobilized lipase less to the solution environment, making the use of PEI-600 as a spacer the most suitable for temperature adaptability.

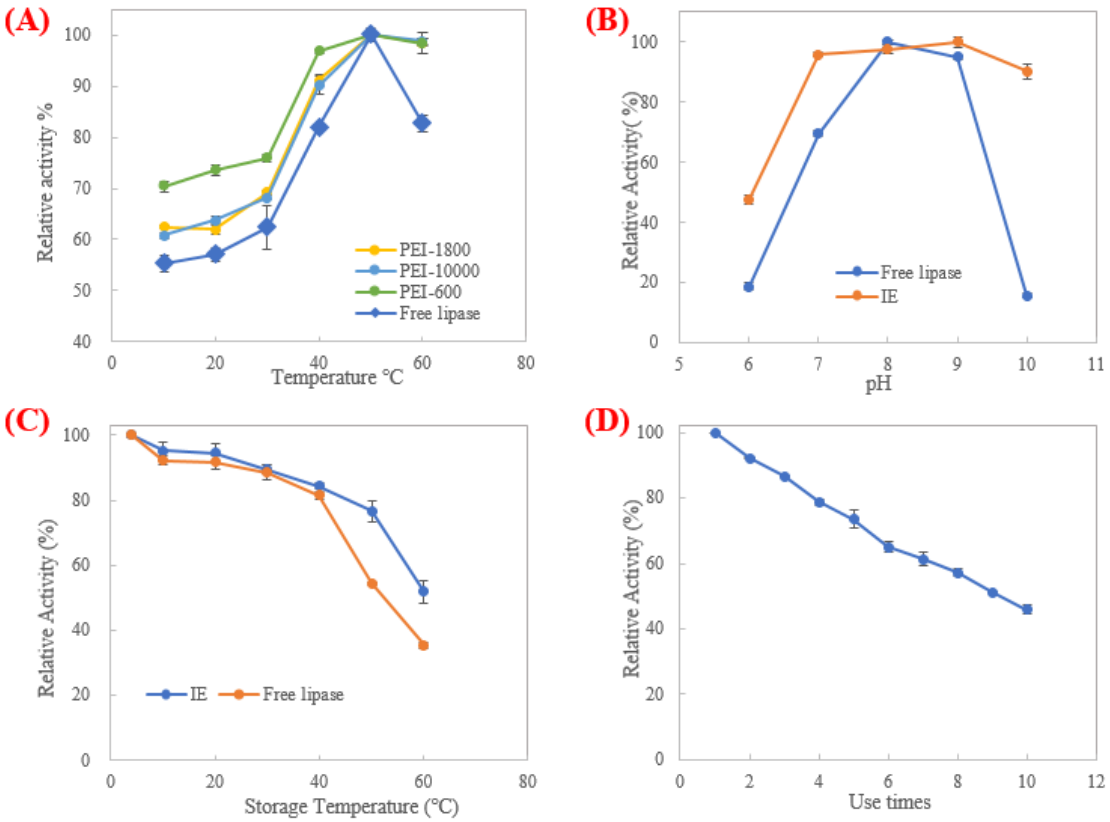

Figure 4-13 Immobilized and free lipase (A) temperature and (B) pH stability; (C) thermal storage stability and (D) IE reusability

4.4.3.2 Optimum pH range

The pH stability of the enzyme is also a crucial factor for assessing the performance of enzyme immobilization. pH can alter the ionization state of enzyme molecules, impacting their configuration and conformation. Enzyme can only exhibit optimal activity when their active sites are under their optimum pH. Sensitivity of enzyme molecules to pH changes inevitably affects their catalysis on substrates[34]. To examine the pH stability of the immobilized lipase, we studied its relative activity within the pH range of 6 to 10 and compared it with the free lipase.

The pH stability of the free enzyme and the immobilized enzyme is illustrated in Figure 4-13(B). After immobilization, there is a notable improvement in the enzyme's pH stability, with a wider threshold pH range. Specifically, for the immobilized lipase, within the pH range of 7-9, the relative activity remains above 95%. Moreover, within the pH range of 6-10, the immobilized lipase exhibits enhanced pH stability compared to the free lipase. At pH 6, the relative activity of the free lipase is 18.61%. At pH 10, the relative activity of the free lipase decreases to 15.77%, while the immobilized enzyme maintains a 90% activity level. After immobilization, the pH stability of the lipase improves, which can be attributed to the "pH memory" theory: the enzyme is fixed under different pH conditions, preserving the corresponding conformations. Then, when the enzyme performs hydrolysis under varying pH conditions, the environment impacts the dissociation of functional groups within the active center differently, altering its conformation and subsequently reducing its catalytic activity[35].

4.4.3.3 Temporal stability

Thermal storage stability is important in enzyme immobilization as it shows how well the enzyme can maintain its activity at high temperatures. Immobilization can create a stable environment for the enzyme, reducing the chance of protein denaturation and loss of activity at high temperatures. In this part, relative activity of free and immobilized lipase was tested after storing them at different temperatures (10-60 ℃) for 24 hours. Figure 4-13(C) demonstrates that storing free and immobilized lipase at 10℃ is the most favorable for maintaining their relative activity, while as temperature increases, their relative activity decreases. Additionally, free lipase exhibits a faster decline in relative activity above 40℃. This immobilization method could enable lipase to maintain its activity at high temperatures. This may be due to the protection of the conformation of lipase through immobilization, which restricts the conformational mobility and thus prevents thermal denaturation[36].

4.4.3.4 Reusability (Operational stability)

Reusability is an important aspect of enzyme immobilization because it allows for the repeated use of the immobilized enzyme, leading to cost savings and increased efficiency. Reusability of immobilized enzymes can gradually decrease due to various factors. These factors may include enzyme leaching, inactivation of the enzyme during reaction cycles. Therefore, considering the potential industrial applications, reusability is an important parameter to evaluate the effectiveness of enzyme immobilization[37]. Figure 4-13 (D) shows the reusability of immobilized lipase, and it can be observed that the relative activity of the immobilized lipase gradually decreases with an increase in the number of cycles. After 10 cycles, the relative activity decreases to 45.9% of the initial value.

4.5. Conclusions

Through systematic optimization of immobilization conditions, we successful immobilized a lipase on magnetic particles functionalized by PDA using PEI or GA as spacer. The immobilized lipase exhibited enhanced thermal stability, reusability, and a broader operational pH and temperature ranges compared to the free lipase. The analyses of enzyme 3D structure confirm that the active sites of the enzyme would be inaccessible in immobilization reactions due to the lack of substrate induction and that PEI would be a more efficient spacer than GA. Furthermore, experiments with PEI of different molecular weights indicate that the spacer length and flexibility may affect the enzyme immobilization efficiency (loading density) and specific activity of immobilized enzymes. The optimal conditions leading to the maximal activity of IE are determined to be 1.86 wt% PEI-1800, lipase concentration 4.25 mg/mL, pH 6.0, an immobilization duration 5 hours, and immobilization temperature of 10°C.

Overall, this study provides valuable insights into the immobilization of lipase on PDA-modified magnetic microparticles, highlighting the influence of PEI molecular weight and immobilization conditions. These findings contribute to the advancement of enzymatic processes, fostering the

development of more efficient and sustainable industrial applications. Further research in this area holds great potential for optimizing enzyme immobilization techniques and expanding their use in diverse industrial sectors

4.6 References

1. Filho, D. G., Silva, A. G. & Guidini, C. Z. Lipases : sources , immobilization methods , and industrial applications. 7399–7423 (2019).
2. Kapoor, M. & Gupta, M. N. Lipase promiscuity and its biochemical applications. *Process Biochemistry* **47**, 555–569 (2012).
3. Ismail, A. R. & Baek, K. International Journal of Biological Macromolecules Lipase immobilization with support materials , preparation techniques , and applications : Present and future aspects. *Int J Biol Macromol* **163**, 1624–1639 (2020).
4. Tan, T., Lu, J., Nie, K., Deng, L. & Wang, F. Biodiesel production with immobilized lipase : A review. *Biotechnol Adv* **28**, 628–634 (2010).
5. Fact, C., Chandra, P., Singh, R. & Arora, P. K. *Microbial Lipases and Their Industrial Applications : A Comprehensive Review*. *Microbial Cell Factories* (BioMed Central, 2020). doi:10.1186/s12934-020-01428-8.
6. Feng, Y. *et al.* Recent advances in enzyme immobilization based on novel porous framework materials and its applications in biosensing. **459**, (2022).
7. Gennari, A., Führ, A. J., Volpato, G., Fernanda, C. & Souza, V. De. Magnetic cellulose : Versatile support for enzyme immobilization - A review. *Carbohydr Polym* **246**, 116646 (2020).
8. Bilal, M., Zhao, Y., Rasheed, T. & Iqbal, M. N. International Journal of Biological Macromolecules Magnetic nanoparticles as versatile carriers for enzymes immobilization : A review. **120**, 2530–2544 (2018).
9. Abreu, I. *et al.* Journal of Pharmaceutical and Biomedical Analysis Magnetic particles for enzyme immobilization : A versatile support for ligand screening. *J Pharm Biomed Anal* **204**, 114286 (2021).
10. Datta, S. & Christena, L. R. Enzyme immobilization : an overview on techniques and support materials. 1–9 (2013) doi:10.1007/s13205-012-0071-7.
11. Torres, R. RSC Advances crosslinker and a versatile tool in enzyme. 1583–1600 (2014) doi:10.1039/c3ra45991h.
12. Khoobi, M. *et al.* Polyethyleneimine-modi fi ed superparamagnetic Fe 3 O 4 nanoparticles for lipase immobilization : Characterization and application. **150**, 77–86 (2015).

13. Deng, H. *et al.* Monodisperse magnetic single-crystal ferrite microspheres. *Angewandte Chemie - International Edition* **44**, 2782–2785 (2005).
14. Deng, Y. *et al.* Preparation of iron-based MIL-101 functionalized polydopamine@Fe3O4 magnetic composites for extracting sulfonylurea herbicides from environmental water and vegetable samples. *J Sep Sci* **41**, 2046–2055 (2018).
15. Solvent-Accessible Surfaces of Proteins and Nucleic Acids Author (s): Michael L . Connolly. **221**, 709–713 (2014).
16. Richards, F. M. Areas, volumes, packing, and protein structure. (1977).
17. Barth, M., Bender, J., Kundlacz, T. & Schmidt, C. Evaluation of NHS-Acetate and DEPC labelling for determination of solvent accessible amino acid residues in protein complexes. *J Proteomics* **222**, 103793 (2020).
18. Tien, M. Z., Meyer, A. G., Sydykova, D. K., Spielman, S. J. & Wilke, C. O. Maximum allowed solvent accessibilites of residues in proteins. *PLoS One* **8**, (2013).
19. Wang, X. *et al.* Immobilization of alcalase on polydopamine modified magnetic particles. *Biochem Eng J* **207**, 109310 (2024).
20. Zhu, Y. *et al.* Covalent immobilization of porcine pancreatic lipase on carboxyl-activated magnetic nanoparticles : Characterization and application for enzymatic inhibition assays. *Materials Science & Engineering C* **38**, 278–285 (2014).
21. Wang, S. nan *et al.* Immobilized alcalase alkaline protease on the magnetic chitosan nanoparticles used for soy protein isolate hydrolysis. *European Food Research and Technology* **239**, 1051–1059 (2014).
22. Ren, Y. *et al.* Facile , high efficiency immobilization of lipase enzyme on magnetic iron oxide nanoparticles via a biomimetic coating. (2011).
23. Ding, C., Sun, H., Ren, J. & Qu, X. Analytica Chimica Acta Immobilization of enzyme on chiral polyelectrolyte surface. *Anal Chim Acta* **952**, 88–95 (2017).
24. Xiao, Z., Zhao, Z., Jiang, B. & Chen, J. International Journal of Biological Macromolecules Enhancing enzyme immobilization : Fabrication of biosilica-based organic-inorganic composite carriers for efficient covalent binding of. *Int J Biol Macromol* **265**, 130980 (2024).
25. Park, A. *et al.* Structural and experimental evidence for the enantiomeric recognition toward a bulky sec-alcohol by Candida antarctica lipase B. *ACS Catal* **6**, 7458–7465 (2016).

26. Zhou, X. *et al.* Immobilization of lipase in chitosan-mesoporous silica material and pore size adjustment. *Int J Biol Macromol* **235**, 123789 (2023).
27. Silveira, T. R. *et al.* An efficient decolorization of methyl orange dye by laccase from Marasmiellus palmivorus immobilized on chitosan-coated magnetic particles. *Biocatal Agric Biotechnol* **30**, 1–10 (2020).
28. Virgen-Ortíz, J. J. *et al.* Polyethylenimine: A very useful ionic polymer in the design of immobilized enzyme biocatalysts. *J Mater Chem B* **5**, 7461–7490 (2017).
29. Wen, L. *et al.* Insight into immobilization efficiency of Lipase enzyme as a biocatalyst on the graphene oxide for adsorption of Azo dyes from industrial wastewater effluent. *J Mol Liq* **354**, 118849 (2022).
30. Panzavolta, F. *et al.* Acetylenic polymers as new immobilization matrices for lipolytic enzymes. *J Mol Catal B Enzym* **32**, 67–76 (2005).
31. de Andrades, D. *et al.* Immobilization and stabilization of different β-glucosidases using the glutaraldehyde chemistry: Optimal protocol depends on the enzyme. *Int J Biol Macromol* **129**, 672–678 (2019).
32. Badoei-dalfard, A., Shahba, A., Zaare, F. & Sargazi, G. International Journal of Biological Macromolecules Lipase immobilization on a novel class of Zr-MOF / electrospun nanofibrous polymers : Biochemical characterization and efficient biodiesel production. *Int J Biol Macromol* **192**, 1292–1303 (2021).
33. Parandi, E. *et al.* Biodiesel production from waste cooking oil using a novel biocatalyst of lipase enzyme immobilized magnetic nanocomposite. *Fuel* **313**, 123057 (2022).
34. Zhao, J., Ma, M., Yan, X., Zhang, G. & Xia, J. Green synthesis of polydopamine functionalized magnetic mesoporous biochar for lipase immobilization and its application in interesterification for novel structured lipids production. *Food Chem* **379**, 132148 (2022).
35. Elias, N. *et al.* Structure and properties of oil palm-based nanocellulose reinforced chitosan nanocomposite for efficient synthesis of butyl butyrate. *Carbohydr Polym* **176**, 281–292 (2017).
36. Mehrasbi, M. R., Mohammadi, J., Peyda, M. & Mohammadi, M. Covalent immobilization of Candida antarctica lipase on core-shell magnetic nanoparticles for production of biodiesel from waste cooking oil. *Renew Energy* **101**, 593–602 (2017).

37. de Andrade Silva, T., Keijok, W. J., Guimarães, M. C. C., Cassini, S. T. A. & de Oliveira, J. P. Impact of immobilization strategies on the activity and recyclability of lipases in nanomagnetic supports. *Sci Rep* **12**, 1–11 (2022).

Chapter 5 Immobilization of lipases on magnetic particles using polyethyleneimine as spacer： effects of spacer length and protein structure

Xinyue Wang[1], Xiao Hong[2], Jason Zhang[1], Christopher Q. Lan[1,]*

[1]: *Department of Chemical and Biological Engineering, University of Ottawa, 161 Louis Pasteur Private, Ottawa, Ontario, Canada, K1N 6N5*

[2]: *Department of Cellular and Molecular pharmacology, University of California, San Francisco, 600 16th street, N316, San Francisco, California, USA, 94158*

* Corresponding author, Department of Chemical and Biological Engineering, University of Ottawa, 161 Louis Pasteur Private, Ottawa, Ontario, Canada

The content of this chapter will be submitted.

5.1 **Abstract**

In this study, we strategically selected three branched polyethyleneimine (PEI) of different molecular weights (Mw) and two lipases of different structures to study the effects of spacer length and protein structure on enzyme immobilization. It was demonstrated that a *Candida antarctica* sourced lipase (LCA) (270.94 kDa), was more sensitive to steric hindrance in the immobilization process but more accessible to substrate once being immobilized in comparison to a *Candida rugosa* sourced lipase (LCR) (57.78 kDa). Using solvent accessible surface analysis and introducing a new concept, atom ratio as benchmark, it was found that all active site residues of LCA were valley residues while the glutamate residue of one of the two active sites of LCR was a peak residue. Furthermore, LCR was found to have 12.5% more peak reactive residues than LCA. These findings were used to explain the sensitivity of LCR to the concentration of spacers in immobilization and its better immobilization efficiency in terms of both loading density and specific activity of immobilized LCR (ILCR) than that of immobilized LCA (ILCA). It was found that the shortest PEI (600 Da) was able to immobilize the largest amount of lipase, likely due to its smaller steric hindrance and therefore better accessibility of the side-chain functional groups of PEI for binding of lipases. On the other hand, ILCA with PEI (1800 Da) and ILCR with PEI (10,000 Da) had the highest specific activities and activities per unit mass immobilized enzyme, due to the interplay between multiple factors. Optimization of LCR immobilization was carried out using response surface methodology (RSM). The optimized conditions, i.e., 0.5 wt% LCR concentration, 29°C, pH 6.9, and 2-hours immobilization, resulted in enhanced thermal, pH, and operational stabilities, broader pH and temperature ranges, and reusability in comparison to the free lipase. The ILCR retained 30% of its activity after nine reuse cycles.

Key Words: Lipase immobilization, Polydopamine-modified magnetic microparticles, Polyethyleneimine, Response surface methodology, Surface modification

5.2 Introduction

Immobilization of enzymes onto solid surfaces to produce immobilized enzymes (IE) have proven to be an important approach to enhance enzyme stability, separability, process controllability, and enable the applications that are not available with free enzymes, e.g., biosensors and reuse of enzymes[1].

Lipase (triacylglycerol acyl hydrolase, EC 3.1.1.3) catalyzes the hydrolysis of triglycerides into free fatty acids, diacylglycerol, monoacylglycerol, and glycerol[2]. It also has high efficiency in catalyzing reactions such as esterification, alcoholysis, and transesterification. These functionalities find lipase extensive applications in industries such as foods, cosmetics, pharmaceuticals, and biodiesels[3–5]. Enzymes are characterized by their high activity and selectivity, functioning under mild experimental and environmental conditions. However, the high cost of enzymes remains a major barrier to their widespread industrial use[6]. To reduce production costs, immobilization techniques are frequently employed, wherein lipase is anchored onto suitable carriers, enabling its repeated use. Immobilization offers several advantages, including improved separability, reusability, and enhanced stability of the lipase. Common immobilization methods include physical adsorption, covalent bonding, crosslinking, and entrapment on solid support materials[7].

Magnetic particles (MP), known for their excellent magnetic responsiveness, straightforward synthesis, controllable size, large surface area, low cost, and ease of modification, are widely used as supports for enzyme immobilization[8]. These materials can be employed for immobilization either through direct physical adsorption or by surface modification. However, enzymes immobilized via direct physical adsorption may suffer from weaker interactions, leading to insufficient immobilization and potential enzyme leaching[9,10]. Additionally, enzyme aggregation on the carrier surface may result in steric hindrance, shielding active sites and reducing enzyme

activity[11]. Therefore, further research is essential to explore the surface modification of magnetic microparticles by grafting specific spacers, aiming to minimize steric hindrance and maintain the activity of immobilized enzymes by addressing issues related to active site shielding. Polyethyleneimine (PEI) is a branched polymer available in various molecular weights, containing numerous amino groups that can react with carboxyl and hydroxyl groups on the enzyme surface, facilitating enzyme immobilization onto the PEI[12]. Substantial research has demonstrated the effectiveness of PEI in immobilizing lipase onto carriers. However, there is limited research directly comparing the effects of different PEI lengths on the immobilization of various lipases.

In this investigation, we studied the immobilization of two lipases on polydopamine (PDA)-modified MP polyethyleneimine (PEI) of three different molecular weights and therefore molecular lengths as spacers. Bioinformatic analysis was employed to compare the types and distribution of surface amino acid residues of the lipases, followed by a discussion on the likelihood of these lipases reacting with PEI. Experimental studies were then conducted to determine which lipase retained higher activity when immobilized with PEI as a spacer. Subsequently, we examined the effects of different molecular weights and concentrations of PEI on the immobilization outcomes. In the next phase, response surface methodology (RSM) was used to first screen the key variables, such as initial lipase concentration, immobilization time, temperature, and pH, that significantly influence the immobilization process. RSM was then employed to optimize these variables, develop a corresponding predictive model, and determine the optimal conditions for lipase immobilization.

5.3 Materials and methods

5.3.1 Materials

Two lipases (one sourced from *Candida sp.*, LCA, and the other from *Candida rugosa*, LCR), 4-Nitrophenyl palmitate, triton X-100, dopamine hydrochloride, and Bradford reagent were procured from Sigma-Aldrich Inc., St. Louis, MO. Bovine Serum Albumin (BSA), branched polyethyleneimine (PEI) with molecular weights of 600, 1800, and 10000, were purchased from Thermo-Scientific, Rockford, IL. Glutaraldehyde (25% solution) was sourced from Electron Microscopy Sciences, Hatfield, PA. Sodium acetate was obtained from VWR Life Science, Solon, Ohio. Iron (III) Chloride Hexahydrate, Ethylene glycol, Tris-base, and Phosphate Buffered Saline (10X solution) were procured from Fisher Scientific.

5.3.2 Preparation of polydopamine modified magnetic particles (MPP)

The synthesis of magnetic microparticles (MP) was conducted using an adapted variant of the conventional solvothermal reduction method[13]. In brief, 2.7 g of $FeCl_3 \cdot 6H_2O$ were weighed and subsequently dissolved in 80 ml of ethylene glycol, followed by stirring the mixture for 30 minutes to yield a yellow solution. Next, 3.6 g of sodium acetate was introduced into the solution, continuing the stirring process for an additional 30 minutes to obtain a homogeneous yellow solution. This solution was then transferred into a 100 ml Teflon-lined stainless-steel autoclave and subjected to a heating process at 200 °C for 24 hours to facilitate the synthesis of the magnetic particles (MP). Post-synthesis, the product was allowed to naturally cool to room temperature (20°C). Subsequently, it was washed thrice with 99% alcohol and dried under vacuum at 40°C overnight. The synthesized MP were then stored at 4°C.

The polydopamine coating layer on the MP was prepared through the surface polymerization of dopamine, with the experimental procedure delineated as follows: Initially, 2 g of the MP, procured

from the aforementioned synthesis process, were weighed and washed twice with 30 ml of Tris-HCl (pH 8.5, 20 mM) solution. Subsequently, these were suspended in 80 ml of Tris-HCl (pH 8.5, 20 mM) solution and subjected to ultrasonic mixing for 30 minutes to ensure thorough dispersion within the solution[14]. Prepare 10 mg/ml dopamine solution 20 mL and stock it. Upon the completion of dispersion of the MP solution, it is mixed with the stocked 20 mL dopamine solution, and the mixture is then placed on a shaker set at 25°C and agitated at a speed of 150 rpm to react for 18 hours. Subsequently, the resultant product, magnetic particles coated with polydopamine (MPP), was washed three times with deionized water and dried under a vacuum at 40°C overnight. Finally, the product is stored at 4°C.

5.3.3 Functionalization of MPP with PEI to produce MPPP

To prepare nanoparticles modified with three length PEIs as spacers, the process is as follows: Initially, 10 mg of MPP is weighed and placed into a 2 ml tube, then added to 2 mL of pH 7.4 PBS buffer solution for rinsing. Subsequently, a series of solutions with varying concentrations are prepared using 99% PEI solutions with different molecular weights. Subsequently, 1 ml of the above spacers solutions is transferred into tubes, and the MPP are subjected to ultrasonic treatment for 30 minutes to ensure full dispersion. Then, they are placed in a shaker at 25°C with a speed of 250 rpm for a reaction duration of 3 hours. After the reaction, the products are washed three times with 1 mL of pH 7.4 PBS solution to remove residual chemicals.

5.3.4 Lipase immobilization to prepare immobilized enzymes (IEs)

For lipase immobilization, dilute the purchased LCA or LCR solution with PBS to intended concentrations. Then, transfer 1 mL of the diluted LCA or LCR solution into the test tube containing pre-set amount of carriers. Place the mixture on a shaker and incubate at 250 rpm and 40°C for 18

hours. After the reaction, drain the supernatant and then wash three times with pH 7.4 PBS solution to ensure the removal of any residual free enzymes from particle surfaces. Combine all supernatants, including that of the reaction mixture and that from each washing step. Measure the total volume and subject it to measurement of proteins concentration for the determination of enzyme loading density.

5.3.5 Characterizations of MP, MPP, MPPP, and IE

The crystallographic structure and chemical composition of the synthesized MPs, MPP, MPPP, and IE were characterized using powder X-ray diffraction (XRD). The morphologies of these particles were examined utilizing scanning electron microscopy (SEM, model JSM-7500F). X-ray Photoelectron Spectroscopy (XPS) was utilized to analyze the composition of surface elements of the MPs, MPP, MPPP, and IEs.

5.3.6 Analysis of lipase structure and amino acid residues on surface

The primary amino acid sequence of the lipase was retrieved from the National Center for Biotechnology Information (NCBI) database (https://www.ncbi.nlm.nih.gov/), and the crystal structure of the lipase (5GV5) was obtained from the Protein Data Bank (RCSB PDB). A comprehensive analysis of the primary sequence of the lipase was conducted to determine the number and proportion of amino acid residues (AAR) carrying functional groups that could form covalent bond with PEI or GA. Subsequently, the PyMOL molecular virtualization system (PyMOL | pymol.org) was employed to examine the three-dimensional structure and generate visual representation of the enzyme surface applying a solvent-accessible surface area (SASA)

cutoff of 2.5 Å² (the resolution of the PDB file is 2.89 Aº). While this cutoff is empirical, it is consistent with previously reported SASA thresholds used to define the enzyme's molecular surface[15,16,17]. An in-depth analysis was then conducted to quantify the number and proportion of these reactive surface residues and depict their distribution on the lipase surface by the PyMOL script 'FindSurfaceResidue.py' (http://pymolwiki.org/index.php/FindSurfaceResidues). Following that, the relative residue solvent accessible surface area (RSA) of individual reactive AAR was calculated by the PyMOL function 'get_sasa_relative', based on the following equation:

$$RSAS = SASA/MaxSASA \quad (1)$$

where SASA is the solvent accessible surface area of an AAR in the 3D structure of the enzymatic protein and MaxSASA the maximum SASA of the AAR, which was retrieved from the literature[18,19].

5.3.7 Determination of protein loading and enzyme activity

In this study, three key parameters are employed to evaluate the efficiency of immobilization: loading density, activity, and specific activity. Loading density denotes the ability of a given quantity of carrier material to effectively immobilize enzymes. It quantifies the mass of enzymes that was bound per unit mass of the carrier, serving as a measure of immobilization capacity of carrier. Activity encompasses the collective enzymatic activity displayed by the free or immobilized enzymes on the carrier. It represents the cumulative activity of all free enzyme in a unit volume or immobilized enzymes on a unit mass of IE and is of practical significance. On the other hand, specific activity focuses on the intrinsic activity possessed by the enzyme immobilized on the carrier. Specific activity of enzymes on IE provides insights into the effects of

immobilization on intrinsic efficiency and performance of the immobilized enzymes and holds relevance for theoretical analysis.

5.3.7.1 Protein concentration and loading density of enzymes

The determination of protein concentration and loading density followed the methods described in my previous research report[20]. Briefly, the enzyme loading density is defined as the mass of enzyme immobilized per unit mass of carrier, was measured using the Bradford method with BSA as the standard. To create a standard curve, prepare BSA solutions (0.25 - 2 mg/mL). Mix 20 μL of each BSA solution (or 20 μL PBS as the blank) with 1 mL of Coomassie Brilliant Blue G-250, incubate for 5 minutes at room temperature, then measure the absorbance at 595 nm. The conversion factor, which is the slope of the BSA concentration vs OD_{595} linear curve, was determined to be 2.522 mg BSA/L per OD_{595} unit. The protein concentration of a sample is calculated by the following equation:

$$C = 2.522\ OD_{595} \times D \qquad (2)$$

Where 2.522 is the conversion factor determined from the BSA standard and D the dilution factor of samples.

To determine the enzyme loading density of an IE, mix 20 μL of appropriately diluted supernatant collected at end of lipase immobilization, and 20 μL of properly diluted lipase solution used in immobilization with 1 mL Coomassie Brilliant Blue G-250. Measure their OD_{595} after 5 minutes of incubation at room temperature to determine the protein concentration of the initial enzyme solution (C_0, mg/l) and the supernatant (C, mg/l). Calculate the loading density of IE using the following equation:

$$q = \frac{(C_0 V_0 - CV)}{m} \qquad (3)$$

where q steps, anding density, which is defined as the mass of enzymatic proteins per unit mass of IE (mg/g), V_0 (mL) the volume of the enzyme solution used in immobilization, V (ml) the total

volume of the supernatant collected at the end of the immobilization, including those from the washing steps, and *m* the mass of carrier, i.e., MPPP used in the immobilization (mg).

5.3.7.2 Assay of enzyme activity

(1) Activity assay

The enzyme activity was assessed using a modified Zhu's[21] method. Specifically, the cleavage of p-nitrophenol palmitate (p-NPP) produced p-nitrophenol (p-NP). To prepare the substrate solution, 50 mg of p-NPP was dissolved in 10 mL of isopropanol and then diluted 10 times with PBS, with Triton X-100 as a surfactant. One milliliter of substrate was added to each sample of IE, followed by sonication for 5 minutes and incubation on a shaker at 220 rpm and 40℃ for 15 minutes. The mixture was then centrifuged, and 200 μL of the supernatant was transferred to 1 mL of 95% ethanol, and the absorbance was measured at 405 nm. The activities of free and IE were determined using a standard curve. One unit of enzyme activity was defined as the amount of enzyme required for producing 1 μmol p-NP per minute under 40℃. The specific activity IE, which is defined as the enzymatic activity per unit mass of IE, was calculated with the following equation:

$$SA_{IE}\left(\frac{U}{mg}\right) = \frac{A_{405}}{k \times t \times m_1} \qquad (4)$$

where A_{405} is the light absorbance at 405 nm wavelength; k the slope of the p-NP standard curve, which is 0.0014 OD/μM; t the reaction time (15 min); and m_1 mass of IE (mg), including carrier (mg) and IE, mg.

The specific activity of enzyme was calculated using the following equation:

$$SA\left(\frac{U}{mg}\right) = \frac{A_{405}}{k \times t \times m_2} \qquad (5)$$

Where m_2 (mg) is the mass enzyme, free or immobilized.

5.3.8 Response Surface Methodology (RSM) to Optimize Immobilization Conditions

5.3.8.1 Plackett-Burman method for variable screening

During the immobilization process, the activity of the immobilized enzyme (IE) is influenced by multiple factors, such as immobilization time, temperature, pH, and initial enzyme concentration. These factors may interact with each other. Therefore, response surface methodology (RSM) is commonly used to study the interactions among these factors. However, RSM typically involves analyzing 2-3 factors. To address this, a Plackett-Burman experimental design is employed to screen for the most significant factors from a larger set, allowing for subsequent optimization of these key factors. The Plackett-Burman experimental design used in this study is detailed in the Table 5-1 and Table 5-2. In a Plackett-Burman design, the estimate represents the effect of a specific factor or variable on the experimental response. It quantifies the magnitude of the effect when altering factors such as temperature, concentration, or pH. The standard error indicates the uncertainty or variability of the estimate, reflecting the extent to which measurement error or random fluctuations may influence the effect. A smaller standard error implies a more reliable estimate, while a larger standard error suggests greater uncertainty in the accuracy of the estimate. The t-value, calculated through a t-test, is used to assess the statistical significance of a factor's effect on the experimental response. The Pr > t value represents the probability associated with the t-value, indicating the likelihood that the observed effect is due to random chance. A lower Pr > t value suggests that the factor's effect is unlikely to be due to random error, thus indicating statistical significance.

Table 5-1 Screening Experimental Variables for LCR Immobilization Using Plackett-Burman Design

Variable	Unit	Symbol	Experimental value	
			-1 （low level）	1 （high level）
Lipase concentration	%wt	X_1	1% wt	3 % wt
Immobilization time	H	X_2	1	2
Immobilization temperature	^{o}C	X_3	20	40
Immobilization pH		X_4	7	8

Table 5-2 Plackett-Burman experimental design

Trial	X_1	X_2	X_3	X_4
1	+1	+1	+1	+1
2	+1	-1	-1	+1
3	+1	+1	-1	-1
4	-1	+1	+1	-1
5	-1	-1	+1	+1
6	+1	-1	+1	-1
7	-1	+1	-1	+1
8	-1	-1	-1	-1

5.3.8.2 Box-Behnke and RSM

To optimize the fixed conditions using the response surface methodology, a Plackett-Burman design was first employed to screen for three variables that significantly influenced the fixed outcome. After selecting three key variables using the Plackett-Burman design, a Box-Behnken design was subsequently employed to conduct a response surface experiment, testing the three factors at three levels, as outlined in Table 5-3 and 5-4.

Table 5-3 Response Surface Analysis of Experimental Variables and Levels

Variable	Unit	Symbol	Experimental value		
			low level	centre	high level
Lipase concentration	%wt	X_1	0.1	0.5	1
Immobilization temperature		X_3	10	25	40
Immobilization pH		X_4	6	7	8

Table 5-4 Box-Behnken Design for Response Surface Analysis

Run	X_1	X_3	X_4
1	0.1	25	6
2	0.1	25	8
3	1	25	6
4	1	25	8
5	0.5	10	6
6	0.5	40	6
7	0.5	10	8
8	0.5	40	8
9	0.1	10	7
10	1	10	7
11	0.1	40	7
12	1	40	7
13	0.5	25	7
14	0.5	25	7

5.3.9 Features of IE

5.3.9.1 Optimum temperature range

To compare the optimal temperature of free and IE, the enzymes were combined with a substrate solution prepared from p-nitrophenol palmitate (p-NPP) and incubated in a shaker at temperatures ranging from 10℃ to 60℃ under identical conditions: the mixture was incubated on a shaker at 40°C with a speed of 250 rpm for 30 minutes. Following the reaction, centrifugation was employed for solid-liquid separation, and the optical density (OD) of the supernatant was measured. The relative activity is defined as the activity value at a specific temperature divided by the highest

activity value obtained across all temperatures tested. This metric is utilized to illustrate the variation in activity value in relation to temperature, with the maximum activity designated as 100%. The conditions for testing stability have been incorporated into the Materials and Methods section.

5.3.9.2 pH range of free and IE

To compare the optimum pH range of free and IE, a series of n-NPP solutions with a pH range of 6 to 10 were prepared. The enzymes were then mixed with these n-NPP solutions, and the mixture was incubated on a shaker at 40°C with a speed of 250 rpm for 30 minutes. After the reaction, centrifugation was used for solid-liquid separation, and the optical density (OD) of the supernatant was measured. The relative activity at different pH conditions was calculated. The relative activity is defined as the activity value at a specific pH, divided by the highest activity value obtained across all pH levels tested. This measure is utilized to illustrate how the activity value fluctuates with changes in pH, setting the maximum activity as 100%.

5.3.9.3 Reusability of free or immobilized enzyme

To evaluate the reusability of the IE, the enzymes will undergo 10 consecutive reaction cycles, with their activities being quantified after each cycle. The activity recorded in the initial cycle will serve as the baseline, designated as 100%. The relative activity for each subsequent cycle will then be calculated in comparison to this initial value, providing a measure of the enzyme's activity retention and stability over multiple uses.

5.4 Results and Discussions

5.4.1 Characterization

5.4.1.1 XRD of MP and IE

The X-ray diffraction (XRD) pattern of the Fe_3O_4 magnetic particles (MP) synthesized via the solvothermal method is depicted in Figure 5-1. Six distinctive peaks were observed at 2θ values of 30.1°, 35.4°, 43.1°, 53.4°, 57°, and 62.5°, corresponding to the crystallographic planes: (2 2 0), (3 1 1), (4 0 0), (4 2 2), (5 1 1), and (4 4 0). These peaks are consistent with the standard pattern for Fe_3O_4, confirming the successful synthesis of the cubic spinel structure of Fe_3O_4[22]. Comparative analysis of the XRD patterns of the magnetic particles (MPs) and the immobilized LCR reveals identical peak positions, indicating that the immobilization of lipase does not alter the lattice structure of the carrier.

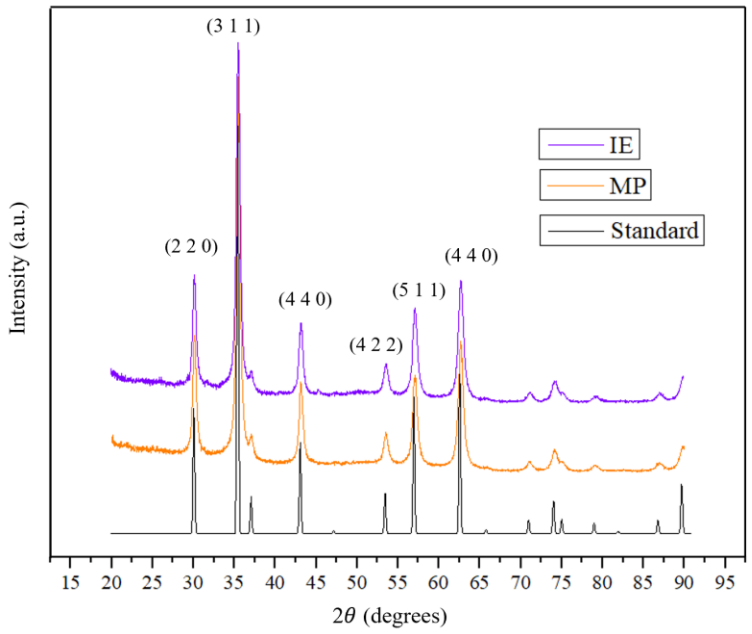

Figure 5-1 XRD pattern of MP and IE (ILCR) as well as the standard

5.4.1.2 morphology

Figure 5-2 presents the Scanning Electron Microscopy (SEM) images of microparticles (MP) synthesized via the solvothermal method and IE. Figures 5-2A and 5-2B respectively show the overall distribution and detailed SEM images of the magnetic particles (MP) synthesized via the solvothermal method. The images reveal that most of the MPs are regular spheroids with smooth surfaces and an average diameter of 800 nm, although there are a few smaller particles. Figures 5-2C and 5-2D respectively display the overall distribution and detailed morphology of the immobilized enzyme (IE). Figure 5-2C indicates that the immobilization of lipase on MPP does not change the overall morphology. The detailed view in Figure 5-2D shows that the incorporation of lipase does not alter the morphology of the carrier.

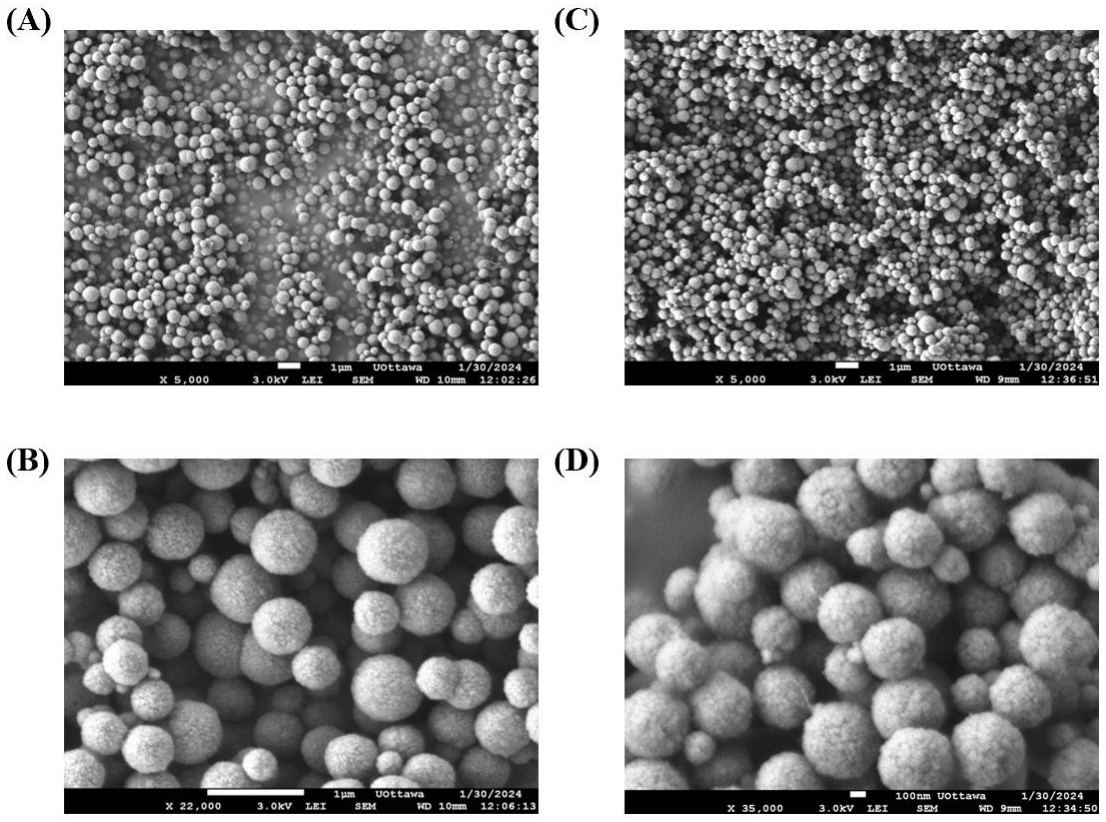

Figure 5-2 SEM images 5000× – original and zoom-out views of MP (A & B) and IE (C & D)

5.4.1.3 X-ray Photoelectron spectroscopy (XPS) of MP and ILCR

To further confirm the successful immobilization of LCR onto the carrier surface, surface elemental analysis of MP and IE was conducted using XPS. As shown in Figure 5-3A, the surface of MP exhibited two prominent peaks corresponding to Fe 2p at a binding energy of 705 eV and O 1s at 528 eV. By comparing the XPS spectra of ILCR, it was observed that ILCR contained additional elements, C and N, corresponding to binding energies of 280 eV and 396 eV, respectively. These peaks were attributed to the amino groups contributed by LCR. Meanwhile, the peak areas of Fe 2p at 705 eV and O 1s at 528 eV decreased after PDA coating, indicating a reduction in the signals of Fe and O due to the formation of a shell-like structure of LCR on the surface of MP[23]. The deconvoluted N 1s spectrum, as illustrated in Figure 5-3B, demonstrates three chemically distinct species within the N 1s region, exhibiting binding energies at 399.0, 399.8, and 400.7 eV, which corresponded to N-H, CNC, and $NH4^{+}$ species present on the surface[24].

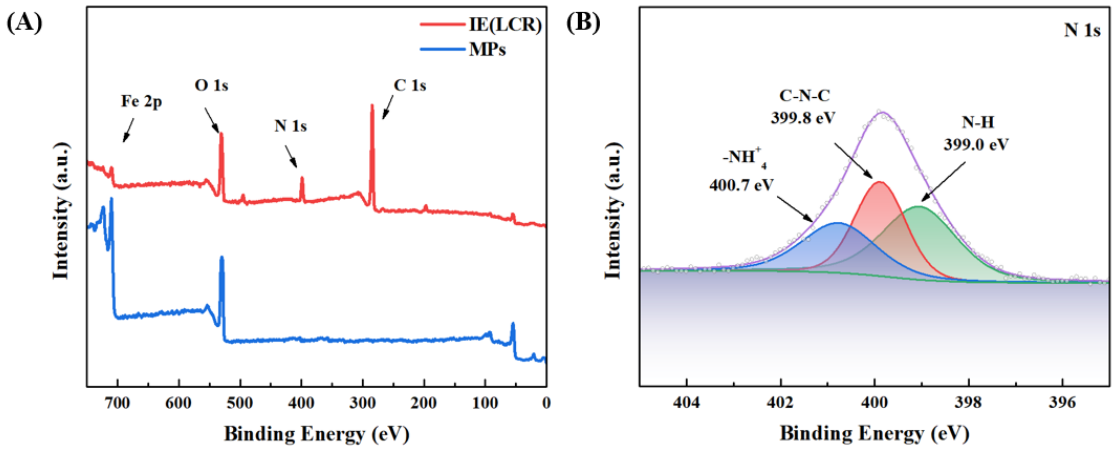

Figure 5-3 XPS spectra of MP and ILCR (A); and deconvolution of the N 1s of ILCR (B)

5.4.2 Distribution of reactive AAR on surfaces of the enzymes

In this study, we strategically selected two lipases, i.e., *Candida antarctica* Lipase B with active Ser105 modified with a phosphonate inhibitor (LCA), and *Candida rugosa* (LCR), for investigation of protein structure on the efficiency of enzyme immobilization. These two lipases are of similar functionality but differ vastly in structure. LCA is an octamer composed of 2,536 amino acid residues, with each monomer consisting of 317 amino acid residues, and a molecular weight of 270.94 kDa. LCR is a monopeptide with a molecular weight of 57.78 kDa and consists of 534 amino acid residues. In other words, the size of LCA is 4.7 times of LCR in terms of molecular weight.

Since the side chain functional groups of PEI are amino groups, which could react with carboxyl and hydroxyl groups, the AAR containing these two functional groups have the potential to covalently bond with PEI for enzyme immobilization and are designated as reactive residues. The distribution of these reactive residues on the surface of the two lipases were determined using solvent accessible surface area (SASA) analysis. The AAR on the surfaces of LCA and LCR were first identified and mapped according to their PDB files, i.e., PDB 5GV5 and PDB 1CRL, respectively, with a cutoff of 2.5 A^2, and shown as the red mesh in Figure 5-4A and 5-4C, respectively. From Figure 5-4A, it can be observed that LCR has two active sites, while LCA, an octamer, has eight active sites (one active site each monomer). The surface was further analyzed to calculate the relative solvent accessible surface areas (RSAS) of each surface AAR to determine the degree of exposure of individual AAR, which is illustrated in Figures 5-4B and 5-4D with the darker areas presenting AAR of larger RSAS and therefore higher exposure levels.

To quantify the AAR distribution on enzyme surface, we further define the **atom ratio** as the ratio between the number of atoms of the functional group and the total number of atoms of an AAR. For instance, the Glu molecule ($C_5H_9NO_4$) has 19 atoms and the Glu residue in a peptide has 16 atoms, whereas the functional group of the Asp residue, i.e., the carboxyl group (-COOH), has 4

atoms. The atom ratio of Glu residue is therefore 4/16, i.e., 25%. Using the atom ratio as the benchmark, we classify a surface AAR with an RSAS equal to or less than its **atom ratio** as a "valley" residue and the surface AAR having an RSAS equal to or higher than 50% as a “peak” residue.

The number of reactive peak and valley residues, including Asp, Glu, Thr, Ser, and Tyr, in LCA and LCR are listed in Table 5-5. The percentages of reactive amino acid residues at peak positions are 5.99% and 6.74% for LCA and LCR, respectively, representing 12.5% more peak reactive AAR on LCR surface than on LCA surface. Furthermore, it is evident that the active site of LCR has much less exposure than that of LCA, as shown in Figures 5-4B and 5-4D, respectively (the darker the blue color, the larger RSAS a residue had, corresponding to a higher level of exposure of an AAR). Indeed, a close analysis of the distribution of active site AAR indicates that a Glu residue of one of the two LCR active sites was a peak residue while all AAR of the active sites of LCA are valley residues. These results, as will discuss more in detail later, may have significant implications to the immobilization of corresponding enzymes.

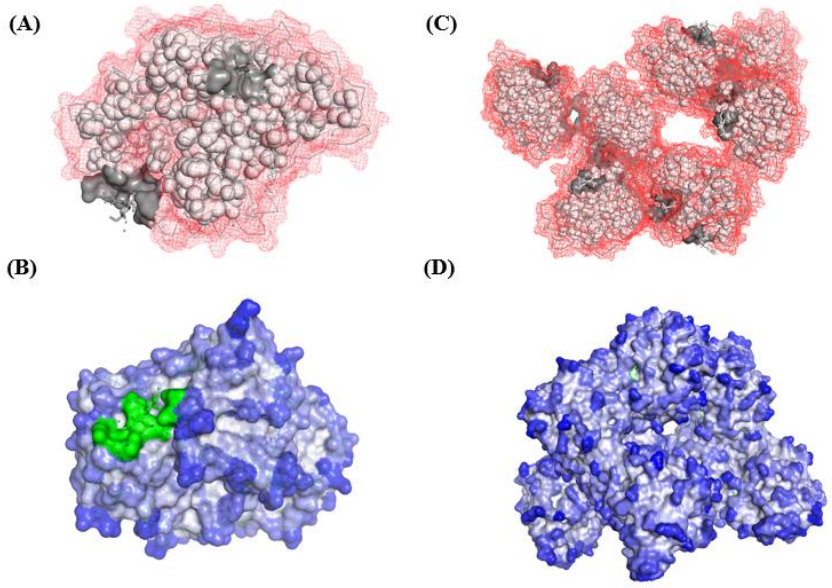

Figure 5-4 Active site (A) and SASA (B) of LCR as well as active site (C) and SASA (D) of LCA

Table 5-5 Number of reactive AAR at valley and peak position in LCA and LCR

Functional group	AAR	Atom Ratio	LCA		LCR	
			Valley	Peak	Valley	Peak
Carboxyl	Asp	30.8	51	14	13	11
	Glu	25.0	22	12	7	5
Hydroxyl	Thr	14.3	96	33	11	7
	Ser	18.2	122	85	23	11
	Tyr	9.5	33	8	11	2
Subtotal	NA	NA	294	152	65	36

Total numbers of AAR in LCA and LCR are 2536 and 534, respectively

5.4.3 Effects of PEI Length and PEI concentration, and enzyme protein properties

We further strategically selected branched PEI of the same structure but of three different molecular weights and therefore lengths, that is, PEI of 600, 1,800, and 10,000 Da, which are designated as PEI-600, PEI-1800, and PEI-10000, respectively, as the spacer, to study the effects of spacer length on the efficiency of enzyme immobilization at varied immobilization temperature, pH, and initial lipase concentration. The branched PEI features have many side-chain amino groups that can bind covalently with the hydroxyl group of Thr, Ser, and Tyr residues, as well as the carboxyl groups of Glu and Asp residues on the enzyme surface.

As shown in Figure 5-5, it is evident that the loading density of both ILCA (A, B, C) and ILCR (D,E,F) increased with the concentration of PEI in the functionalization buffer, regardless of its molecular weight, until plateauing at a critical PEI concentration, with only one exception. The exception was ILCR with PEI-600, which did not plateau within the tested PEI concentration of up to 325 mg/L. The existence of a critical PEI concentration indicates that either the surface of the MPP was saturated or the number of side-chain functional groups of PEI accessible for enzyme

immobilization reached saturation levels when PEI concentration was beyond the critical concentration in the functionalization reaction mixture.

As shown in Table 5-6, while the critical concentrations of different PEI molecules were very different when expressed in molar concentration, they were very similar when expressed in mass concentration when compared for the same lipase under certain conditions. For ILCA, the critical concentrations were approximately 50.0 g/L for both PEI-600 and PEI-1800 but was 25 g/L.

It is worth noting that the three PEI molecules of different molecular weights have the same repeating units. Therefore, different PEI molecules of the same masses, although would have very different numbers of moles, would have similar moles of repeating units and therefore side-chain functional groups. The fact that PEI-600 and PEI-1800 had critical PEI concentrations that are very different in molar concentration but similar in mass concentration indicate that 1) the MPP surface was not saturated by PEI molecules in the tested range; 2) the side-chain functional groups of PEI-600 and PEI-1800 were equally available for enzyme immobilization; and 3) the immobilized LCA enzyme proteins immobilized on these two different PEI were equally accessible for substrates, when these two PEI molecules were involved. On the other hand, the fact that the critical mass concentration of PEI-10000 was only half of that of PEI-600 and PEI-1800 suggests that the long PEI-10000 molecules had steric hindrance that reduced the accessibility of either the side-chain functional groups of PEI for LCA immobilization, or immobilized LCA for substrates, or both. It is very intriguing to notice that for ILCR, PEI-10000 and PEI-1800 had similar critical mass concentration, but the critical concentration of PEI-600 was not reached at the highest concentration tested, i.e., 325 g/L. This could be tentatively explained by the fact that the Mw of LCR (57.78 Da) is on 21.3% of that of LCA (270.94 Da), making it less subjected to steric hindrance of long PEI molecules as a reactant in enzyme immobilization. This argument is reinforced by the fact that, as shown in Table 5-6, the maximum molar loading densities of LCR almost double that of LCA. It

should be noted that the molar densities of both ILCR and ILCA were similar for all the three difference PEI spacers for a given enzyme, i.e., LCR or LCA, with ILCA of PEI-600 being the only exception. The fact that PEI-600 offered a significantly larger plateaued loading density is in alignment with the notion that LCA, due to its larger Mw, is more sensitive to steric hindrance in the immobilization process when PEI spacers on MPPP were large (1800 Da and beyond). This results also indicate that the accessibility of immobilized enzyme to substrates is likely a lesser concern, if not entirely negligible, in this setting since the larger LCA should be more accessible than the smaller LCR after being immobilized on PEI spacers except for those on or near the tips of the PEI residues.

Comparing the immobilization results of LCA and LCR, it can be observed that LCA has a higher loading density than LCR at the same conditions. This can be attributed to the higher molecular weight of LCA (270.94 Da) compared to LCR (57.78 Da). Indeed, when expressed in mmol/g, as shown in Table 5-6, LCR exhibits a higher loading density compared to LCA. In other words, a greater number of enzymatic molecules could be immobilized per unit mass of the carrier for LCR than LCA. Furthermore, the ILCR exhibits higher specific activity than ILCA. Consequently, it can be concluded that LCR is more suitable than LCA for immobilization using PEI as the spacer.

The activities per unit mass of IICA showed a very different pattern than that of ILCR. For ILCA, the activity increased with PEI concentration and then plateaued after the critical PEI concentration, following the trend of loading density, although there was a decrease of activity with ILCA when PEI-600 was used as the spacer, which is likely an outlier. For ILCR, however, a highly pointed peak of the activity versus PEI concentration profile was observed with each of all the three different PEI spacers and all located in the plateaued loading density regimes.

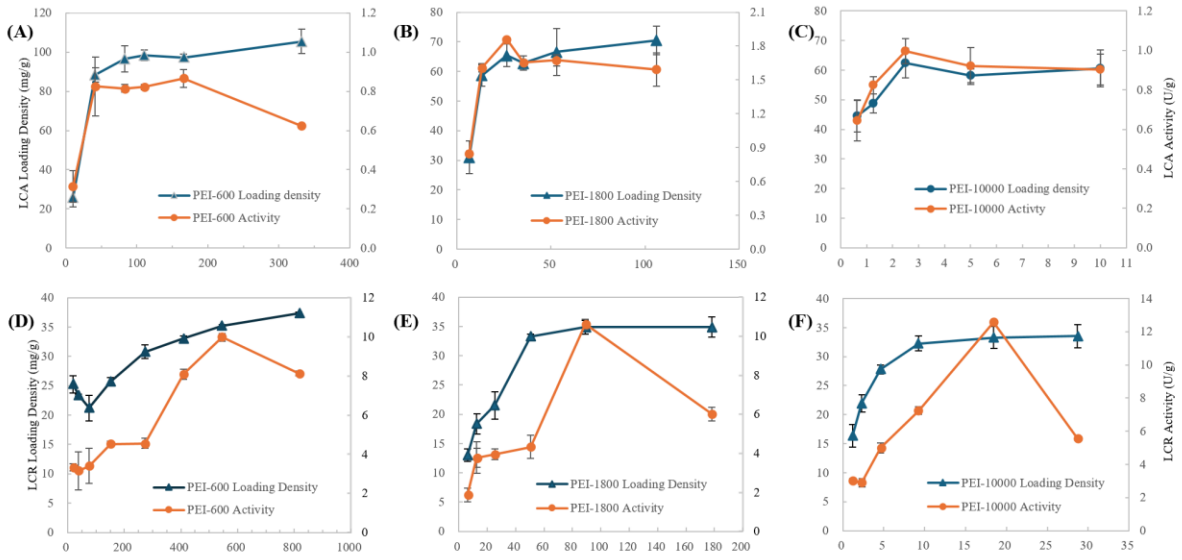

Figure 5-5 Effects of PEI length and concentration on loading density and activity

Figure 5-6 depicts the specific activity vs PEI concentration profiles of different IE. For ILCA, the specific activities followed a general trend of decreasing specific activity with increasing PEI concentration, likely due to an increasing steric hindrance. However, the IICR profiles exhibited a very different pattern with specific activity fluctuating at low PEI range, reaching a peak value, and then significantly decreasing in the high PEI concentration range. The different patterns of ILCA and ILCR profiles might be tentatively explained as follows. Firstly, as afore discussed, all the AAR of the active sites of LCA are valley residues while a Glu residue of one of the two active sites of LCR is a peak residue. Therefore, the active site of LCR would be more likely to bind to the spacer through a reaction between the carboxyl group of the Glu residue and a side-chain amino group of the PEI spacer and the probability of that reaction would increase with PEI concentration. While random modification of active site usually leads to the reduction of enzymatic activity, it has been widely reported that some modifications might enhance enzyme selectivity or/and activity[25]econdly, the relatively small molecular size of LCR make it, when immobilized through a side-chain amino group of PEI away from the tip position, more sensitive to the steric hindrance

of the long PEI molecules. Both of these two likely effects would be more severe at high PEI concentration and hence the rapid decrease of specific activity of ILCR after the optimal PEI concentration.

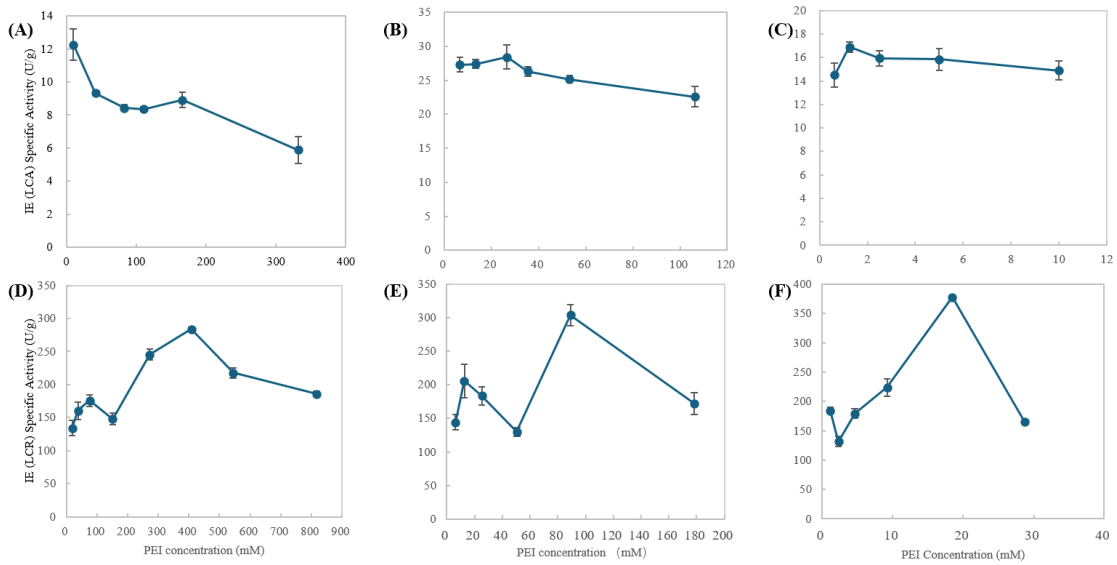

Figure 5-6 Dependence of specific activity of ILCA (A-C) and ILCR (D-F) on PEI concentration when PEI-600, PEI-1800, or PEI-10000 was used as the spacer.

It can be observed in Table 5-6 that for LCA, MPP-1800 is the most effective carrier in maintaining the highest specific activity, retaining 66.54% of that of the free enzyme. In the case of LCR, MPP-10000 proves to be the most effective, retaining 61.72% specific activity of the free enzyme. The reduction in specific activity after enzyme immobilization could be tentatively attributed to factors such as steric hindrance that limited the accessibility of immobilized lipases to substrates, conformational changes of enzymes that reduced the affinity of active sites to substrates, alterations in the microenvironment, substrate diffusion limitations, and improper immobilization site selection that might obstruct the active site. In particular, as aforementioned, the LCR is much smaller than LCA and the immobilized LCR would be more sensitive to hindrance of long PEI

spacer. This could help explain why the longest PEI, i.e., PEI-10000 retained the highest specific activity of this lipase.

Table 5-6 Loading density, activity, and specific activity of ILCA and ILCR using PEI of different Mw as spacers

Lipase	Carrier	Critical PEI Conc. (mM)	Critical PEI Conc. (g/L)	Loading Density (mg/g)	Loading Density (μmol/g)	SA_{IE}* (U/g IE)	SA* (U/g protein)
LCS	FE	NA	NA	NA	NA	NA	42.68
	MPP-600	83.00	49.80	105.43	0.389	0.87	9.34
	MPP-1800	26.56	47.80	65.42	0.241	1.86	28.40
	MPP-10000	2.50	25.00	62.47	0.231	0.99	16.00
LCR	FE	NA	NA	NA	NA	NA	608.16
	MPP-600	544.55	326.73	37.35	0.646	9.98	267.21
	MPP-1800	50.52	90.94	34.88	0.604	10.61	304.22
	MPP-10000	9.22	92.2	33.51	0.580	12.58	375.41

5.4.4 Optimization of LCR immobilization using Response surface methodology (RSM)

The Plackett-Burman method allows for the selection of the three most significant experimental variables from a larger set. As indicated by the partial regression coefficients and significance tests in Table 5-7, the primary factors affecting the immobilization of LCR are initial LCR concentration, temperature, and pH. Therefore, these three factors were selected for further response surface optimization in subsequent experiments to determine the optimal immobilization conditions.

Table 5-7 Significance of variables on activity of LCR-IE

Variable	Estimate	Standard Error	t-value	Pr>t	Significance
LCR concentration	-0.4838	0.106	-4.576	0.020	1
Immobilization time	-0.0065	0.106	-0.061	0.955	4
Immobilization	0.0765	0.106	0.724	0.522	3
Immobilization pH	0.1588	0.106	1.502	0.230	2

Subsequently, using the selected LCR concentration, immobilization temperature, and pH, a Box-Behnken design was employed with the enzyme activity as the response variable. This led to the following quadratic regression equation (5-6). The response surface and contour plots for the model are shown in Figure 5-7. These plots indicate that the model is stable. Calculations based on the model suggest that the optimal immobilization conditions are as follows: LCR concentration of 0.5 wt%, immobilization temperature of 29°C, and pH of 6.9. Meanwhile, using PEI with a molecular weight of PEI-10000 at a concentration of 0.43 mM and an immobilization time of 2 hours, the predicted maximum activity is 10.04 U/mg.

$$Y_{activity} = -67.303 + 12.910X_1 + 0.104X_3 + 21.088X_4 - 13.888X_1^2 - 0.002X_3^2 - 1.534X_4^2 + 0.008X_1 \cdot X_3 + 0.128X_1 \cdot X_4 - 0.001X_3 \cdot X_4 \quad (5\text{-}6)$$

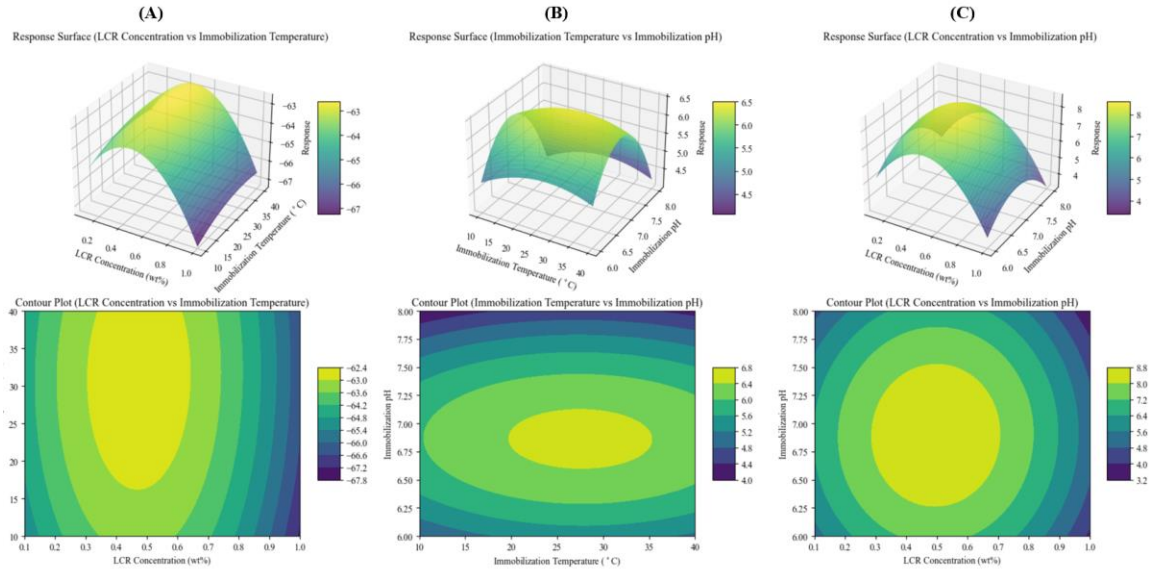

Figure 5-7 Response surface curves and contour plots for the three significant variables affecting LCR activity. (A) Effect of LCR concentration and immobilization temperature; (B) Effect of immobilization temperature and pH; (C) Effect of LCR concentration and pH.

5.4.5 Performance of IE

5.4.5.1 Optimum temperature range

The optimal temperature range of lipase can change following immobilization. Generally, immobilizing an enzyme provides a stable microenvironment, reducing the likelihood of protein denaturation and preserving activity at higher temperatures. However, immobilization can also increase the diffusion resistance of substrates reaching the active site. As temperature rises, the frequency of collisions between substrate and enzyme molecules also increases, potentially accelerating the reaction rate[26].Therefore, it is crucial to evaluate the changes in the optimal reaction temperature and temperature range after enzyme immobilization. This study compares the optimal temperature range of free lipase and immobilized LCR over a temperature span of 10 to 60°C.

In Figure 5-8, within the temperature range of 10 to 50°C, the relative activity of both free lipase and immobilized enzyme (IE, LCR) increases with rising temperature, reaching their highest relative activity at 50°C. Throughout the 10 to 50°C range, the relative activity of ILCR is consistently higher than that of free lipase. However, as the temperature continues to rise from 50 to 60°C, the relative activity of both enzymes significantly declines, with free lipase showing a more pronounced loss of activity. At 60°C, ILCR retains 86% of its relative activity, while free lipase retains only 66%. This indicates that ILCR exhibits greater thermal stability compared to free lipase. The enhanced stability of the immobilized enzyme is primarily due to the immobilization process, which increases the rigidity of the enzyme structure, preventing denaturation or conformational changes at high temperatures, thereby slowing the decline in enzyme activity[27].

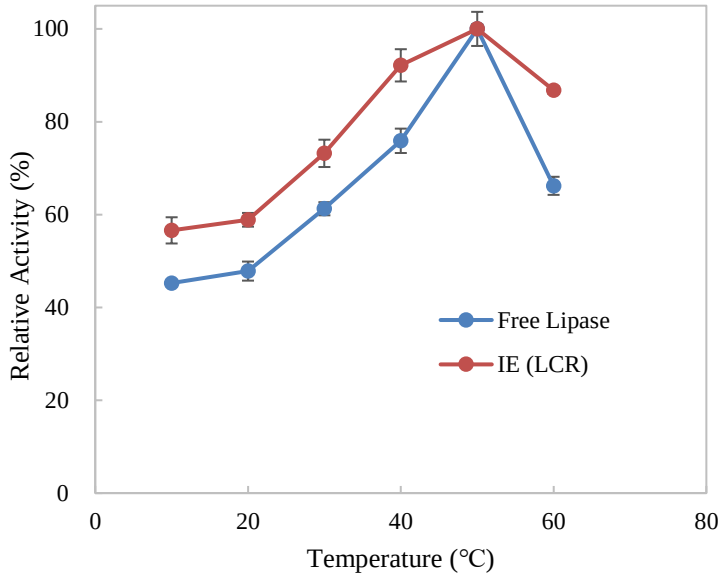

Figure 5-8 Free and immobilized LCR optimum temperature

5.4.5.2 Optimum pH range

pH stability is a critical factor in evaluating the performance of enzyme immobilization. Variations in pH can alter the ionization state of enzyme molecules, thereby affecting their configuration and conformation. Enzymes can only exhibit optimal activity when their active sites are at the optimal pH. The sensitivity of enzyme molecules to pH changes inevitably influences their catalytic efficiency on substrates[26]. To assess the pH stability of the IE, we evaluated its relative activity across a pH range of 6 to 10 and compared it with that of the free lipase.

The pH stability of the free enzyme and the immobilized enzyme is illustrated in Figure 5-9 (A). After immobilization, there is a notable improvement in the enzyme's pH stability, with a wider threshold pH range. Specifically, within the pH range of 6 to 10, the IE demonstrated superior pH stability compared to the free lipase. At pH 6, the relative activity of the free lipase was 59.73%, which is lower than the 67.5% observed for the IE. Both forms exhibited optimal activity at pH 8. At pH 9 and 10, the relative activity of the free lipase was consistently lower than that of the IE.

Following immobilization, the pH stability of the lipase improves, which can be attributed to the 'pH memory' theory. This theory suggests that the enzyme, when immobilized under various pH conditions, retains the corresponding conformations. Consequently, when the enzyme catalyzes hydrolysis under varying pH conditions, the environment affects the dissociation of functional groups within the active center differently. This alteration in conformation subsequently impacts the enzyme's catalytic activity[28].

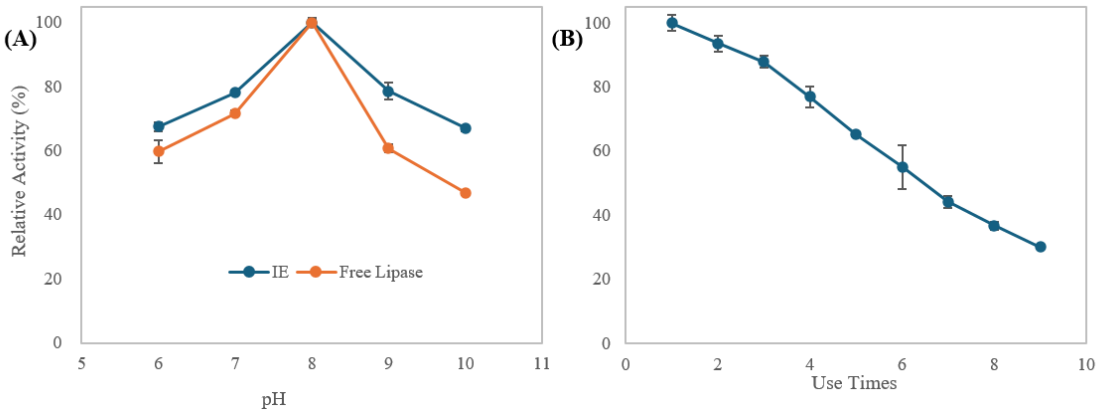

Figure 5-9 (A) pH stability of IE and free lipase; (B) reusability of IE

5.4.5.3 Reusability

Reusability is a crucial aspect of enzyme immobilization, as it enables the repeated use of the immobilized enzyme, resulting in cost savings and enhanced efficiency. However, the reusability of immobilized enzymes may gradually diminish due to factors such as enzyme leaching and inactivation during reaction cycles. Consequently, in the context of potential industrial applications, assessing reusability is an essential parameter for evaluating the effectiveness of enzyme immobilization[29]. Figure 5-9 (B) illustrates the reusability of the IE. It is observed that the relative activity of the IE progressively declines with an increasing number of cycles. After 9 cycles, the relative activity has decreased to 30% of its initial value.

5.5 Conclusions

In this study, we investigated the immobilization of two lipases, i.e., LCR and LCA, on polydopamine (PDA)-modified magnetic microparticles using three branched polyethyleneimine (PEI) of vastly different molecular weights and therefore lengths but same repeating units as spacers. The two lipases are of different sources and different molecular weights, structure, and distribution of reactive amino acid residue distribution on surface.

Both lipases were successfully immobilized using any of the three spacers and the immobilized lipases demonstrated significant improved thermal, pH, and operational stabilities, broader operational pH and temperature ranges, and satisfactory seperability that allowed reuse of the immobilized lipases.

The LCR exhibited larger loading density during the immobilization process and higher specific activity after being immobilized when the same PEI was used as the spacer when compared to LCA. This is tentatively explained by 1) its much smaller molecular weight than LCA, rendering much smaller steric hindrance and therefore larger accessibility to the side-chain functional groups (i.e., the amino groups) away from the tips of the PEI residues on the MPPP surface; and 2) LCR has 12.5% more reactive AAR as peak residues on its surface than LCA, leading to larger reactivity with PEI of LCR than LCA. Furthermore, it was found LCR has one peak Glu residue in one of its two active sites while all active site residues of LCA are valley residues. This difference is used to hypothetically explain the sensitivity of immobilized LCR on PEI concentration in term of specific activity. Additionally, PEI with a molecular weight of 600 Da was able to immobilize the highest amount of lipase, while P EI with a molecular weight of 10,000 Da maintained higher total activity and specific activity of the immobilized enzyme (IE). These findings underscore the critical

role of PEI in the immobilization process and emphasize the importance of optimizing the molecular weight of the spacer molecule to achieve optimal enzyme performance.

The effects of PEI length were mainly attributed to two aspects: 1) steric hindrance to free lipase proteins during the immobilization process, which would reduce the accessibility of the side-chain functional groups of PEI other than those on or near the tips of the PEI residues on MPPP surface; and 2) steric hindrance of substrate molecules, which would reduce the accessibility of immobilized lipases to substrates other than those near or on the tips of PEI residues. A critical concentration of PEI, beyond which the loading density was plateaued, was identified for each of the combinations other than PEI-600 for LCR. Using the enzymatic activity per unit mass of IE as the criterion, PEI-1800 and PEI-10000 was determined to be the most suitable for LCA and LCR, respectively.

To optimize the immobilization of LCR using PEI-10000, we applied the Plackett-Burman method to first screen variables, including LCR concentration, immobilization time, temperature, and pH. The analysis of experimental data identified LCR concentration, immobilization pH, and temperature as the key factors significantly affecting enzyme activity of ILCR. Subsequently, response surface methodology (RSM) was employed to optimize these variables and develop a predictive model for determining the optimal immobilization conditions. The optimal conditions were determined to be LCR concentration 0.5 wt%, immobilization temperature 29°C, immobilization pH 6.9, and immobilization time 2 hours.

Having established the optimal immobilization conditions, we then evaluated the enzymatic performance of the IE. Our results demonstrated that the IE exhibited a wider optimal pH range and improved thermal stability compared to the free LCR. Additionally, the IE maintained 30% of its activity even after being used 9 times, highlighting its reusability and durability.

This study provides valuable insights into the immobilization of lipase on magnetic microparticles, emphasizing the importance of spacer molecular weight and optimized conditions in achieving high enzyme performance. The results contribute to the development of more efficient and sustainable enzymatic systems, with potential applications in various industries, including biocatalysis, food processing, and pharmaceuticals.

5.6 Reference

1. Maghraby, Y. R., El-Shabasy, R. M., Ibrahim, A. H. & Azzazy, H. M. E. S. Enzyme Immobilization Technologies and Industrial Applications. *ACS Omega* **8**, 5184–5196 (2023).
2. Filho, D. G., Silva, A. G. & Guidini, C. Z. Lipases : sources , immobilization methods , and industrial applications. 7399–7423 (2019).
3. Kapoor, M. & Gupta, M. N. Lipase promiscuity and its biochemical applications. *Process Biochemistry* **47**, 555–569 (2012).
4. Ismail, A. R. & Baek, K. International Journal of Biological Macromolecules Lipase immobilization with support materials , preparation techniques , and applications : Present and future aspects. *Int J Biol Macromol* **163**, 1624–1639 (2020).
5. Tan, T., Lu, J., Nie, K., Deng, L. & Wang, F. Biodiesel production with immobilized lipase : A review. *Biotechnol Adv* **28**, 628–634 (2010).
6. Fact, C., Chandra, P., Singh, R. & Arora, P. K. *Microbial Lipases and Their Industrial Applications : A Comprehensive Review*. *Microbial Cell Factories* (BioMed Central, 2020). doi:10.1186/s12934-020-01428-8.
7. Feng, Y. *et al.* Recent advances in enzyme immobilization based on novel porous framework materials and its applications in biosensing. **459**, (2022).
8. Gennari, A., Führ, A. J., Volpato, G., Fernanda, C. & Souza, V. De. Magnetic cellulose : Versatile support for enzyme immobilization - A review. *Carbohydr Polym* **246**, 116646 (2020).
9. Bilal, M., Zhao, Y., Rasheed, T. & Iqbal, M. N. International Journal of Biological Macromolecules Magnetic nanoparticles as versatile carriers for enzymes immobilization : A review. **120**, 2530–2544 (2018).
10. Abreu, I. *et al.* Journal of Pharmaceutical and Biomedical Analysis Magnetic particles for enzyme immobilization : A versatile support for ligand screening. *J Pharm Biomed Anal* **204**, 114286 (2021).
11. Datta, S. & Christena, L. R. Enzyme immobilization : an overview on techniques and support materials. 1–9 (2013) doi:10.1007/s13205-012-0071-7.
12. Khoobi, M. *et al.* Polyethyleneimine-modi fi ed superparamagnetic Fe 3 O 4 nanoparticles for lipase immobilization : Characterization and application. **150**, 77–86 (2015).
13. Deng, H. *et al.* Monodisperse magnetic single-crystal ferrite microspheres. *Angewandte Chemie - International Edition* **44**, 2782–2785 (2005).

14. Deng, Y. *et al.* Preparation of iron-based MIL-101 functionalized polydopamine@Fe3O4 magnetic composites for extracting sulfonylurea herbicides from environmental water and vegetable samples. *J Sep Sci* **41**, 2046–2055 (2018).
15. Solvent-Accessible Surfaces of Proteins and Nucleic Acids Author (s): Michael L . Connolly. **221**, 709–713 (2014).
16. Richards, F. M. Areas, volumes, packing, and protein structure. (1977).
17. Barth, M., Bender, J., Kundlacz, T. & Schmidt, C. Evaluation of NHS-Acetate and DEPC labelling for determination of solvent accessible amino acid residues in protein complexes. *J Proteomics* **222**, 103793 (2020).
18. Tien, M. Z., Meyer, A. G., Sydykova, D. K., Spielman, S. J. & Wilke, C. O. Maximum allowed solvent accessibilites of residues in proteins. *PLoS One* **8**, (2013).
19. Wirnsberger, G., Pritišanac, I., Oberdorfer, G. & Gruber, K. Flattening the curve—How to get better results with small deep-mutational-scanning datasets. *Proteins: Structure, Function and Bioinformatics* **92**, 886–902 (2024).
20. Wang, X. *et al.* Immobilization of alcalase on polydopamine modified magnetic particles. *Biochem Eng J* **207**, 109310 (2024).
21. Zhu, Y. *et al.* Covalent immobilization of porcine pancreatic lipase on carboxyl-activated magnetic nanoparticles : Characterization and application for enzymatic inhibition assays. *Materials Science & Engineering C* **38**, 278–285 (2014).
22. Wang, S. nan *et al.* Immobilized alcalase alkaline protease on the magnetic chitosan nanoparticles used for soy protein isolate hydrolysis. *European Food Research and Technology* **239**, 1051–1059 (2014).
23. Ren, Y. *et al.* Facile , high efficiency immobilization of lipase enzyme on magnetic iron oxide nanoparticles via a biomimetic coating. (2011).
24. Ding, C., Sun, H., Ren, J. & Qu, X. Analytica Chimica Acta Immobilization of enzyme on chiral polyelectrolyte surface. *Anal Chim Acta* **952**, 88–95 (2017).
25. Ikebe, J., Suzuki, M., Komori, A., Kobayashi, K. & Kameda, T. Enzyme modification using mutation site prediction method for enhancing the regioselectivity of substrate reaction sites. *Sci Rep* 1–11 (2021) doi:10.1038/s41598-021-98433-7.

26. Zhao, J., Ma, M., Yan, X., Zhang, G. & Xia, J. Green synthesis of polydopamine functionalized magnetic mesoporous biochar for lipase immobilization and its application in interesterification for novel structured lipids production. *Food Chem* **379**, 132148 (2022).
27. Silveira, T. R. *et al.* An efficient decolorization of methyl orange dye by laccase from Marasmiellus palmivorus immobilized on chitosan-coated magnetic particles. *Biocatal Agric Biotechnol* **30**, 1–10 (2020).
28. Elias, N. *et al.* Structure and properties of oil palm-based nanocellulose reinforced chitosan nanocomposite for efficient synthesis of butyl butyrate. *Carbohydr Polym* **176**, 281–292 (2017).
29. de Andrade Silva, T., Keijok, W. J., Guimarães, M. C. C., Cassini, S. T. A. & de Oliveira, J. P. Impact of immobilization strategies on the activity and recyclability of lipases in nanomagnetic supports. *Sci Rep* **12**, 1–11 (2022).

Chapter 6 Conclusion and prospects

In summary, this thesis explores the use of polydopamine-functionalized magnetic microparticles as carriers for the immobilization of alcalase and lipase. The study investigates the effects of two types of spacers, glutaraldehyde (GA) and polyethyleneimine (PEI), as well as three different lengths of PEI on the immobilization outcomes. The thesis also optimizes the immobilization conditions and evaluates the performance of the immobilized enzymes. The main findings of this thesis are as follows:

(1) Micron-sized magnetic particles were successfully synthesized using the solvothermal method and subsequently coated with polydopamine (PDA) through DA's self-polymerization process. Characterization results, including X-ray diffraction (XRD), Fourier-transform infrared spectroscopy (FTIR), vibrating sample magnetometry (VSM), and X-ray photoelectron spectroscopy (XPS), confirmed the successful deposition of the PDA coating on the magnetic particles and demonstrated that the coating did not significantly affect the magnetic properties of the carrier. Scanning electron microscopy (SEM) analysis further verified the spheric morphology of the coated carriers.

(2) Alcalase was successfully immobilized onto the carrier using glutaraldehyde (GA), with optimized immobilization conditions determined to be a pH of 7.5, a GA concentration of 0.23 μg/mL, an alcalase concentration of 6.1 mg/mL, and an immobilization time of 4 hours. The immobilized enzyme exhibited an extended pH and temperature range, and after 14 cycles of reuse, it retained 78.66% of its original activity.

(3) Lipase (LCS) was successfully immobilized using two different spacers, i.e., glutaraldehyde (GA) and polyethyleneimine, as well as three PEI molecules of different molecular weights and therefore lengths. It was revealed that PEI, which has multiple amino groups as functional group to form covalent bonds with carboxyl amino acid residues and hydroxyl amino acid residues, had superior enzymatic protein immobilization efficiency than GA. The lipase immobilized with PEI as spacer also had much higher specific enzymatic activities than those with GA as spacer. When comparing lipase immobilization with PEI of three molecular weights, i.e., PEI-600, PEI-1800, and PEI-10000, PEI-600 Da exhibited optimal efficiency in lipase immobilization, whereas PEI-1800 Da maintained the highest specific enzymatic activity.

(4) A new concept, i.e., atom ratio, was proposed in this study as the benchmark for the identification of valley residues that are inaccessible to reactions other than the enzymatic reaction that involves the configuration change introduced by specific substrate(s). Analysis on the distribution of surface amino acid residues indicate that all the AAR of reactive sites are valley residues. Furthermore, all peak AAR that are reactive to PEI and GA are well distanced from the active sites of lipase, which is LCS. The optimal immobilization conditions were determined to be a lipase concentration of 4.25 mg/mL, pH 6, immobilization time of 5 hours, and an immobilization temperature of 10°C. Performance studies on the immobilized lipase indicated a broader optimal pH range and enhanced thermal stability compared to the free enzyme. Additionally, the immobilized lipase retained 50% of its activity after 10 reuse cycles.

(5) By comparing the immobilization of LCS and LCR using three different lengths of PEI, both bioinformatic analysis and experimental results indicated that lipase LCR yielded better immobilization outcomes. Response surface methodology (RSM) was employed to optimize the

immobilization conditions, which were determined to be 0.5 wt% LCR concentration, 29°C, pH 6.9, and 2 hours of immobilization. The immobilized lipase exhibited enhanced thermal stability, a broader optimal pH range, and improved reusability, retaining 30% of its activity after nine reuse cycles.

(6) This thesis systematically investigated the effects of different molecular weights of enzymes and spacer lengths on immobilization performance across three distinct projects. A clear trend emerged, demonstrating that the reusability of immobilized enzymes decreases as the length of the spacer increases. As shown in Table 6-1, alcalase immobilized using GA retained 79% of its activity after 10 cycles of reuse, highlighting the robustness of this immobilization strategy. In contrast, for lipases immobilized using PEI spacers of varying lengths, a significant decline in reusability was observed with increasing spacer length. Specifically, lipases immobilized with PEI-1800 retained 50% of their activity after 10 cycles, while those immobilized with the longer PEI-10000 spacer retained only 30% of their activity after 9 cycles. These findings underscore the critical role of spacer selection in enzyme immobilization, emphasizing a trade-off between spacer length and the operational stability of the immobilized enzyme. Future studies should further explore the underlying mechanisms of this trade-off and optimize spacer design for specific applications.

Table 6-1 Comparison of reusability across three projects

Enzyme	Enzyme Molecular Weight (kDa)	Spacer	Activity Retention (%)/Cycles of Use
Alcalase	27.41	GA	79%/14
LCS	270.94	PEI-1800	50%/10
LCR	57.78	PEI-10000	30%/9

Due to time and resource constraints, we have to leave several interesting avenues for future works based on the findings of this thesis, which are outlined as follows:

(1) Practical Application Studies: Investigate the real-world performance of immobilized lipases in various applications, such as esterification, transesterification, and hydrolysis reactions.

(2) Exploration of Alternative Spacers: Experiment with different spacers beyond GA and PEI, such as polyethylene glycol (PEG) and polyacrylic acid (PAA), to assess their impact on enzyme immobilization.

(3) Bioinformatics-Driven Directional Modification: Utilize bioinformatics to guide the targeted modification of enzyme molecules, aiming for directional immobilization to reduce randomness and improve immobilization efficiency.